Water Environmental Remediation in Organically Polluted Reservoir via Anoxification Recovery Using Underwater LED Irradiation

ホンリキット, ダオルアン

Water Environmental Remediation in Organically Polluted Reservoir via Anoxification Recovery Using Underwater LED Irradiation

HONGLIKITH DAOLUANG

2022

Table of contents

LIST OF FIGURE CAPTIONS

List of table captions

Chapter 1 Introduction

In a closed water body with an excessive inflow of organic matter, one of the most serious environmental issues is anoxification occurring in the deeper layer due to the low transparency in hot seasons. In particular, in the hypolimnion occurred in the organically polluted deep-water reservoirs, the insufficient underwater light intensity inhibits the production of dissolved oxygen (DO) by phytoplankton and aquatic plant photosynthesis (Elçi 2008; Hasan et al. 2013). In addition, the thermal stratification stemming from low transparency restraints the vertical transport of DO from the surface layer to the bottom layer, resulting in the occurrence of anoxic water in the hypolimnion (Sahoo and Luketina 2006; Wendt-Potthoff et al. 2014). Anoxification leads not only to the death of aquatic life but also to an increase in nutrients. The former is due to the depletion of oxygen and is linked to the breakdown of aquatic ecological systems (Rast, W., and Lee, G.F. 1978; Chapra and Canale 1991). The latter denotes the elution of dissolved inorganic phosphorous and nitrogen from the bottom sediment (Hupfer and Lewandowski 2008) and accelerates the eutrophic state, such as the excessive growth of phytoplankton known as cyanobacterial blooms (Vadeboncoeur et al. 2003; Jahan et al. 2010). Moreover, anoxification is linked not only to the generation of toxic hydrosulfide but also to the accumulation of sludge, including metal sulfides and undecomposed organic matter on the bottom bed. The bottom mud damages the aquatic biosphere (Wendt-Potthoff et al. 2014). Therefore, for the environmental conservation and restoration of water in organically polluted water bodies, it is important to develop effective counter measures against anoxification, and establish a technique to recover the anaerobic state.

Currently, conservation technologies for aquatic environments in closed water bodies have been put to practical use, and the applications of sand covering, dredging, and aeration in organically polluted water areas have already been reported. Although these countermeasures have shown some advantageous outcomes for aquatic environmental conservation, various problems, such as unsustainability of improvements and economic problems, have been pointed out (Ogawa et al. 2009; Kido et al. 2014). Because the improvement technique based on these physical methods has a large influence on aquatic ecosystems, it is desirable to develop new technologies for aquatic environment restoration and environmental harmony.

In recent years, a water quality improvement technique for anoxification recovery via the promotion of phytoplankton photosynthesis using underwater LED irradiation has been developed as a new technology (Minato et al. 2012; Yamanaka et al. 2012; Minato et al. 2014;

Harada et al. 2016). This technology can be applied by focusing on the poor underwater light environment, which is caused by dissolved and particulate organic matter. Anoxification can be recovered by artificially improving the underwater light environment using an LED light source, such as a fish-luring light, and its effect is stemming from oxygen production via phytoplankton photosynthesis. In addition, this solution may be linked to the improvement of water and bottom sediment environments with recovery from anaerobic to aerobic states (Harada et al. 2016). This improvement method may overcome the problems pointed out in other physical techniques, such as dredging, sand covering, and aeration, and can be considered as a new technology for the conservation of aquatic environmental harmony into account. However, there are few research reports on the effectiveness of water quality improvement by underwater LED irradiation, and it is difficult to say that the basic knowledge on this technology is sufficiently acquired.

Chlorophyll-a (Chl-a), which is a major photosynthetic pigment in plants, mainly absorbs light within the blue wavelength band (435 nm to 480 nm) and the red wavelength band (610 nm to 750 nm) in the visible light spectrum. In addition, it is generally pointed out that the blue and red color spectra contribute to an increase in the chlorophyll production rate and the growth of algae (Chen et al. 2010), and that the photosynthesis rate of plants is strongly influenced by the ratio of the photon quantity within blue and red color spectra. However, there are many unclear points about the relationship between the photosynthesis rate of phytoplankton and the optical spectrum of the irradiation light (Wang et al. 2007; Takada et al. 2011; Minato et al. 2012). Following this point, Harada et al. (2016) quantitatively evaluated the effectiveness of underwater LED irradiation as a water environmental remediation technology using a cylindrical water tank. In particular, they focused on the influence of the ratio of red to blue light (R/B ratio) on the biochemical changes in DO and Chl-a. They found that irradiation with the mixed wavelength range could more quickly recover anoxia or hypoxia because of the increase in photosynthesis rate, compared to a single-color wavelength range of the red or blue spectrum. However, in the experimental system by Harada et al. (2016), filamentous algae adhering to LED lamps contributed more strongly to the continuous maintenance of sufficient DO concentration compared to phytoplankton. In other words, the water environmental remediation effects were estimated in only a limited space in the vicinity of the light source in their research approach. Considering the application of this technology to actual water bodies, it is essential to examine the possibility of recovery from anoxification using LEDs in an experimental system where phytoplankton, rather than filamentous algae, can multiply without the influence of underwater objects.

The photon flux density in a region away from the light source becomes weaker because the underwater light from the LED lamp is attenuated in the direction of irradiation. Therefore, it is necessary to understand the effects of water environmental remediation under conditions in which the optical intensity is lower than the optimum light quantum for photosynthesis. In addition, even in the region close to the light source, the mixed light of red and blue color spectra is anything but strong under the normal output of electric power, and the photon quantity is at the lowest limit in the range of the optimum quantum for photosynthesis. Because the general artificial light irradiation has a limit of light intensity at a relatively low level for photosynthesis, the contrivance of the LED irradiation method, which are able to increase the photosynthesis rate or to promote oxygen production, is required to effectively recover the anoxic state. One possible solution is to use of RGB full-color underwater LED lamp as a light source. Simply, photon intensity of LED irradiation can increase by adding the green spectrum (500´ nm to 560 nm) to the two-color (red and blue) spectrum. That is, it is expected that the mixed RGB irradiations have advantages such as, faster improvement in the DO environment and better maintenance of a healthy DO level (more than 4 mg/L) than the two-color red and blue spectrum (Honglikith et al. 2022). As dissolved oxygen is core factor for living aquatic organism, the minimum acceptable limit of DO level must be 4 mg/L because most fishes could not survive if DO is lower than 4 mg/L and aquatic life would be affected. DO level is strongly recommended higher than 4 mg/L that there will no experience oxygen depletion (Caraco et al. 2000; Radwan et al. 2003; Kaushik et al. 2012). However, how much intensity of the green color band is required to promote algal growth, and how much intensity of the red and blue spectra is required for phytoplankton photosynthesis under the condition of limited photon intensity remain unknown. Therefore, to design optimal conditions for the optical spectrum in LED irradiation, quantitatively evaluating the anoxification recovery effect is necessary by understanding the influence of LED irradiation on the promotion of phytoplankton photosynthesis under each of the RGB irradiation spectra.

In addition, examining the water environmental remediation effects considering the initial anaerobic condition as well as spectral condition of LED irradiation is important for the following reasons. The initial anaerobic condition depends on the duration in the anoxic state and the potential of maintaining a reductive state, and can be characterized by concentrations of materials stemming from anaerobic decomposition processes, such as denitrification, iron reduction, and sulfate reduction, of organic matter (Oniki et al. 2017; Thach et al. 2017, 2018a). A strong reductive state caused by long-term anoxification causes the increases of oxidizable

substances such as sulfide, ferrous ion, and undecomposed organic matter. High concentration of nutrients, as well as nutrients such as dissolved inorganic nitrogen (DIN) and dissolved inorganic phosphorous (DIP). It is guessed that the high concentration of oxidizable substances prior to LED irradiation has a disadvantage for recovering from the anoxic state because it links to excessive oxygen consumption via oxidation reactions. Meanwhile, it is presumed that high concentrations of phosphate-phosphorus (PO_4-P) and ammonia-nitrogen (NH_4-N) eluted from sediment under anaerobic conditions prior to beginning the LED irradiation will an advantage for promoting the phytoplankton photosynthesis rate. Therefore, the initial water quality parameters characterized by the anaerobic state at the beginning of LED irradiation strongly influence the water environmental remediation via anoxification recovery.

Backed by the subjects mentioned above, this study focuses on LED irradiation experiments at the laboratory level for understanding the effect of anoxification recovery through oxygen production by phytoplankton without the influence of filamentous algae adhering the underwater objects. The experiments aim to evaluate the influences of two factors, spectral distribution and photon intensity of the RGB illumination, and initial water quality concentrations that reflected the anaerobic reductive potential prior to beginning the LED irradiation, on the anoxification recovery and water environmental remediation. In particular, the influence of optical conditions for irradiating LEDs on oxygen production by phytoplankton photosynthesis are examined via two different preparative scales of indoor water quality experiments on a beaker-scale and a relatively large water tank-scale. This thesis consists of five chapters as following.

In Chapter 2, the outline of LED irradiation experiments is described. The irradiation experiments in this study is performed by irradiating environmental water samples from an actual reservoir at the laboratory scale and by monitoring the changes in water quality parameters related to organic pollution and eutrophication. The concrete contents in this chapter were concerning a targeted water body for environmental water and bed material collecting, experimental systems on a beaker-scale and water tank-scale, used underwater LED lamps, and the continuous measurement and scheduled observation of water quality parameters. In particular, the explanation for experimental systems describes how to generate anoxification on beaker-scale and water tank-scale, as well as how to illuminate the anoxic water for excluding the influence of filamentous algae adhering to LED lamp.

In Chapter 3, beaker-scale experiments are performed to evaluate the impacts of the optical spectrum and LED light intensity on the maintenance of healthy aerobic conditions, as

well as the anoxification recovery by promoting oxygen production by phytoplankton photosynthesis. In these experiments, the experimental condition of weak light intensity assumes a point far from the light source to evaluate the effective irradiation range for water quality improvement, not only limited range in the vicinity of light source. The specific objective is to estimate the effectiveness of widening optimum intensity for photosynthesis to cover the entire visible light region by adding the green spectrum to two-color mixed (red and blue) spectrum under limited maximum LED output. In addition, LED irradiation experiments assumes an organically polluted water body where concentrations of NH_4-N, PO_4-P, and hydrogen sulfide are expected to increase under strong reductive conditions due to long-term anoxification. The influences of LED irradiation of anoxic water with a strong reductive state on biochemical dynamics of water quality are examined to acquire the essential findings concerning the application of the proposed water quality improvement method to actual water areas.

In Chapter 4, LED irradiation experiments aim to examine the influence of optical conditions and initial anaerobic conditions on water environmental remediation are performed on water tank-scale to enhance the reliability of experimental results. The water tank-scale experiments consist of three series. The first series is to determine the effects of single-color irradiation (red, green, and blue spectra) on the growth of phytoplankton, fluctuations in DO, and recovery from long-term anoxification. The single-color irradiation experiments are performed to relatively evaluate the effect of the green spectrum on promoting the oxygen production via phytoplankton photosynthesis when compared to red and blue spectra under the optical condition such that photon intensity is marginally sufficient and would not strongly restrict photosynthesis. The experimental results might provide essential knowledge for discussing the effectiveness of water environmental remediation using RGB full-color underwater LED lamp irradiation. The second series is to examine the improvement of water quality during the recovery from anaerobic state under weak light intensity conditions, which is markedly lower than the effective photon flux density for photosynthesis. Concretely, experiments using mixed RGB irradiation (R:B:G = 1:1:1) is conducted to evaluate the influence of the weak light intensity that was as low as one-tenth and one-twentieth of optimum light quantum for photosynthesis, under initial anaerobic conditions which are represented as a strongly reductive state and are reflected by high concentrations of sulfide and nutrients. The experimental outcomes might be applied to the evaluation of spatial range in the irradiating direction from LED lamp, which allows for good anoxification improvement. The third series is to evaluate the influence of initial anaerobic conditions on water environmental remediation effects under weak light intensity. To achieve this purpose, mixed RGB irradiation experiments are performed under two different

experimental condition concerning initial water quality parameters characterized by concentrations of oxidizable substances (sulfide and ferrous ion), and nutrients (ammonium and phosphate ions). The experimental findings might give an information for understanding the dependencies of anoxic recovery effect and maintenance of a healthy aerobic condition on the duration in anoxic state prior to the beginning of LED irradiation.

Lastly, the general conclusions and recommendation for the general implementation of the above-described LED irradiation experiment are pointed out in Chapter 5.

Chapter 2 Materials and Methods

2.1 Study area

LED irradiation experiments describes in the next section are performed using environmental water and bed material collected from an actual reservoir at the laboratory scale and by monitoring the changes in water quality parameters while irradiating anoxic water. This targeted water body was an agricultural reservoir situated in a deforested area in the Ito campus of Kyushu University, Fukuoka Prefecture, Japan. This reservoir was constructed as an irrigation water resource and a flood control reservoir. It had a surface area of approximately 13 800 m^2, storage capacity of approximately 75 000 m^3, and maximum water depth of approximately 8 m (**Fig.2.1**). The logged wood chips acquired at the time when the forested area had developed into the campus was covered with the developed land, including the vicinity of the targeted reservoir. As a result, this reservoir was affected by excessive inflow levels of dissolved organic matter from humified logged wood chips during heavy rainfall. Therefore, water environment was degraded because of low transparency and insufficient underwater light intensity due to high amount of dissolved organic matter (Harada et al. 2014; Do et al. 2015; Thach et al. 2018a).

The characteristics of seasonal change in water environment were summarized as follows (Thach et al. 2018b). The thermal stratification started to occur in April because of a significant difference in temperature between water surface and bottom water layer (temperature deviations of up to 10 ºC) with its structure consisting of an epilimnion, thermocline, and hypolimnion. From April to August, the water temperature gradient increased so that a stable thermocline could be found at 2 m - 4 m. Since in the middle of May, DO showed a distribution similar to the vertical profile of water temperature. That is, the DO profile had a three-layer structure with a top layer in a largely saturated state, a rapidly decreasing quick change layer, and a hypoxic bottom layer. The hypolimnion was in an anoxic condition at depths ≥ 6 m~7 m until June, and its range was expanded since July. In particular, in August, hypoxia developed at ≥ 2.5 m when strong stratification formed with the large water temperature difference of approximately 20 °C between water surface and bottom bed. However, thermal stratification was weakened due to radiative cooling at water surface since mid-September. Owing to the development of a mixing layer in the fall season, water depth zones with a sufficient DO concentration enlarged to ≤ 4 m in October and ≤ 6 m in November. Thus, DO environment improved across all zones in the vertical direction, starting with destratification, which occurred

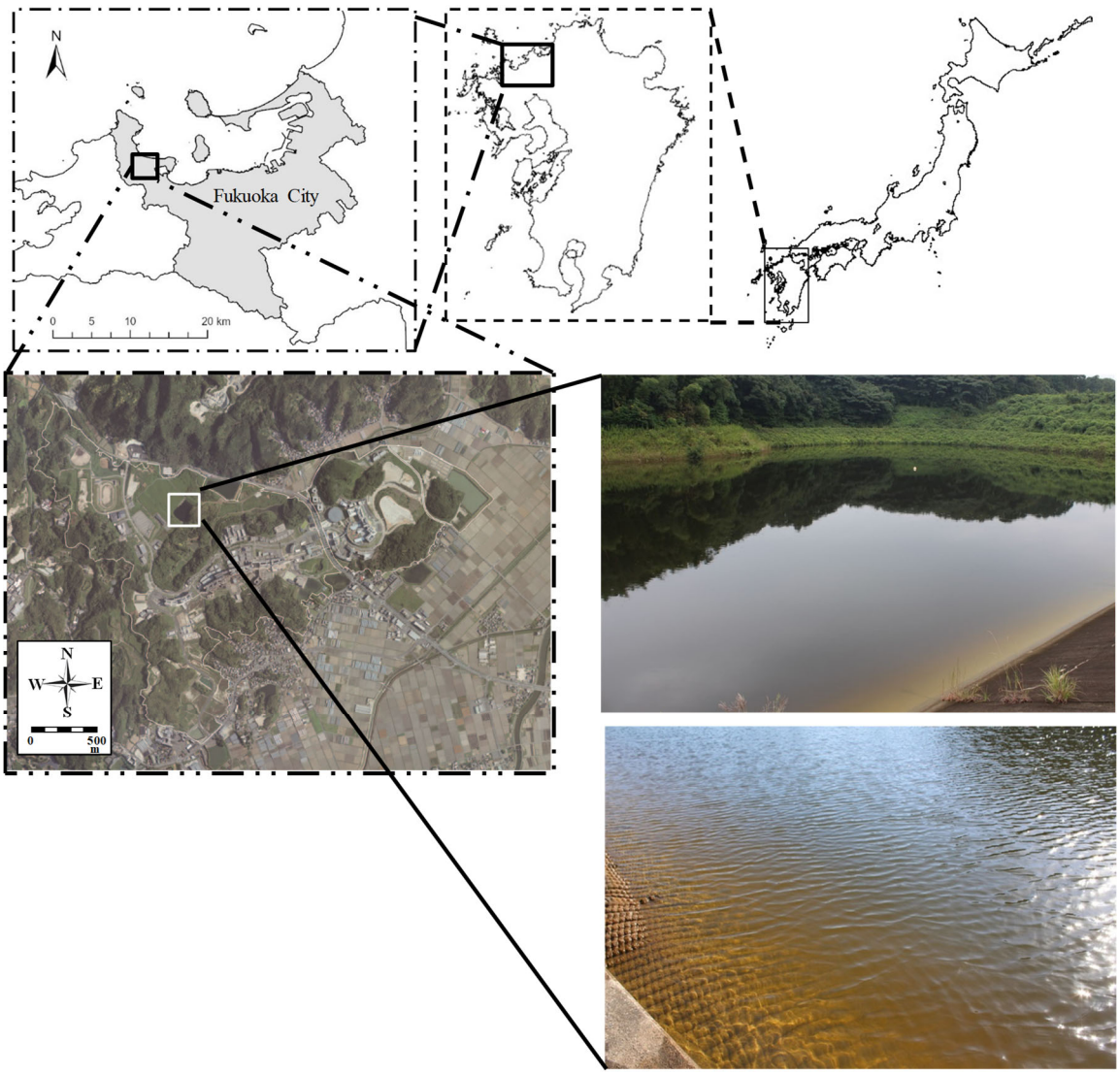

Fig. 2.1 Targeted reservoir situated in the Ito campus of Kyushu University, Fukuoka Prefecture, Japan

by the development of vertical circulation in mid-November or early December. Therefore, the strong reductive state with an oxidation reduction potential (ORP) of –200 mV above the bottom mud lasted in a long-term of approximately 8 months, resulting in elution of nutrients from the bottom sediment, and generation of hydrogen sulfide. In particular, PO_4-P, NH_4-N and sulfide increased to high concentrations of approximately 0.25 mg/L, 3.0 mg/L and 700 mg/L, respectively. The aim of this study is to establish water environmental remediation via anoxification recovery in such an organically polluted reservoir.

2.2 LED irradiation experiments on a beaker-scale and a water tank-scale

The purpose of LED irradiation experiments is to examine how much artificial light irradiation could contribute to water environmental remediation in anoxic water through the recovery from the anaerobic state in two stages. In the first stage, beaker-scale method is used to obtain a fundamental knowledge of water environmental remediation, considering the influence of spectral characteristics of LED irradiation with RGB on the water quality dynamics. This irradiation experiment is conducted in a volume of 0.5 L because small beakers are convenient for handling the preparation and setting for water quality experiments. In the second stage, the experimental scale is expanded to a water tank with a volume of 50 L to improve the credibility of experimental results.

In this study, water environmental remediation is applied to the above-mentioned organically polluted water bodies, where concentrations of sulfide, NH_4-N, and PO_4-P would increase to a high level by strong reductive state. Because it is difficult to take a sample of the excessive anoxic water at the bottom, aerobic water sampled at water surface is artificially converted to anaerobic water using a specific experimental setup. Meanwhile, bed material with strong reductive state is used for laboratory experiments by sampling bottom mud during anoxification, and the used sediment had physicochemical properties with ORP of –176.5 mV, pH of 7.40, EC of 0.068 mS/cm, sulfide level of 0.154 mg/g and ignition loss of 11.62 %. This study do not focus on the effect of initial reductive state of sediment surface on water environmental remediation upon LED irradiation but focuses on the impact of photon flux density, in which lights are emitted to the anoxic water. Therefore, the control for bottom sediment is not set in first- or second-stage experiments.

In both stages, an RGB full-color underwater LED lamp (LA1-24RGB, Marintec Inc.) with a diameter of 0.9 m and a height of 0.51 m is used as the light source. This is commercially available as a fish-luring underwater light and has a four-sided structure with 60 LED elements

corresponding to RGB color components per side. It is possible to adjust the photon flux density for each color and irradiate samples using monochromatic light or mixed color light with an arbitrary spectral distribution (component ratio of red, blue, and green color light intensities). In this study, in light of previous results of Harada et al. (2016), the following two stages are adopted to exclude the influence of an underwater object that would induce the overgrowth of filamentous algae adhering to LED lamp.

The beaker-scale experiments in the first stage consists of four irradiation experiments, and each set is performed under different experimental conditions concerning the optical spectrum and LED intensity, as stated below. In each case, approximately 100 tall-beakers of 0.5 L at a height of 0.15 m filled with bed material (approximately 0.1 L) and environmental water (approximately 0.4 L) are prepared. The prepared beakers are divided into two groups of irradiation and control. The water surfaces in all beakers are covered with little amount of liquid paraffin (also called white oil) to block the supply of oxygen from the atmosphere (i.e., reaeration) to regenerate the conditions similar to a hypolimnion in a stratified water body. As shown in **Fig. 2.2**, beaker-scale experiments are designed not only by setting up the above-mentioned underwater LED lamp in a transparent acrylic water tank (diameter of 0.3 m and height of 1 m) filled with pure water but also by placing 24 beakers in two tiers along the periphery of the water tank. By utilizing two sets of water tanks and LED lamps in a single irradiation experiment, 48 beakers are provided per experimental condition. Lights are perpendicularly emitted from LED lamp to beaker walls, and just a small part of bed material is irradiated at the light source-side in this experimental system. However, the surface of bottom sediment is directly unaffected by the LED irradiation. Therefore, aerobic and anaerobic conditions of bottom surface do not depend on the emitted light itself but on the DO concentration above the sediment. Because beakers do not provide a suitable habitat for filamentous and adherent algae, the generation of these algae is suppressed even when beakers are exposed to LED irradiation. It is possible to conduct a beaker-scale irradiation experiment assuming a spatially wide range without the influence of LED lamp installations by adjusting the light intensity, outside limited range in the vicinity of light source. Other beakers that are not used for LED irradiation experiments are maintained in a container with complete light blocking as a control condition. All beakers in the two groups of irradiation and control experiments are kept under dark conditions to inhibit oxygen production by photosynthesis derived from other light sources, except for LED irradiation; they are also kept in a thermostatic temperature-controlled room at a temperature of 20 ^{o}C.

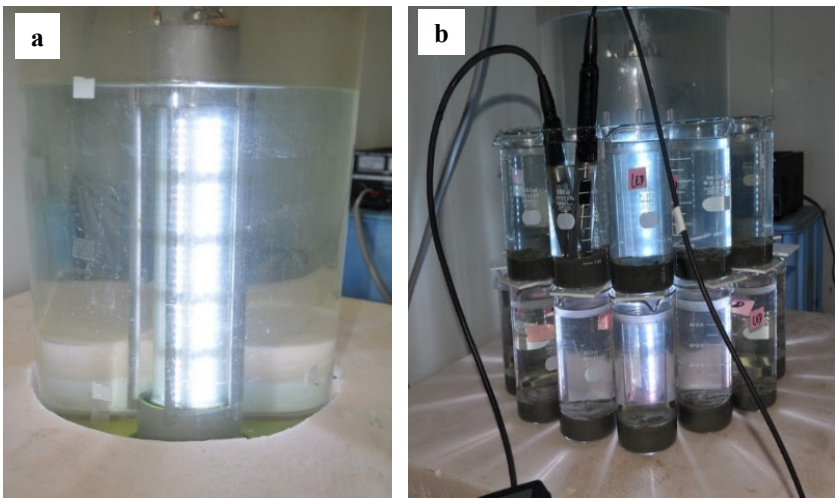

Fig. 2.2 The design for beaker-scale irradiation experiments. a) An RGB underwater LED lamp installed in a trans-parent acrylic water tank filled with pure water, and b) 24 tall-beakers of 0.5 L placed in two tiers along the periphery of the water tank

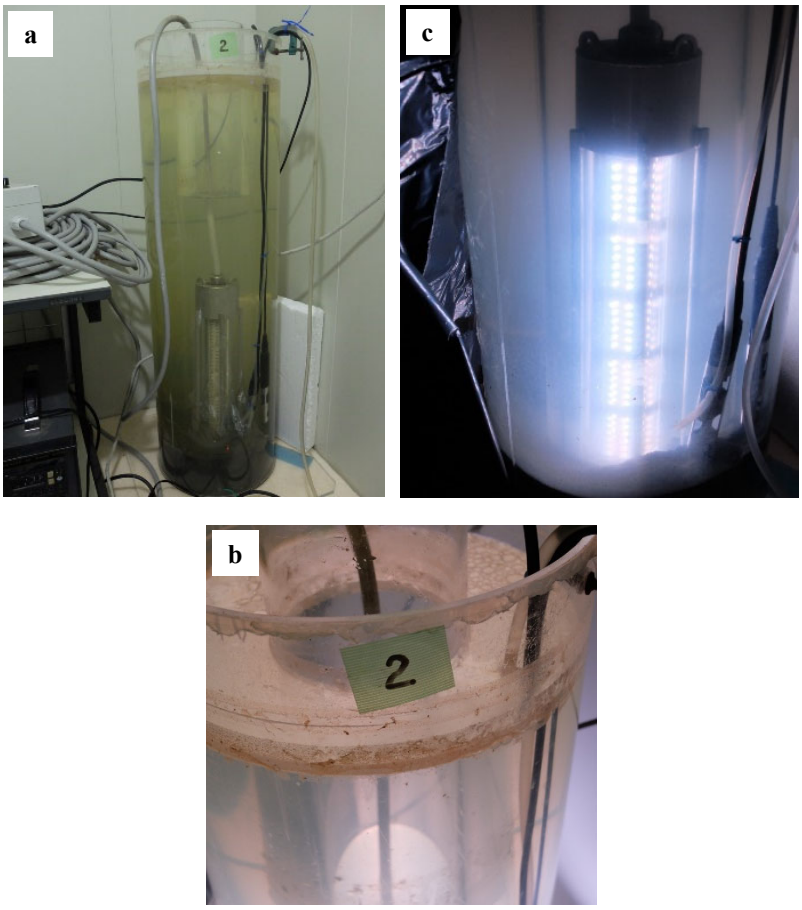

Fig. 2.3 The design for water tank irradiation experiments. a) General view of the experimental system. b) The small cylindrical tank filled with pure water for installing the underwater LED lamp, and c) environmental water irradiated using an LED lamp

The water tank-scale LED irradiation in the second stage is carried out in a transparent acrylic water tank with a diameter of 0.3 m and a height of 1.25 m. The environmental water and reductive bed material sampled on the above-mentioned reservoir are prepared at heights of approximately 1 m and 0.15 m, respectively, in this water tank. In this experimental system, the underwater LED lamp is installed in a transparent acrylic cylinder, which is set at the center of the water tank, as shown in **Fig. 2.3**. It is a small cylindrical tank with a diameter of 0.13 m and a height of 1 m filled with pure water. By secluding the LED lamp from the environmental water using a small cylinder, it is possible to neglect the impact of filamentous algae adhering to underwater objects on the oxygen production by algal photosynthesis. Surfaces of the bottom mud in water tank-scale experiments are never irradiated because LED lamps are pointed up-right in the sediment. Therefore, bottom sediment is unaffected by LED irradiation. Three series of irradiation experiments in total are performed in the second stage, and three cylindrical water tank systems are utilized par one series. All water tank systems are set up in a thermostatic room controlled at a constant temperature of 20ºC. It is possible to inhibit the production and supply of DO via photosynthesis and reaeration, not only by keeping water tanks under dark conditions but also by covering the water surface with liquid paraffin during the experimental period, re-sulting in the simulated generation of a hypolimnion in a stratified water body.

One of primary purposes in this study is to examine the recovery from anaerobic condi-tions with a strong reductive state caused by long-term anoxification above the bottom sediment through both beaker-scale and water tank-scale experiments. For this purpose, LED irradiation experiments are initiated from the time point when the water body is in a strong reductive state such that the oxidation-reduction potential (ORP) reached approximately –400.0 mV, and also phosphorous, ammonium, and sulfide concentrations remarkably increased due to anaerobic reductive reactions. In the first stage of beaker-scale experiments, anoxic water is generated in tall-beakers by maintaining water sample under dark conditions for more than two weeks before beginning the LED irradiation experiments. In addition, in the water tank-scale experiments, it takes approximately two months for the ORP of the environmental water to be lowered to a strong reductive state of approximately –400.0 mV. The time it takes aerobic conditions to be converted to anaerobic conditions seemed to differ in two stages because DO is consumed in a shorter period over the entire range of 0.5 L beakers via an aerobic reaction when compared to the water tank. LED irradiation experiments in both stages are initiated after confirming the remarkable increase in phosphorous, ammonium, and sulfide concentrations due to anaerobic organic matter decomposition.

The duration in both beaker-scale and water tank-scale experiments are approximately 2 months following a 24 hour-cycle with 12 hour-on/12 hour-off LED irradiation, and the photon flux density and optical spectrum of the irradiating light are determined according to the experimental conditions described below in the next chapter. This periodic irradiation is performed based on the finding that the photosynthesis in the light period could be activated by the periodical change of light included the dark period. In addition, the imitation of daytime and nighttime by controlling the irradiation times would lead to environmentally conscious water environmental remediation.

2.3 Water quality monitoring

Comprehensively understanding the temporal changes in DO is essential and important for assessing the anoxification recovery effects. In both beaker-scale and water tank-scale experiments, DO is continuously measured at 20 minute-interval using a fluorescent DO meter (ProODO, YSI). The fluorescent DO electrode shows a fast response time and excellent measurement accuracy and repeatability, enabling a continuous and stable measurement in a still fluid environment. Also, ORP is an effective index to understand an anaerobic biochemical dynamic of water quality. Under anoxic state, reduction half-reactions through inorganic compounds containing oxygen occur in stages, and begin with high ORP. The major biochemical reductions in aquatic environments are denitrification, iron reduction, and sulfate reduction, and it is possible to roughly know which stage of reduction half-reaction occurs by measuring the ORP. To grasp an anaerobic condition from the viewpoint of biochemical reactions, the ORP measurement electrode was made of platinum, and the reference electrode was made of silver chloride. Although potential (Eh) conversions using a hydrogen standard electrode were not performed, an approximate Eh value was calculated by adding 200.0 mV to the measured value. In beaker-scale LED irradiation experiments, DO and ORP meters are set in one of the 48 beakers for continuous measurements. In the water tank-scale irradiation experiments, these meters are fixed at 0.1 m above the bottom sediment in each water tank.

In addition to the continuous observation, water quality parameters related to organic pollution and eutrophication are measured on a regular basis as mentioned below for about 2 months after the start of LED irradiation. In both cases, water quality analyses are scheduled about 11 h after putting on LED lamps. In addition, in both beaker-scale and water tank-scale experiments, optical spectrum and irradiating light intensity are measured using an illuminance spectrophotometer (CL-500A, Konica Minolta Inc.) in conjunction with the scheduled water

quality observations. The details of scheduled observations in each experiment are presented below.

In beaker-scale experiments, water quality parameters are analyzed for 2-4 beakers, which are randomly selected per observation to eliminate bias among samples. Scheduled observations are performed twice per week at intervals of 2 or 3 days during first month of experiment and every 7 days during second month of experiment. Before measuring water quality parameters, the liquid paraffin, covering the water surface is removed using lipophilic and hydrophobic oil absorption sheets in advance. The water samples are taken from the selected beakers are combined, and this integrated sample is used for water quality analyses. In water tank-scale experiments, water samples for the analysis of water quality parameters are collected based on the siphon principle through a polyvinyl chloride tube fixed at 0.1 m above the bottom sediment, similar to the continuous observation of DO and ORP. In this experiment, the sampling volume per time is approximately 0.5 L in each cylindrical water tank, and the frequency of scheduled observations is twice per week at intervals of 2 or 3 days.

Major water quality parameters and their analytical measurements are follows: (a) Chl-a is analyzed using a fluorophotometer (Aquafluor, TURNER DESIGNS) and solvent extraction of chlorophyll with N,N-dimethylformamide; (b) nitrate-nitrogen (NO_3-N) and sulfate ion (SO_4^{2-}) is measured using an ion chromatograph (DX-320, Dionex); (c) PO_4-P and total phosphorus (TP) are analyzed using absorption spectrophotometry (DR5000, HACH) based on the ascorbic acid reduction molybdenum blue method; (d) total nitrogen (TN) is measured based on an ultraviolet absorption spectrophotometry using DR5000; (e) total iron ion (TFe), which was defined as the sum of ferrous ion (Fe^{2+}) and ferric ion (Fe^{3+}), are analyzed based on the 2,4,6-tris (2-pyridyl)-1,3,5-triazine method using DR5000; (f) the sulfide concentration is measured using DR5000 based on the ethylene blue method, and this analysis included S^{2-} liberated from hydrogen sulfide, hydrogen sulfide ion, and soluble metal sulfides (including iron sulfide) due to the presence of sulfuric acid; (g) NH_4-N is measured by utilizing a colorimetric titration-type ammoniacal nitrogen meter (AT-2000, Central Kagaku Corp.); (h) total organic carbon (TOC) and dissolved organic carbon (DOC) are measured using a TOC analyzer (Sievers 900, GE Analytical Instruments) based on a wet ultraviolet oxidation reaction and selective membrane conductometric technology; (i) ultraviolet light absorption at 254 nm (E254) is measured using DR5000 as an indicator of humic acids and other dissolved organic matter.

To roughly understand the phytoplankton composition and monitor the temporal changes associated with it, in vivo Chl-a concentration measurements at class-differentiated

algae levels are carried out using a multi-wavelength excitation fluorometer (FluoroProbe, bb-Moldaenke). Based on the fluorescence excitation spectra obtained by exposing chlorophyll to LED light at six different wavelengths, phytoplankton could be classified into four classes as follows: Chlorophyceae (green algae), cyanobacteria (blue-green algae), diatom/dinoflagellates, and cryptophytes; in vivo Chl-a concentration of each class was measured (Beutler et al. 2002). As diatoms and dinoflagellates have similar spectra, these species could not be differentiated, and the integrated Chl-a was expressed as the sum of their concentrations.

Chapter 3 Influence of Optical Spectrum on Remediating Anoxic Water Environment by Beaker-scale Experiments

3.1 Introduction

The anoxic recovery effects by LED irradiation would be strongly affected by not only light intensity but light quantity because this technology is based on promoting an oxygen supply by phytoplankton photosynthesis. Because a light intensity decays in the irradiating direction due to absorption and scattering of dissolved or particulate matter, an extreme lowering of photosynthesis rate by a low photon intensity is an obstacle to an anoxification recovery. To properly evaluate the spatial range which allows for good anoxification improvement by LED irradiation, it is an essential topic to estimate the influence of weak light intensity on the oxygen production by phytoplankton photosynthesis. In addition, it is important to determine an ideal spectral distribution in LED irradiation for phytoplankton photosynthesis. The only mixed light of red and blue color spectra cannot necessarily ensure the optimum photon flux density for phytoplankton photosynthesis under normal output of electric power, although two color bands play a most important role in photosynthesis in the visible light. Because the general artificial light irradiation has a limit of light intensity at a relatively low level for photosynthesis, the contrivance of LED irradiation method, which are able to increase the photosynthesis rate or to promote oxygen production, is required to effectively recover the anoxic state.

To acquire fundamental knowledge concerning the influence of optical spectrum and light intensity of LED irradiation on water quality dynamics, indoor water quality experiments are performed using an RGB full-color underwater LED lamp. In this research, beaker-scale experiments, which require a smaller amount of environmental water and bed sediment are adopted as the first approach to reduce the labor for building experimental systems. The concrete aim is to estimate the effectiveness of widening optimum intensity for photosynthesis to cover the entire visible light region by adding the green spectrum to two-color (red and blue) spectra under limited maximum LED output. Therefore, irradiation experiments are conducted by illuminating anoxic water from outside beaker. The experimental condition of weak light intensity assumes a point far from the light source to evaluate the effective irradiation range for water environmental remediation, not only limited range in the vicinity of light source. In addition, indoor water quality experiments assume an organically polluted water body where concentrations of NH_4-N, PO_4-P, and hydrogen sulfide are expected to increase under strong reductive conditions due to long-term anoxifcation. The influences of LED irradiation of anoxic

water with a strong reductive state on biochemical dynamics of water quality were examined to acquire the essential findings concerning the application of the proposed water environmental remediation method to actual water areas.

3.2 Experimental conditions

The experimental conditions are classified into optical conditions concerning LED irradiation and initial water quality conditions. The former was a primary experimental condition to examine the influence of spectral features of LED irradiation on water quality dynamics via the recovery from the anaerobic state, and it was characterized by RGB color bands and optical intensity. The photosynthetic rate, which is an essential key point in the preservation of a satisfactory oxygen environment, is most strongly related to both the blue wavelength band and the red wavelength band in the visible light. In addition, according to Minato et al. 2012, the optimum photon flux density for phytoplankton photosynthesis is 50–180 μmol/ (m^2 s), and this range is equivalent to approximately 25–90 μmol/(m^2 s) when it is evaluated by the sum of photons of blue wavelength band and red wavelength band in the sunlight spectrum. In this study, the strong and weak light intensities in LED irradiation experiments are determined by referring to the range of 25–90 μmol/(m^2 s) for the optimum photon flux density required for phytoplankton photosynthesis. Beaker-scale experiments are designed to examine the effectiveness of adding the green visible spectrum to the mixed red and blue spectra to increase phytoplankton photosynthesis.

Therefore, LED irradiation experiments in this scale are conducted under four optical conditions, labeled as Cases A-1 to A-4**,** by setting the optical spectrum and intensity as experimental conditions, as summarized in **Table 3.1.** First, optical spectrum conditions are divided into two groups as follows: Two-color spectra (Cases A-2 and A-4), and the three-color RGB spectra (Cases A-1 and A-3). The former is set based on the contribution of red and blue spectra to algal growth. The latter focuses on the green spectrum to increase the optimum level of photosynthesis within entire visible light region. The influence of the presence or absence of the green spectrum on water quality dynamics is examined by comparing these groups. Next, the light intensity is divided into two groups based on the range of optimum photon flux density for phytoplankton photosynthesis. Cases A-1 and A-2 are corresponded to the lower limit of the optimum range. Cases A-3 and A-4 are represented weak light conditions, which severely restricted photosynthesis as an optical limiting factor.

Cases A-1 to A-4 are characterized by a combination of above conditions. In Cases A-1

and A-3, the photon flux densities of red, blue, and green spectra are set such that R:B:G = 1:1:1. In Cases A-2 and A-4, the photon quantities of red and blue spectra are adjusted so that the R/B ratio is approximately 1.0, under the condition that the photon flux density of the green spectra is zero. The photon quantities of red and blue spectra in Cases A-1 and A-2 are determined so that the sum of both densities in two cases are approximately equal. Therefore, the total photon flux density of visible light region in Case A-1 was larger than that in Case A-2 because of the inclusion of the green spectrum. For Cases A-3 and A-4 the total photon density of visible light region is extremely small, approximately 10.0 μmol/(m^2 s), in comparison with the optimum light intensity for photosynthesis, and the R/B ratio is approximately 1.0. The sum of the photon quantity of red and the blue spectra for Case A-3 is smaller than that of Case A-4 because Case A-3 includes the green spectrum, and the total photon quantum of visible rays is equivalent in both cases.

The primary purpose in the first stage is to examine the recovery from anaerobic conditions, in which a strong reductive state caused an increase in NH_4-N, PO_4-P and sulfide. To achieve this objective, the anaerobic water prepared in beakers before beginning LED irradiation experiments for two months is maintained for a long period (about three weeks for beaker-scale experiments). Therefore, initial water quality conditions in each case is reflected by the anaerobic reductive reactions under a strongly reduced state of ORP = –400.0 mV (Whitmire and Hamilton 2005), as shown in **Table 3.2**. The characteristics of anoxic water are summarized as follows. First, NO_3-N decreased to almost zero due to denitrification (Robert Hamersley et al. 2009). Next, NH_4-N and PO_4-P show relatively high concentrations because of the elution from sediment due to the anaerobic decomposition of organic matter (Gordon and Higgins 2007). In addition, TFe level increases under anaerobic conditions, indicating that ferrous ion (Fe^{2+}) is eluted from sediment to water due to iron reduction (Lijklema 1980; Roden and Edmonds 1997). Therefore, the increase in PO_4-P mainly resulted from the iron reduction. Furthermore, sulfide concentration obviously increases owing to the sulfate reduction that is generated under strong reducing conditions (Luther et al. 2003; Zerkle et al. 2010). From the above, initial water quality of LED irradiation experiments in all cases is characterized by anaerobic reductive reactions, such as denitrification, iron reduction, and sulfate reduction. Therefore, it is a key point to examine the influence of high concentrations of nutrients and reductive substances in anoxification recovery using LED irradiation.

Table 3.1 Optical spectrum and intensity of LED irradiation for the beaker-scale experiments

Case	LED	Intensity μmol/(m^2 s)	Visible light (360 nm~780 nm)	Blue band (435nm~480 nm)	Red band (610nm~710 nm)	Green band (500nm~570 nm)	R/B ratio
A-1	RGB	Strong	82.1	24.9	26.5	25.6	1.1
A-2	RB	Strong	57.7	26.9	25.6	0.4	1.0
A-3	RGB	Weak	10.0	3.1	3.2	3.0	1.0
A-4	RB	Weak	10.0	4.3	4.7	0.2	1.1

Table 3.2 Initial water quality parameters at the start of LED irradiation in all cases

Case	ORP (mV)	DO (mg/L)	Chl-a (μg/L)	Sulfide (μg/L)	NH_4-N (mg/L)	PO_4-P (mg/L)	NO_3-N (mg/L)	TFe (mg/L)
A-1	–381.4	0.3	0.8	46.7	2.17	0.16	0.01	1.47
Control	–381.4	0.3	0.8	46.7	2.17	0.16	0.01	1.47
A-2	–426.0	0.4	0.7	96.7	2.50	0.23	0.01	1.87
Control	–426.0	0.4	0.7	96.7	2.50	0.23	0.01	1.87
A-3	–411.3	0.3	0.4	46.0	2.43	0.24	0.01	1.79
Control	–411.3	0.3	0.4	46.0	2.43	0.24	0.01	1.79
A-4	–411.3	0.3	0.4	46.0	2.43	0.24	0.01	1.79
Control	–411.3	0.3	0.4	46.0	2.43	0.24	0.01	1.79

3.3 Results and discussion

3.3.1 Remediation effects under strong light intensity conditions

Under the condition of sufficient photon density in red and blue spectra for phytoplankton photosynthesis, the effects of the green spectrum on the improvement of water quality are examined by comparing results between Cases A-1 and A-2. **Figure 3 .1** shows the continuously measured results for DO and ORP under these conditions. In both cases, the change in DO could be characterized by three points as follows: (1) The time lag between the beginning of LED irradiation experiments and the start of increase in DO; (2) the drastic increase in DO with a fluctuation of the 24 hour-cycle after anoxification recovery; (3) the shift in DO to the steady-state expressed as a sinusoidal variation via a gradual decrease after the peak value. These characteristics of DO variations were explained through the changes in PO_4-P, TFe, NH_4-N, sulfide, NO_3-N, class-differentiated Chl-a and total Chl-a as in shown **in Fig.3.2** as well as ORP in **Fig.3.1**. The goal was to quantitatively estimate the effects of improved water quality from viewpoint of the production and consumption of oxygen based on the similarities and differences between two cases. In the following sections, *t* denotes the elapsed time from the start of LED irradiation.

1) Water quality dynamics until recovery from anoxification

First, the temporal changes in ORP, sulfide, and Chl-a levels after the start of the increase in DO (i.e., anoxification recovery) are investigated. The time required to recover from the anoxic state in Cases A-1 and A-2 is 6 days and 10 days, respectively. The following remarkable features are observed over time for ORP, sulfide, and total Chl-a levels before anoxification recovery. For a few days after beginning LED irradiation experiments (until $t = 2$ d for Case A-1 and $t = 5$ d for Case A-2), ORP remained at approximately −400.0 mV, which is a strong reducing state when compared to initial conditions, and sulfide is maintained at the same high level as initial value. Meanwhile, ORP increases in the negative range during putting on LED lamps ($t = 2$ d to 6 d for Case A-1 and $t = 5$ d to 10 d for Case A-2). Such a fluctuation in ORP means that the strong reducing condition is weakened despite the anoxic state. In addition, sulfide level began to decline at $t = 2$ d for Case A-1 and at $t = 5$ d for Case A-2, and they reach almost zero when water samples in beakers recovered from the oxygen-free state. The disappearance of sulfide means that the oxidation of sulfide to SO_4^{2-} occurred in the presence of oxygen (Morse 1990; Nielsen and Vollertsen 2021). Furthermore, we confirm the increase in Chl-a levels of the dominant species belonging to cryptophytes in both cases, at $t = 5$ d for Case A-1 and $t=7$ d

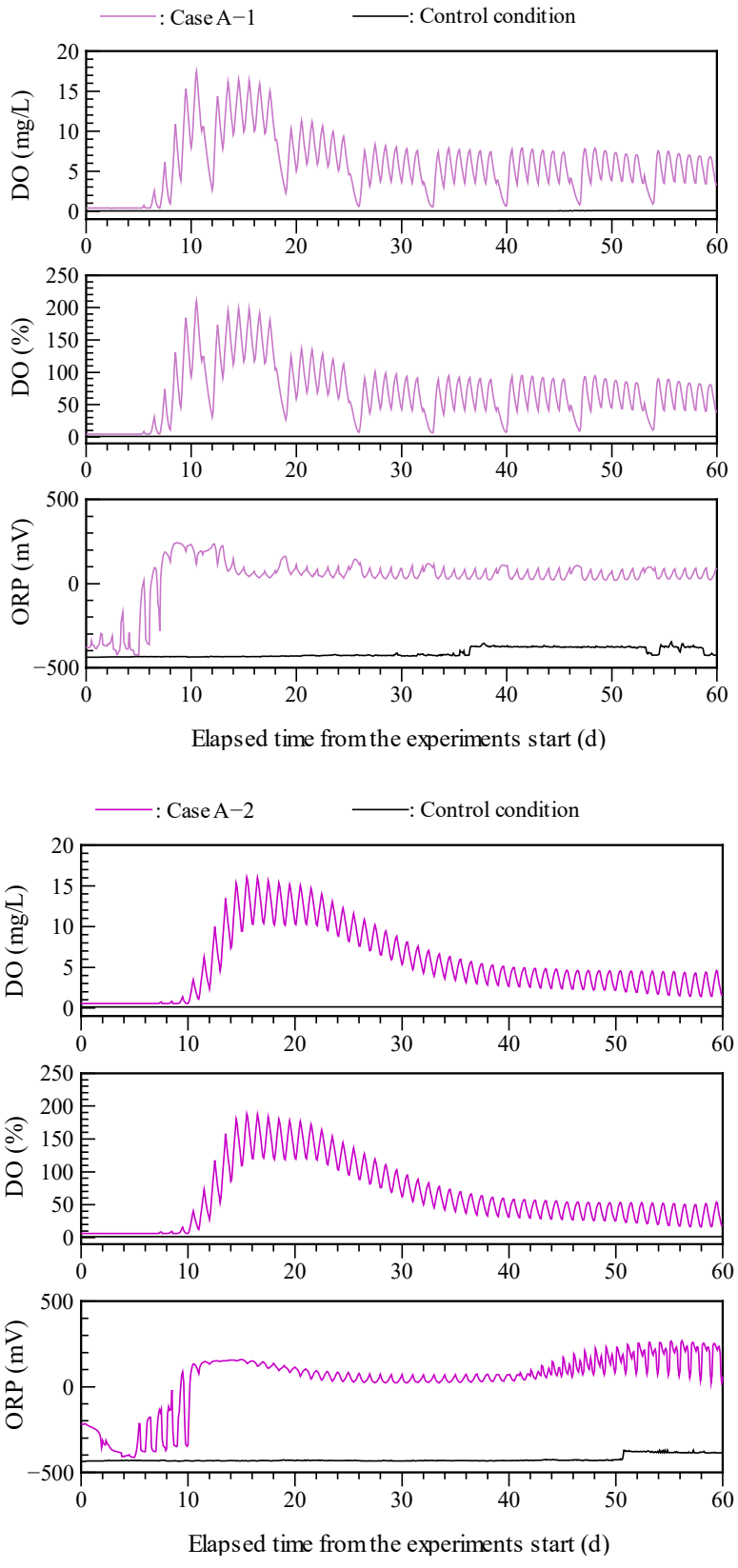

Fig. 3.1 Continuously measured DO and ORP in Cases A-1 and A-2

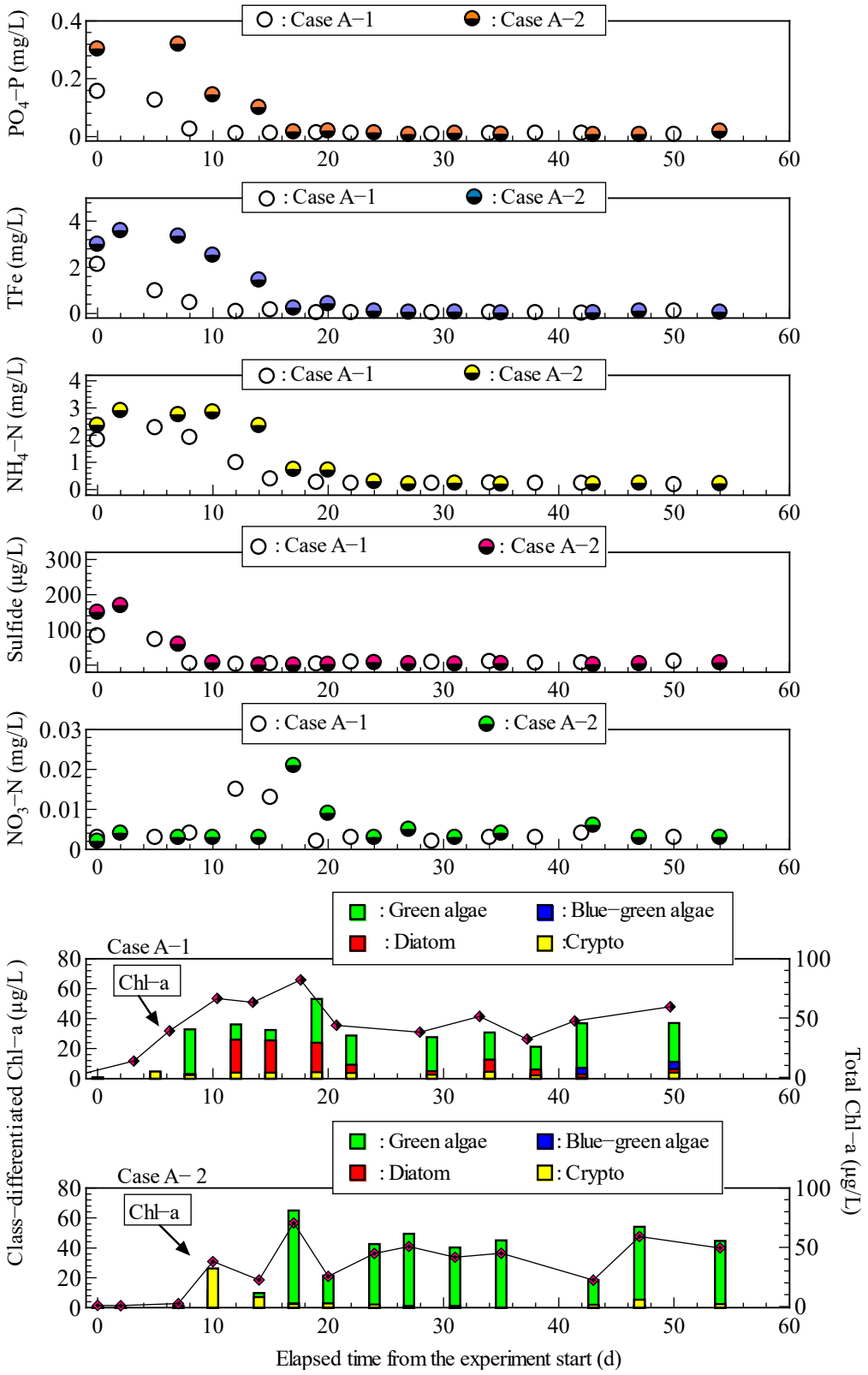

Fig.3.2 Periodically measured PO_4-P, NH_4-N, sulfide, NO_3-N, TFe, class-differentiated Chl-a and Total Chl-a in Cases A-1 and A-2

for Case A-2. Therefore, not only the increase in ORP and Chl-a levels but also the disappearance of sulfide indicates that oxygen is produced via phytoplankton photosynthesis between t = 2 d to 6 d for Case A-1 and t = 5 d to 10 d for Case A-2. From the above results, the reason why the anoxic state in beakers is maintained despite LED irradiation may be divided into two factors according to the time elapsed from the initiation of the irradiation experiment. For a couple of days immediately after initiating the irradiation (t < 2 d for Case A-1, and t < 5 d for Case A-2), the anoxic state could be maintained because oxygen production by algae photosynthesis do not occur regardless of sufficient light intensity conditions. It is considered that no oxygen production in the absence of light for about 2 weeks until the start of LED irradiation might lower the response of phytoplankton to light. That is, the delay in oxygen production by photosynthesis arose because the long-term absence of light leads to the decreased photo-responsiveness of phytoplankton. This decreased photo-responsiveness should be considered as a factor for the occurrence of a time lag between the initiation of irradiation experiment and the beginning of increase in DO. Although cryptophytes are generated as the dominant algae after t = 2 d for Case A-1 and t = 5 d for Case A-2, the amount of oxygen production is assumed to be small because their photosynthetic capacity is small when compared to other algal groups. It is assumed that it take a long time for phytoplankton, such as green algae with a high photosynthetic capacity, to recover from the reduced photo-responsiveness under the change from continuous absence of light to the presence of it. Thus, the oxygen consumption, which is accompanied by the oxidation of reductive substances, such as sulfide, would exceed the oxygen production, resulting in a continued anoxic state even though DO is produced by phytoplankton photosynthesis between t = 2 d to 6 d for Case A-1 and t = 5 d to 10 d for Case A-2. In both cases, excessive oxygen consumption is reflected in the high initial concentration of sulfide. Therefore, the time required to solve anoxification might depend not only on the recovery from the reduced photo-responsiveness of phytoplankton but also on the concentration of oxidizable substances generated under anaerobic conditions.

There are differences in the effectiveness of recovery from the anoxic state between Cases A-1 and A-2 such that the increases in phytoplankton and DO in Case A-1 occurs at an earlier stage compared to that in Case A-2. The increase in phytoplankton is confirmed after t = 2 d for Case A-1 and after t = 5 d for Case A-2. This result indicates that the photo-responsiveness in Case A-1 is recovered earlier than that in Case A-2. Considering that the photon quantity of red and blue spectra in both cases is approximately the same, the comparison between Cases A-1 and A-2 show that the presence or absence of the green spectrum strongly

influence the activation of phytoplankton exposed in the absence of light in long-term. Therefore, both photo-responsiveness and photosynthesis rate of phytoplankton could be enhanced by including the green spectrum along with red and blue spectra, and as a result, the anoxic state could be quickly solved. In addition, since the dominant phytoplankton species is cryptophytes until DO start to increase in both cases, the influence of the green spectrum on the species composition of plankton is small.

2) Water quality dynamics following DO increase

DO in Cases A-1 and A-2 sharply increase to a very high peak value of approximately 17.0 mg/L in approximately 5 days after recovery from the anoxic state, and then the supersaturation of approximately 200.0 % is maintained for several days. In both cases, the total Chl-a concentration increases to a maximum value of 60.0 μg/L to 80.0 μg/L as DO concentration increase. In addition, because the proportion of green algae contributing to the total Chl-a concentration is high, the dominant species changed from cryptophytes to green algae. The rapid increase in DO is due to the growth of green algae; therefore, the photosynthetic capacity would be higher than that in cryptophytes. Because these results are common in Cases A-1 and A-2, the above-mentioned features are not affected by the presence or absence of the green spectrum. PO_4-P and NH_4-N, which retain a high concentration due to the strong reducing state when DO = 0, decrease abruptly after the recovery from anoxic conditions and decrease to around zero when DO reach the peak value. This decrease is attributable to the uptake by phytoplankton, mainly green algae (Wang et al. 2006; Mackay et al. 2020; Zhang et al. 2020). As the temporal rates of decrease in PO_4-P and NH_4-N concentrations are relatively large, it is assumed that oxygen production is caused by the proliferation of phytoplankton with a very high photosynthetic rate. As a result, in both cases, Chl-a increases to a hypertrophic level exceeding 75.0 μg/L and DO also increases to a supersaturation level of approximately 200.0 %. It is considered that these high concentrations could be due to the excessive increase in PO_4-P and NH_4-N eluted from the sediment under long-term strong reducing conditions before beginning LED irradiation. In addition, no adherent algae or submerged plants are observed in beaker-scale experiments, and it is considered that interspecific competition with such large algae would not arise, resulting in the massive growth of phytoplankton.

Sulfide is disappeared via an oxidation reaction occurring under aerobic conditions immediately after recovery from the anoxic state, and ORP rapidly change from negative to positive. The anaerobic state is quickly recovered to an aerobic state, and the effect of water

environmental remediation is obvious regardless of the presence or absence of the green spectrum during LED irradiation. During the increase in DO, TFe also decreases to almost zero. Fe^{2+} ions, which are generated in large amounts via iron reduction under strong reducing conditions before LED irradiation, are oxidized to Fe^{3+} ions upon recovery from the anaerobic state to aerobic state. Fe^{3+} ions could form an insoluble iron compound with phosphate ions, and the compound is deposited on the sediment, resulting in a decrease in TFe (Morse 1990; Barry et al. 1994; Burke and Banwart 2002). Therefore, the decrease in PO_4-P with the increasing DO is not only due to the uptake by phytoplankton for photosynthesis but also due to the combination with Fe^{3+} ions, concentration of which increased upon the oxidation of Fe^{2+} ions.

Cases A-1 and A-2 shows the similarities in terms of a rapid increase in DO with fluctuations during the 24 hour-cycle after anoxification recovery, and there are no differences in the peak value of DO and during the time required to reach the peak between these cases. In addition, there are no differences in the species composition of the phytoplankton, dominated by the green algae, as well as the variation of Chl-a as the DO increase between Cases A-1 and A-2. Although the time of recovery from the anoxic state could be advanced by including the green spectrum in LED irradiation, it is considered that the presence or absence of the green spectrum had a little influence on the water quality dynamics as the increase in DO.

3) Water quality dynamics after DO reach its peak value

In both Cases A-1 and A-2, the saturation degree of DO declines from supersaturation to a value lower than 100 % with the fluctuation of 24 hour-cycle after increasing to the peak value. It then reaches a steady state in which the increase and decrease are sinusoidal. In Case A-1, DO shows a steady state within the range of 4.0 mg/L to 8.0 mg/L approximately 10 days after it has reached the peak value. In addition, DO maintains a saturation degree of approximately 60.0 % on average for one cycle after t = 25 d. Meanwhile, DO in Case A-2 decreases, showing a smooth curve from the peak value to the steady state after approximately t = 20 d. Additionally, DO changes within the range of 2.0 mg/L to 5.0 mg/L after about t = 40 d. In Case A-2, DO decreases by approximately 10.0 mg/L from the peak value and reach an equilibrium with a saturation degree of approximately 50.0 % on average for one cycle. Thus, the temporal change in DO in both cases show similar features, reaching a steady state with periodic variations via the decrease from a peak value of approximately 200.0 % to a saturation degree below 100.0 %. In contrast, the differences in both cases could be confirmed as follows: The time required to shift from the peak value to the steady state; the average concentration of 24 hour-

cycle; the amplitude of the sinusoidal variation. In particular, DO in Case A-2 decreases to a poor oxygen level of 2.0 mg/L during putting out the light. Meanwhile, DO in Case A-1 shows a maintained concentration of 4.0 mg/L or more during putting out the light. This difference indicates that Case A-1 shows a higher improvement effect when compared to Case A-2 in terms of the sustained preservation of a healthy DO environment. The factors that caused these differences during the change in DO are considered hereinafter.

Because Chl-a in both cases fluctuate in the range of 20.0 μg/L to 60.0 μg/L and shows an average value of approximately 40.0 μg/L, there is not a big difference in the growth rate of phytoplankton between two cases. DO reaches the sufficient healthy concentration even though adherent algae and filamentous algae do not generate and growth throughout the irradiation experiment period. Therefore, phytoplankton concentration could stably be maintained at a eutrophic level because an interspecific competition with large algae do not occur under LED irradiation of 50–80 μmol/(m^2 s), and the healthy DO environment could be preserved only by phytoplankton photosynthesis. Phytoplankton in Case A-2 is mainly composed of green algae until the end of irradiation experiment. In contrast, in Case A-1, the appearance of blue-green algae in addition to green algae is confirmed as the dominant species when Chl-a increases after t = 50 d. In both cases, NH_4-N and PO_4-P shows low concentrations of 0.20 mg/L and 0.01 mg/L, respectively, and NO_3-N remains almost zero regardless of the change in DO after initiation of LED irradiation. Generally, the observed concentrations of dissolved inorganic nitrogen (DIN) and dissolved inorganic phosphorus (DIP) in eutrophic water areas do not denote the available nutrients for algal photosynthesis, but the remaining nutrients that are not ingested by algae. Therefore, low concentrations of DIN and DIP, regardless of high concentration of Chl-a, involve in the intake by photosynthesis and the supply into water by respiration and mineralization are balanced. That is, the biochemical matter cycle of DIN and DIP shift to an equilibrium state after t = 18 d. This balanced dynamic lead to a stable increase in the DO in both cases, and the oxygen production of phytoplankton is hardly affected by the nutrient limitation arising from the lack of NH_4-N and PO_4-P in both cases. The differences in temporal changes in DO and Chl-a between the two cases seems to be unrelated to the limiting factors (nutrients, water temperature, and underwater light intensity) toward photosynthesis. Therefore, the results not only shows that the photosynthetic rate (the oxygen production rate) in Case A-1 is more promoted when compared to Case A-2 but also that blue-green algae with higher photosynthetic capacity emerged in Case A-1 due to the green spectrum in LED irradiation. Considering this, it is possible to determine the advantage of the green spectrum in phytoplankton photosynthesis.

4) Reduction effects in nitrogen, phosphorous and organic matter

Based on the scheduled observation results shown **in Fig.3.3**, water environmental remediation upon anoxification recovery are examined by focusing on the concentrations of TN, TP, TOC, DOC, and E254 at the end of the LED irradiation experiment. **Table 3.3** shows the comparisons of the final results with the initial concentrations in LED irradiation experiments for Cases A-1 and A-2. In addition, comparisons of the final results between the irradiation and control groups are summarized in **Table 3.3**. By comparing the results between the end and the beginning of LED irradiation for each case, it is possible to evaluate the amounts of nitrogen, phosphorus, and organic carbon which are reduced upon recovery from the anaerobic state to aerobic state. In addition, by referring to the results at the end of Cases A-1 and A-2 along with those of control condition, it is examined how much anoxification recovery inhibited the increase in nitrogen, phosphorus, and organic matter concentrations caused by the elution from sediment due to anaerobic biochemical reactions.

Comparing the results at the beginning and end of LED irradiation experiment, it is found that both TN and TP dramatically decrease after 2 months, regardless of the presence or absence of the green spectrum. TN in Case A-1 finally decreases from initial concentration of 2.03 mg/L to 0.77 mg/L (decrease by 1.26 mg/L). This result indicates that nitrogen concentrations over 1.00 mg/L are reduced through the aerobic matter cycle in which phytoplankton played a leading role. Also, initial concentration of TN in the control condition increases to 2.48 mg/L due to the persistence of anoxic state in the absence of light for 2 months, and the increase is due to the elution of NH_4-N from sediment. Therefore, LED irradiation in Case A-1 blocks the elution of NH_4-N by recovering anoxification, resulting in the reduction of nitrogen concentrations by 0.45 mg/L. In Case A-2, TN concentrations decreases by approximately 60 % when compared to the initial concentration, similar to Case A-1, and there is no difference in the maintenance and reduction of TN between Case A-1 and Case A-2. Also, the initial concentration of TP in Cases A-1 and A-2 decline from 0.30 mg/L to 0.12 mg/L and from 0.31 mg/L to 0.10 mg/L, respectively. LED irradiation with strong light intensity for 2 months is sufficiently effective in reducing TP concentration because phosphorous levels (over 0.10 mg/L) are reduced, and the reduction rate is about 60 % to 70%.

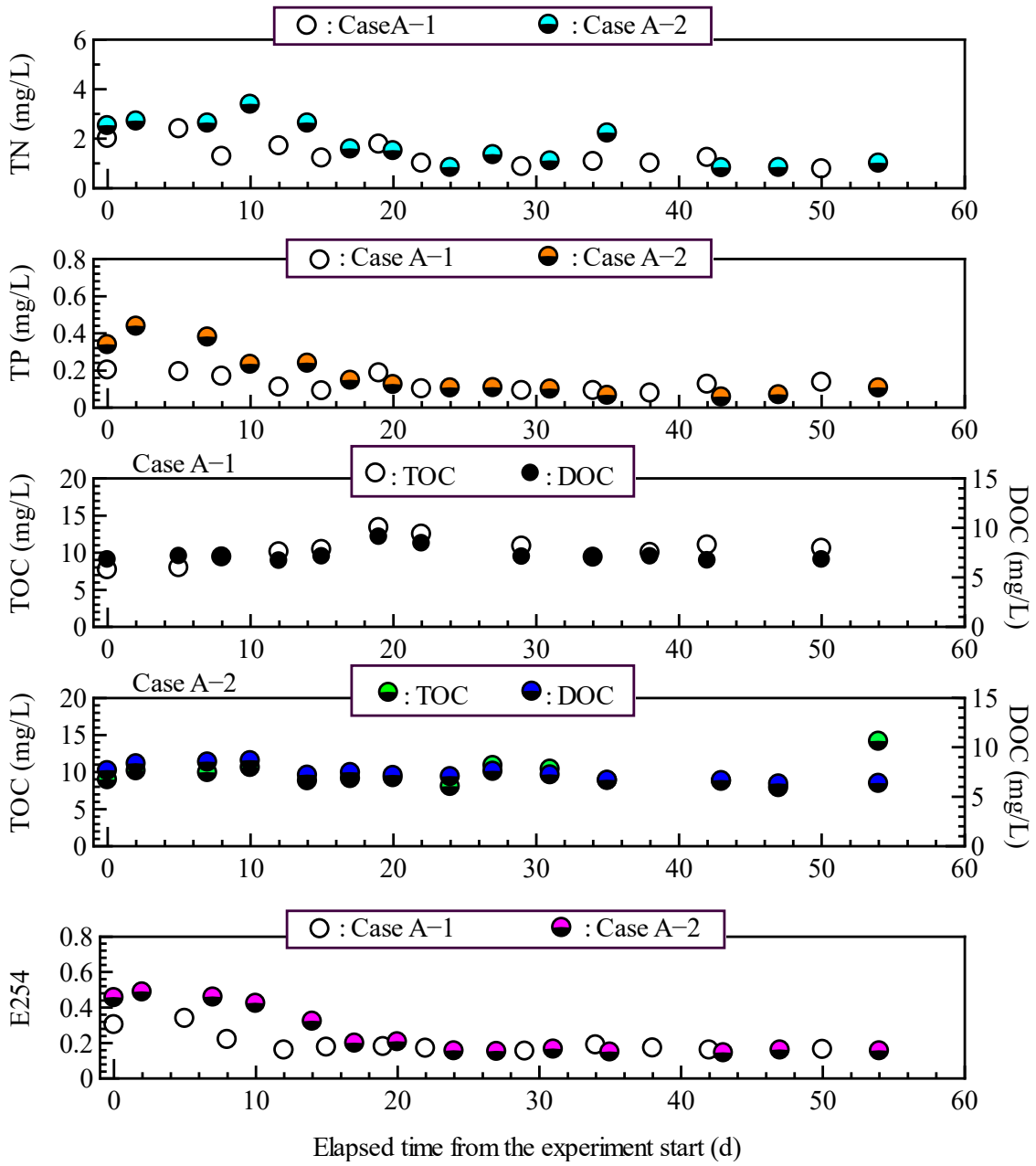

Fig. 3.3 Periodically measured TN, TP, TOC, DOC, and E254 in Cases A-1 and A-2

Table 3.3 Comparisons of the initial and final TN, TP, TOC, DOC, and E254 measurements in the LED irradiation group and the final results under control conditions in Cases A-1 and A-2

Water quality parameters	Case A-1				
	(a) Start	(b) End	(c) Control	(b) /(a)	(b) /(c)
TN (mg/L)	2.03	0.77	2.48	0.38	0.31
TP (mg/L)	0.30	0.12	0.32	0.40	0.38
TOC (mg/L)	7.69	10.50	9.07	1.37	1.16
DOC (mg/L)	6.79	6.79	9.02	1.00	0.75
E254	0.30	0.16	0.41	0.53	0.39

(a) and (b) : the initial and final concentrations in the LED irradiating condition, (c): the final concentrations in the control condition.

Water quality parameters	Case A-2				
	(a) Start	(b) End	(c) Control	(b) /(a)	(b) /(c)
TN (mg/L)	2.52	0.99	3.26	0.39	0.30
TP (mg/L)	0.31	0.10	0.35	0.32	0.29
TOC (mg/L)	8.92	14.10	12.08	1.58	1.17
DOC (mg/L)	7.61	6.34	9.60	0.83	0.66
E254	0.35	0.16	0.44	0.46	0.36

(a) and (b) : the initial and final concentrations in the LED irradiating condition, (c): the final concentrations in the control condition.

Here, TFe drastically decreases from 2.12 mg/L to 0.01 mg/L in Case A-1 and from 3.00 mg/L to 0.01 mg/L in Case A-2 upon LED irradiation for 2 months. As mentioned above, these decreases are mainly caused by the insoluble iron compound where Fe^{3+} was increased via oxidation of Fe^{2+} after anoxification recovery and formed with phosphoric acid. Therefore, the reduction of TP upon LED irradiation is resulted from the inorganic chemical chelate formation, as well as the aerobic matter cycle, through phytoplankton intervention. Meanwhile, TP in the control condition almost do not increase from the initial concentration during 2 months without the elution of PO_4-P from the sediment because iron reduction is terminated in the experimental preparation phase. This result indicates that the anaerobic state causes a switch from iron reduction to sulfate reduction because of continuous and strong reducing state.

Meanwhile, TOC in Cases A-1 and A-2 increases upon LED irradiation for 2 months, unlike TN and TP. The increase in TOC is attributed to an increase in particulate organic matter. That is, phytoplankton grow to the eutrophic level by LED irradiation with strong light intensity, resulting in an increase in particulate organic matter, including zooplankton and withered phytoplankton. However, because the increasing rates are not so high (approximately 1.5), the influence of phytoplankton growth on water quality as an organic pollutant is not extremely high. In addition, there is no significant increase or decrease in the DOC levels in Cases A-1 and A-2. One remarkable result in both cases is a significant decrease in E254 levels. That is, the hardly decomposable component of dissolved organic matter, such as humic acid, can be decomposed under aerobic conditions. According to the results under control condition, E254 levels increases by approximately 1.3 times when compared to the initial value during the 2 months. Meaning that it is possible to restrain the elution of dissolved organic matter from the sediment because of the anoxification recovery and the maintenance of the aerobic state, which means the inhibition of organic pollution derived from the internal load. Therefore, the decrease in E254 levels could be evaluated as a water environmental remediation effect. In both Cases A-1 and A-2, nitrogen and phosphorous concentrations are reduced via the aerobic matter cycle, in which phytoplankton played a leading role. Moreover, the increase in dissolved organic matter estimated as E254 is chemically restrained by the recovery of water and sediment under aerobic conditions. There is no significant difference in the decrease rates of TN, TP, and E254 upon LED irradiation for 2 months between Cases A-1 and A-2. Therefore, the green spectrum hardly affects the water quality-improving effects of long-term irradiation where nitrogen and

phosphorous concentrations are reduced through the aerobic matter cycle. Furthermore, nutrient and E254 levels increases due to anaerobic biochemical reactions inhibited by the aerobic sediment.

3.3.2 Remediation effects under weak light intensity conditions

Under extremely low photon intensity of visible light for phytoplankton photosynthesis, the effects of the green spectrum on water environmental remediation are examined by comparing experimental results between Cases A-3 and A-4. **Figure 3.4** shows the continuously measured DO and ORP under these experimental conditions. As discussed in the previous section, the anoxification recovery effects were examined by referring to the regularly measured results of water quality parameters, such as PO_4-P, TFe, NH_4-N, sulfide, NO_3-N, class-differentiated Chl-a and total Chl-a are summarized in Fig.3.5, according to the temporal change in DO.

1) Water quality dynamics until anoxification recovery

Cases A-3 and A-4 require 18 days and 26 days for DO to start increasing, respectively, and both cases require a longer time to recover from the anoxic state to aerobic state when compared to Cases A-1 and A-2. In particular, ORP in both Cases A-3 and A-4 maintain a strong reducing state of approximately –400.0 mV for 10 days or more days after the initiation of LED irradiation (t < 12 d for Case A-3 and t < 16 d for Case A-4). In addition, the anaerobic decomposition of organic matter proceeded for t < 4 d regardless of LED irradiation because sulfide, PO_4-P and NH_4-N increase when compared to the initial values. This result indicates that the reduced photo-responsiveness of phytoplankton inhibit oxygen production via photosynthesis for t < 4 d. Meanwhile, in both Cases A-3 and A-4, sulfide linearly start to decrease after t = 4 d and reached zero at t = 10 d. Therefore, sulfide seems to disappear due to oxidation between t = 4 d and 10 d. In addition, PO_4-P and NH_4-N tend to decrease after t = 4 d, and these decreases seem to be a result of the nutrient intake by phytoplankton under LED irradiation. The above-mentioned results prove that a slight amount of oxygen is produced by phytoplankton photosynthesis after t = 4 d in both Cases A-3 and A-4. In addition, ORP varies toward zero in the negative range during putting on LED lamp after t =12 d for Case A-3 and after t = 16 d for Case A-4, and the reducing state is temporarily weakened despite DO = 0. Therefore, oxygen production occurs before anoxification recovery. Because the level of oxygen products seems very low due to a low Chl-a concentration of around 5.0 μg/L under weak light intensity; the oxygen is consumed via oxidation reactions of oxidizable

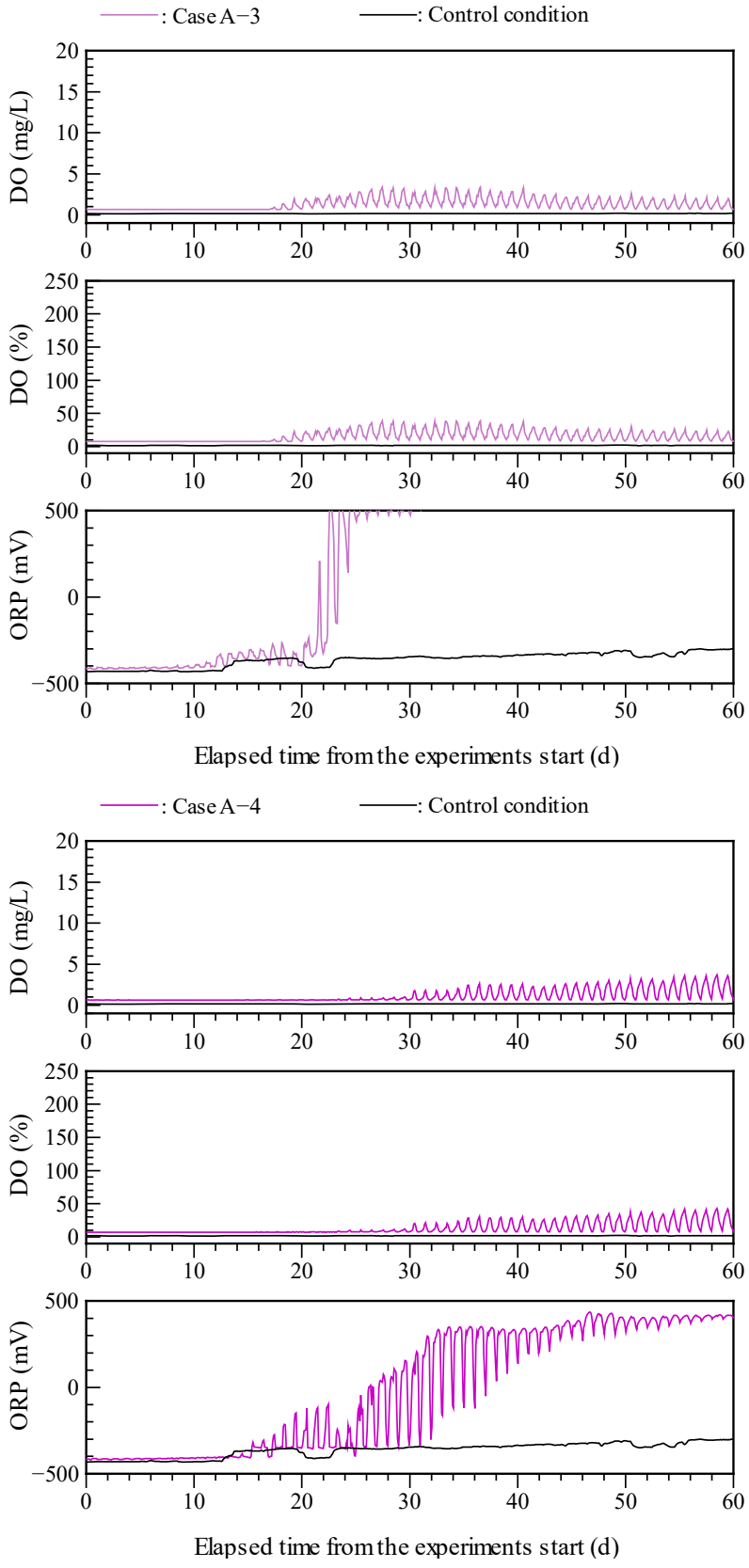

Fig. 3.4 Continuously measured DO and ORP in Cases A-3 and A-4

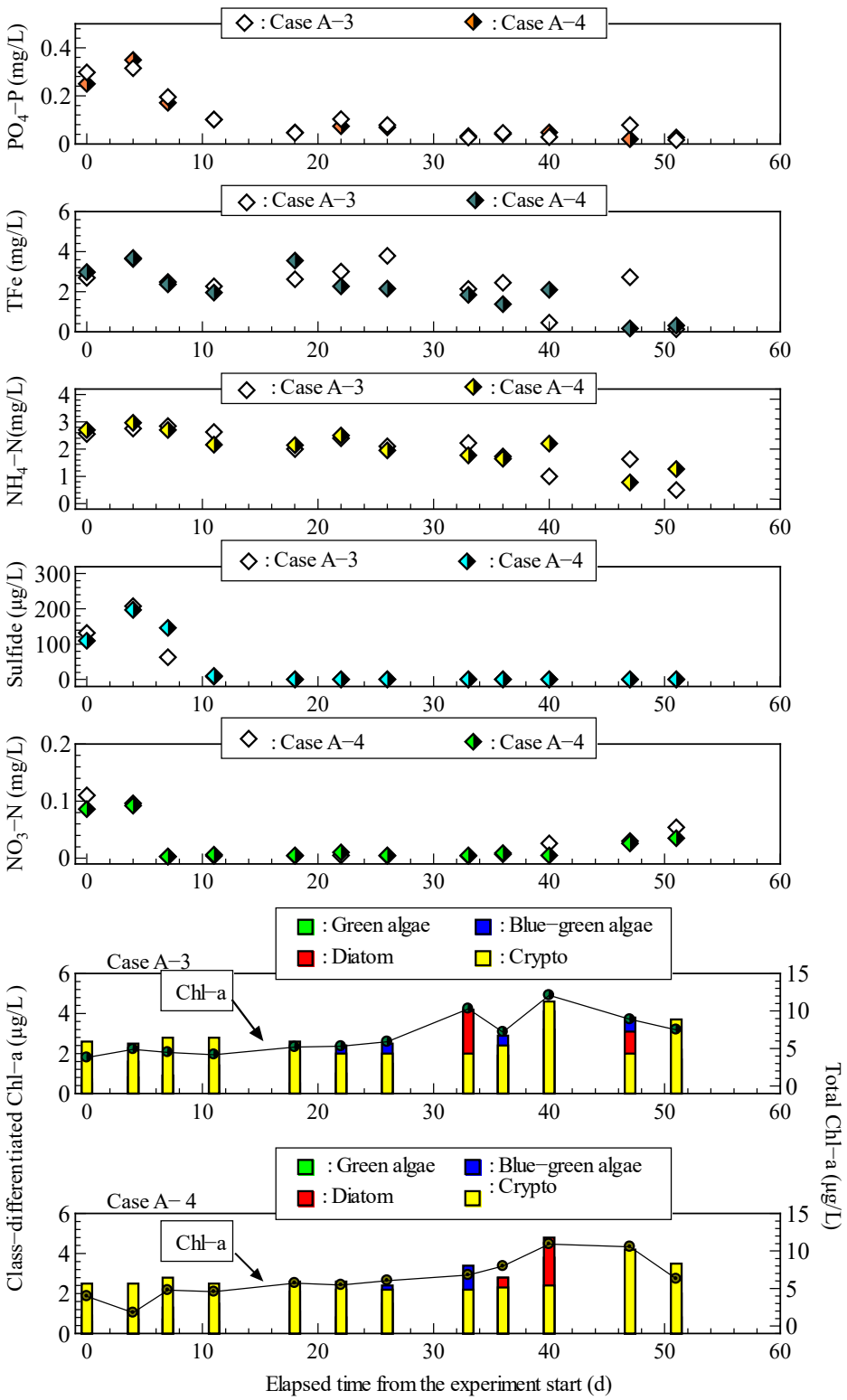

Fig.3.5 Periodically measured PO_4-P, NH_4-N, sulfide, NO_3-N, TFe, class-differentiated Chl-a and Total Chl-a in Case A-3 and A-4

substances in high concentration seem to exceed the oxygen production, resulting in lengthening of anoxic state. From the above, the duration of anoxia under weak light intensity conditions could be divided into two from the viewpoint of the presence or absence of oxygen production by photosynthesis, similar to the strong light conditions in Cases A-1 and A-2.

From the similarities between Cases A-3 and A-4, the time requires to recover from the reduced photo-responsiveness of phytoplankton is not related to the presence or absence of the green spectrum. In addition, considering the results of Cases A-l and A-2, the timing at which oxygen production by photosynthesis began hardly depended on light intensity. That is, the influence of the optical spectrum in LED irradiation on the recovery from the reduced photo-responsiveness of phytoplankton is small. However, Cases A-3 and A-4 shows DO increase at different time points; the recovery from anoxification takes 18 days for Case A-3 and 26 days for Case A-4. That is, the deviation between oxygen production and oxygen consumption differs in Cases A-3 and A-4. Because the temporal changes in TFe and Chl-a until the increase in DO level do not differ between two cases, oxygen consumption via oxidation reactions of oxidizable substances, as well as phytoplankton respiration, seems to be at the same level between Cases A-3 and A-4. In addition, until the increase in DO (t = 4 d to 19 d for Case A-3 and t = 4 d to 29 d for Case A-4), the period where changes in the concentrations of PO_4-P and NH_4-N are observed for Case A-3 are analogous to that for Case A-4. Indicating that the impacts of nutrient limitations on the photosynthesis rate of phytoplankton are the same in both cases. Therefore, it is difficult to regard the nutrient inhibition of PO_4-P and NH_4-N as the reason why the anoxification of Case A-3 could be solved earlier than that of Case A-4. The photon densities of the red and blue spectra in Case A-3, including the green spectrum, are smaller than those in Case A-4 because the total photon density of the visible light region is set to be the same in both cases, as shown in **Table 3.1**. Even though red and blue spectra are considered as the effective optical spectrum for algal photosynthesis, the anoxic state in Case A-3 is recovered earlier than that in Case A-4.

There is no clear difference in the total amount and species composition of phytoplankton during the anoxic state for $t > 4$ d between both cases, where Chl-a are low at approximately 5.0 μg/L and cryptophytes account for about 50 % of the total Chl-a. From the above, it can be concluded that the influence of red and blue spectra on the total amount and species composition of phytoplankton is small, and the green spectrum plays an important role in promoting the photosynthetic rate under the low light intensity of 10.0 μmol/(m^2 s).

2) Temporal changes in DO after anoxification recovery

In Case A-3, DO fluctuates with the 24 hour-cycle after anoxification is solved at t = 18 d, and it shows a maximum concentration of approximately 3.0 mg/L at t = 30 d. After this peak, the DO in Case A-3 reaches a steady state with an amplitude of approximately 2.0 mg/L from t > 50 d onwards via fluctuations within the range less than 3.0 mg/L. This temporal change is similar to that in Cases A-1 and A-2. Meanwhile, the change of DO in Case A-4 shows a periodic variation within 24 hour-cycle from t = 26 d, but it differs from the temporal changes under other experimental conditions because it is unsteady, and the stroke gradually widen until the end of irradiation. Next, we focus on the changes in ORP values. In Case A-3, ORP values from t = 12 d to 25 d change with a wide up and down in the range of negative to positive values according to the increase in DO during switching on the light and the decrease of it during putting out the light. After t = 25 d, ORP maintains a constant value of 500.0 mV, even though DO temporarily decreases to almost zero during putting out the light. Therefore, DO environment seems to be completely recovered from the anaerobic state to aerobic state, and the oxidative condition could be maintained for t > 25 d. Meanwhile, ORP in Case A-4 fluctuates with large amplitude in the range of negative to positive values during t = 29 d to 40 d, and the improvement of ORP from the reducing state to the oxidative state requires a long-term of 40 days. From the above results, it is found that the large differences between Cases A-3 and A-4 could be caused in the improved DO environment by the spectrum conditions of LED irradiation. The reason why there are differences in the anoxification recovery between Cases A-3 and A-4 are described below.

Chl-a concentrations after anoxification recovery (t > 29 d for Case A-3 and t > 40 d for Case A-4) fluctuates within the range of 5.0 μg/L to 10.0 μg/L and are somewhat higher than those when DO start to increase. This result indicates that a small increase in phytoplankton levels could be expected even if the photon flux density is weak, approximately one-fifth lower than the limit of the optimum photon density for photosynthesis. Case A-3 and Case A-4 are similar such that diatom/dinoflagellate and cryptophytes, whose photosynthetic capacities are relatively low, account for about 50 % of the total Chl-a levels, and that green algae levels do not increase dominantly unlike Cases A-1 and A-2 under strong photon conditions. From the measurement of class-differentiated Chl-a concentrations, it is determined that blue-green algae exist with a slight component ratio until the end of irradiation experiments, and their impact on

DO production seem to be small. Therefore, the deficient maintenance of the aerobic state during LED irradiation is mainly due to photosynthesis by cryptophytes and diatom/dinoflagellate. Besides, low production of oxygen is attributed not only to the low concentration of phytoplankton but also to the low photosynthesis rate of diatom/dinoflagellate and cryptophytes. In addition, it is though that the influence of the green spectrum on the growth of phytoplankton is small because there are no big differences in the concentration and species composition of phytoplankton between two cases. However, as mentioned above, the green spectrum has a large impact on the amount of DO production via photosynthesis. Therefore, it could be considered that the difference in oxygen production due to the presence or absence of the green spectrum do not affect the amount and species composition of phytoplankton.

In Cases A-3 and A-4, PO_4-P decrease from about 0.30 mg/L to about 0.04 mg/L between t = 4 d and 18 d, and low concentration of 0.02 mg/L is maintained from t = 30 d. Because there is no obvious decrease in TFe, low PO_4-P concentration is not due to insolubilization by the Fe^{3+} bonding, whereas it was mainly related to the intake by phytoplankton. PO_4-P shows a constant value of 0.02 mg/L after t = 30 d, where the balance between the use via photosynthesis and the supply into water due to respiration and mineralization is maintained, and it is considered that the biochemical dynamic of PO_4-P shifts to the equilibrium state. Therefore, the impact of phosphorus-limitation on phytoplankton photosynthesis do not temporally change after t = 18 d, and we could exclude the influence of PO_4-P from the limiting factors concerning temporal variation of oxygen production. In other words, low PO_4-P concentration do not affect the differences not only in anoxification recovery time but also in the change of DO between Cases A-3 and A-4.

Meanwhile, NH_4-N in both Cases A-3 and A-4 gradually decrease from about 2.50 mg/L to approximately 2.00 mg/L in approximately 40 days after beginning LED irradiation experiments. This result indicates that the nutritious condition for photosynthesis during this period is due to phosphorus-limitation, and that oxygen is produced under a condition such that PO_4-P is more actively consumed by phytoplankton than NH_4-N. Although NH_4-N for Case A-3 remarkably decreases to a low constant concentration of about 0.30 mg/L from the time DO reach a peak concentration at t = 50 d, DO reaches a stationary state represented by a periodic variation less than 2.0 mg/L after t = 50 d. This dynamic seems to be attributed to the balance in the supply and the intake of nutrients. Therefore, it is guessed that the biochemical dynamic of NH_4-N might be shifted to the equilibrium state due to the active uptake of ammonia by phytoplankton since t = 50 d. Meanwhile, NH_4-N in Case A-4 fluctuates in the range of 0.50

mg/L to 1.50 mg/L after t = 50 d, and its biochemical dynamics do not shift to a balanced state, unlike those observed in Case A-3. In Case A-4, the ammonium available for photosynthesis adequately remain in water until the end of LED irradiation experiment, and the biochemical dynamics of NH_4-N do not reach the equilibrium state, resulting in an unsteady state of DO. Therefore, such a difference in the NH_4-N dynamics should have been reflected in the change in DO between Cases A-3 and A-4. From the above, it is determined that the green spectrum promoted the intake of NH_4-N by phytoplankton and accelerated the balanced state of nutrient dynamics; as a result, the unsteady change in DO transform more quickly to a steady state. The advantage of the green spectrum is found out such that the improvement of DO environment appears more quickly. When the results in Case A-4 are compared to those in Case A-3, the stroke of daily variation in DO is eventually large, and its maximum value is approximately 4.0 mg/L. Such a difference seems to be reflected under the optical spectrum conditions in which the photon flux densities of red and blue spectra for Case A-4 are larger than Case A-3.

3) Reduction effects in nitrogen, phosphorous and organic matter

The improvement effects of water environment upon LED irradiation with weak light intensity for 2 months are detected by measuring the decrease in nitrogen, phosphorus, and organic carbon as shown in **Fig.3.6** and **Table 3.4**. **Figure 3.6** shows the scheduled observation of TN, TP, TOC, DOC, and E254 in Cases A-3 and A-4. **Table 3.4** summarizes the comparisons of the final results with the initial concentrations in each case, as well as the comparisons of the final results between the irradiation and control conditions.

The initial concentration of TN in Case A-3 reduces from 2.77 mg/L to 1.09 mg/L. Also, the initial TN concentration of 3.42 mg/L in Case A-4 is finally lowered to 1.90 mg/L. In both cases, high levels in nitrogen are dramatically reduced during 2 months, and the reduction rates under weak light intensity are same as those under strong light intensity. Also, the initial concentration of TP in Cases A-3 and A-4 decrease from 0.33 mg/L to 0.13 mg/L and from 0.30 mg/L to 0.12 mg/L, respectively, and the reduction rates in both cases are about 60 %. The reduction of TP upon the LED irradiation for 2 months is equal to that under strong light intensity for Cases A-1 and A-2. In addition, the final concentrations of TN and TP in Cases A-3 and A-4 are remarkably lower than those in the control group, and it is plausible to expect an inhibitory effect on the increased nutrients concentrations derived from the anaerobic biochemical reactions. Therefore, nitrogen and phosphorous concentrations are reduced due to the aerobic matter cycle in which phytoplankton plays a leading role even though

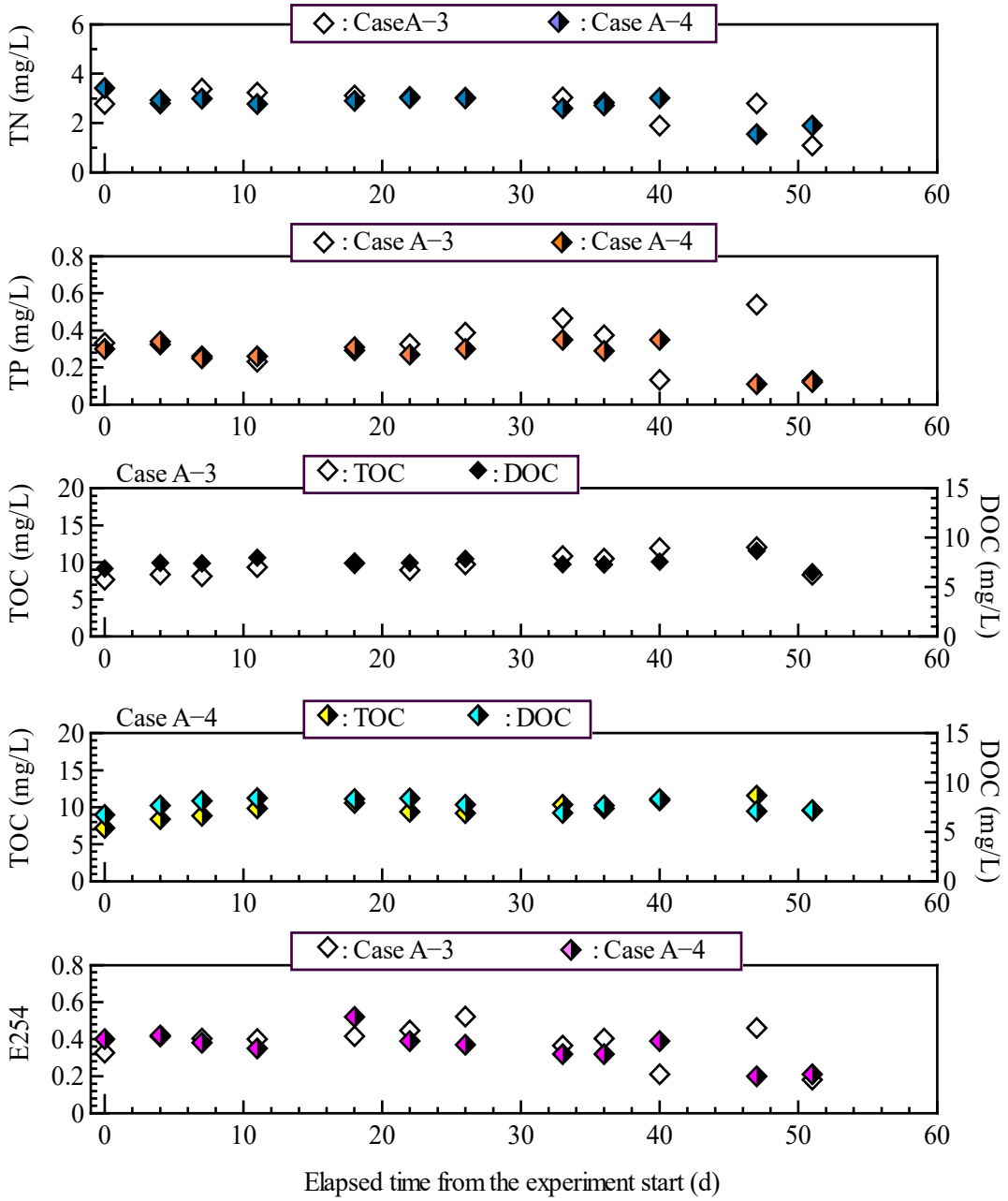

Fig. 3.6 Periodically measured TN, TP, TOC, DOC, and E254 in Cases A-3 and A-4

Table 3.4 Comparisons of the initial and final TN, TP, TOC, DOC, and E254 measurements in the LED irradiation group and the final results under control conditions in Cases A-3 and A-4

Water quality parameters	Case A-3				
	(a) Start	(b) End	(c) Control	(b) /(a)	(b) /(c)
TN (mg/L)	2.77	1.09	3.02	0.39	0.36
TP (mg/L)	0.33	0.13	0.35	0.39	0.41
TOC (mg/L)	7.66	8.34	10.35	1.09	0.81
DOC (mg/L)	6.89	6.49	6.51	0.94	1.00
E254	0.33	0.18	0.68	0.55	0.26

(a) and (b) : the initial and final concentrations in the LED irradiating condition, (c): the final concentrations in the control condition.

Water quality parameters	Case A-4				
	(a) Start	(b) End	(c) Control	(b) /(a)	(b) /(c)
TN (mg/L)	3.42	1.90	3.02	0.56	0.63
TP (mg/L)	0.30	0.12	0.35	0.40	0.38
TOC (mg/L)	7.22	9.55	10.35	1.32	0.92
DOC (mg/L)	6.74	7.20	6.51	1.07	1.11
E254	0.37	0.21	0.68	0.57	0.31

(a) and (b) : the initial and final concentrations in the LED irradiating condition, (c): the final concentrations in the control condition.

the oxygen production is strongly restricted due to the approximately one-fifth lower limit of the optimum photon intensity for photosynthesis. Because there is no unequivocal difference in the reduction rates of TN and TP concentrations between Cases A-3 and A-4, the green spectrum hardly affects water environmental remediation in terms of nitrogen and phosphorous levels. The significant decreases in TOC and DOC concentrations between the start and end of LED irradiation for 2 months could not be observed, unlike nitrogen and phosphorous concentrations.

TOC concentration in both Cases A-3 and A-4 slightly increase from the initial values compared to the results of Cases A-1 and A-2. Such a slight increase is attributed to insufficient reproduction of phytoplankton under light limitation for photosynthesis, unlike under strong light intensity conditions. In addition, similar to Cases A-1 and A-2, DOC levels at the beginning and the end of LED irradiation for 2 months show the same concentration. However, E254 levels in both Cases A-3 and A-4 obviously decline upon LED irradiation for 2 months, similar to Case A-1 and A-2. The final value of E254 levels under control conditions obviously increase by a factor of approximately two from the initial value, whereas E254 levels at the end of the LED irradiation experiment in both Cases A-3 and A-4 decreased by approximately 50 % in 2 months. This result means that LED irradiation with weak light intensity could effectively restrain the increase in the concentrations of dissolved organic matter, which is due to elution from the sediment under anaerobic conditions, regardless of the presence or absence of the green spectrum. In addition, E254 levels are reduced as a result of the aerobic decomposition of hardly decomposable dissolved organic matter, even though it takes a long time to recover anoxification and DO temporally changes in the low level less than 3.0 mg/L.

3.4 Conclusions

In this chapter, the impacts of optical spectrum and LED light intensity on the maintenance of healthy aerobic conditions are evaluated on beaker-scale experiments. In particular, this chapter focuses on the effectiveness of increasing the optimum spectra for photosynthesis by adding the green spectrum to two-color spectrum (red and blue). The knowledge and outcomes acquires by beaker-scale experiments can be summarized as follows from four viewpoints.

The photo-responsiveness and photosynthesis rate of phytoplankton could be enhanced in the presence of the green spectrum regardless of light intensity, and the anoxic state could be quickly recovered. In particular, LED irradiation with the three-color mixed RGB spectra

played an important role in promoting oxygen production when compared to mixed light of red and blue spectra under low light intensity.

Under high intensity light, DO rapidly increases to supersaturation after anoxification recovery due to the growth of green algae possessing high photosynthetic capacity regardless of the green spectrum. However, LED irradiation, including the green color band, has an advantage such that the healthy DO environment is preserved without a decrease to poor oxygen levels in the absence of light

Under the weak light intensity that is as low as a tenth of the optimum light quantum for photosynthesis, it takes a long period for anoxification recovery. In LED irradiation with RGB spectrum, the supply and intake of NH_4-N and PO_4-P for phytoplankton shift to an equilibrium state after anoxification recovery, resulting in the maintenance of the aerobic state without lowering the ORP to a reducing state in the absence of light unlike mixed light of red and blue spectra.

The water environmental remediation by solving the long-term anoxification under both strong and weak light intensity conditions are reflected in decreased TN and TP upon LED irradiation for 2 months regardless of the green spectrum. These results indicate the reduction of DIN and DIP through the aerobic matter cycle, in which phytoplankton plays a leading role. In particular, phosphate formed a particulate inorganic chemical chelate with ferric ions generated by the oxidation of ferrous ions after recovering the anaerobic condition, resulting in the reduction of TP. In addition, water environmental remediation by recovery formed anaerobic state to aerobic includes the inhibition of PO_4-P and NH_4-N elution from the sediment.

Chapter 4 Influence of RGB Spectra and Initial Anaerobic Conditions on Water Environmental Remediation by Water Tank-scale Experiments

4.1 Introduction

As determined from the results of Cases A-1 and A-2 in the beaker-scale experiments, LED irradiation of anoxic water is sufficiently effective for water environmental remediation under strong light intensity conditions, such that the photon quantity of LED irradiation is in the optimum intensity range for phytoplankton photosynthesis. In particular, LED irradiation, which includes three-color mixed RGB spectra, exhibits a satisfactory effect in improving water quality in the early recovery from anoxification. Therefore, it is key to assess the recovery effects from long-term anoxic state at positions far from a light source, such that the photon emitted from LED source is weaker than the optimum intensity for photosynthesis. In addition, one of the most significant outcomes of beaker-scale experiments is the result obtained by comparing the temporal change in DO between Cases A-3 and A-4. That is, mixed RGB irradiations have advantages such as, faster improvement in the DO environment and better maintenance of a healthy DO level than two-color red and blue spectrum. Therefore, to design optimal conditions for the optical spectrum in LED irradiation, quantitatively evaluating the anoxification recovery effect is necessary by understanding the influence of LED irradiation on the promotion of phytoplankton photosynthesis under each of RGB irradiation spectra. Moreover, the anoxification recovery effect and the maintenance of a healthy DO level would be determined by promoting the oxygen production via phytoplankton photosynthesis exceed oxygen consumption via the oxidation reactions of oxidizable substances present in high concentration. That is, the increases in nutrients and oxidizable substances stemming from anaerobic decomposition processes in the anoxic state would strongly influence the effects of water environmental remediation by LED irradiation. Therefore, it is an important topic to evaluate influences of low photon intensity on the biochemical dynamic of DO considering the initial anaerobic conditions which would characterize concentrations of water quality parameters at the beginning of LED irradiation.

In this chapter, the effectiveness of water environmental remediation by underwater LED irradiation in anoxic water is experimentally examined from three viewpoints. First, the influence of each RGB spectrum on maintaining a healthy DO level is examined as the first series according to the single-color irradiations, which are sufficient for phytoplankton photosynthesis despite their marginal light intensity. Next, mixed RGB irradiation experiments are

conducted as the second series under the condition of weak light intensity which corresponded to a point far from the light source to evaluate the effective irradiation range for water environmental remediation, not only limited range in the vicinity of light source. Finally, the influences of initial anaerobic conditions on the anoxification recovery are examined as the third series under mixed RGB irradiation having extremely low photon intensity when compared to the optimal photon intensity requires for photosynthesis. In this chapter, the reliability of the experimental results is enhanced by scaling up from beakers to water tank. That is, LED irradiation experiments are conducted in cylindrical water tanks, which represented the hypolimnion of an organically polluted water body, under a higher experimental precision when compared to beaker-scale experiments. In all series, the impacts of experimental conditions on the water environmental remediation effects are examined considering the time required to increase DO, time required to recover from the anoxic state, and characteristics of temporal changes in water quality parameters, such as DO, Chl-a, DIN, and DIP, after recovering from anoxification. The outcomes in this chapter might provide essential knowledge for discussing the effectiveness of water environmental remediation when underwater LED irradiation to conserve and restore the aquatic environment is applied in actual organically polluted water areas.

4.2 Effects of single-color irradiation on water environmental remediation

4.2.1 Experimental conditions

In the first series, anoxic water with a strong reductive potential and subjected to long periods of anoxification is irradiated with each single-color wavelength of red, blue, or green spectrum. Here, the optimum photon flux density for phytoplankton photosynthesis is 50–180 μmol/(m^2 s) (Minato et al. 2012). Therefore, this series, supplied with photon intensity that is marginally sufficient and would not strongly restrict photosynthesis, aim to determine the effects of single-color irradiation on the growth of phytoplankton, fluctuations in DO, and recovery from long-term anoxification. The first series of experiment includes LED irradiation experiments with three water tanks label as Case B-1 (red spectrum), Case B-2 (green spectrum), and Case B-3 (blue spectrum). The photon intensity in each single-color spectrum is adjusted to approximately 40–50 μmol/(m^2 s) as the optical condition, such that phytoplankton photosynthesis would not be strongly inhibited by limited light. The irradiation experiments start almost two months after the anoxic water sample is prepared. The experimental conditions regarding the optical spectrum and intensity of LED irradiation of the first series are summarized in **Table 4.1**.

Table 4.1 Optical spectrum and intensity of LED irradiation in the first series

Case	Color	Visible light (360 nm~780 nm) μmol/(m^2 s)	Blue band (435 nm~480 nm) μmol/(m^2 s)	Green band (500 nm~570 nm) μmol/(m^2 s)	Red band (610 nm~710 nm) μmol/(m^2 s)
B-1	R	46.10	0.39	0.51	45.2
B-2	G	45.61	0.79	44.37	0.45
B-3	B	42.84	42.43	0.25	0.16

Table 4.2 Initial conditions of main water quality parameters associated with the anaerobic state in the first series

Case	DO (mg/L)	Chl-a (μg/L)	Sulfide (μg/L)	NH_4-N (mg/L)	PO_4-P (mg/L)	NO_3-N (mg/L)	TFe (mg/L)
B-1	0.13	0.17	380.5	1.23	0.279	0.004	1.23
B-2	0.08	0.08	307.0	1.04	0.248	0.002	0.94
B-3	0.19	0.09	237.5	0.97	0.176	0.005	0.63

The initial water quality in the first series is determined by long-term anoxification and is characterized as following the anaerobic biochemical reactions under a strongly reductive state. NO_3-N is almost absent due to denitrification, which occurs as the first reaction in cascade anaerobic decompositions of organic matter. Fe^{2+} would be eluted from the bottom sediment because of iron reduction under anaerobic conditions, consequently, increasing TFe. Additionally, iron reduction would increase PO_4-P due to the release of PO_4^{3-} from an insoluble Fe compound with Fe^{3+} deposited in the sediment. In addition, sulfate reduction would occur under a stronger reductive state, resulting in a high concentration of sulfide in the anoxic water. Moreover, NH_4-N concentration would be relatively high due to the isolation of ammonium ions from organic matter accompanying catabolism by anaerobic microbes. Therefore, the initial anaerobic conditions in the first series are summarized in **Tables 4.2** as those with high concentrations of oxidizable substances and nutrients under a strong reductive potential.

4.2.2 Results and discussion

The influences of single-color irradiation (red, green, and blue spectra) having marginally sufficient photon intensity on water environmental remediation are estimated from viewpoints of anoxification recovery, maintenance of a healthy DO level, and reductions of nitrogen, phosphorous, and organic matter. **Figure 4.1** shows the results of continuously monitored DO concentration in Case B-1 (red spectrum), Case B-2 (green spectrum), and Case B-3 (blue spectrum). **Figures 4.2** and **4.3** illustrate the scheduled measurements results of PO_4-P, TFe, NH_4-N, sulfide, NO_3-N, Chl-a, TN, TP, TOC, DOC, and E254 in the first series. In the following, t denotes the elapsed time from the start of the LED irradiation experiment.

1) Dynamics of water quality until anoxification recovery

The anoxic states of DO = 0 are maintained for $t < 14$ d in Case B-1, $t < 16$ d in Case B-2, and $t < 12$ d in Case B-3 without an increase in DO immediately after initiating the LED irradiation. According to mixed RGB irradiation experiments on beaker-scale, the reasons for the time lag between beginning the LED irradiation experiments and increasing DO concentration are explained by mainly referring to the continuously measurement results of ORP as follows. First, oxygen production by photosynthesis is prevented because the reduced photo-responsiveness of phytoplankton originated from long-term absence of light, until the start of the LED irradiation experiments; consequently, the anoxic state continued despite LED irradiation with marginally sufficient light intensity. Second, although minimal DO is produced by phytoplankton photosynthesis, many oxidative substances consume more oxygen

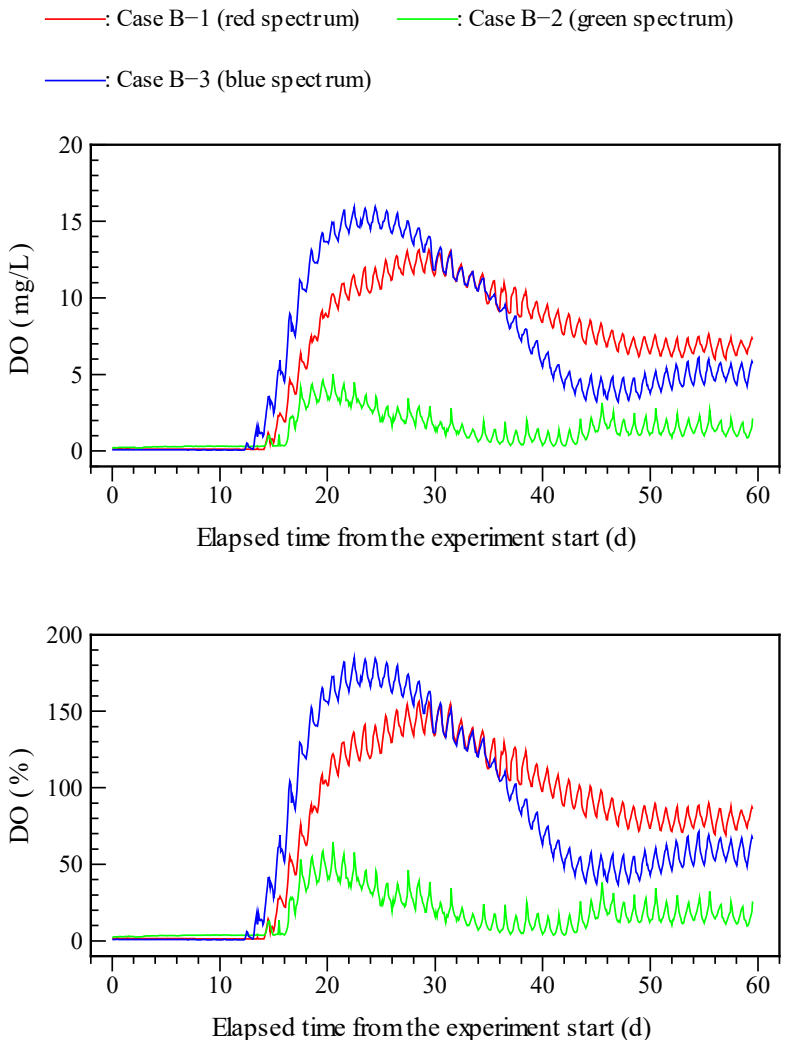

Fig.4.1 Continuously monitored DO concentration and saturation in Case B-1 (red spectrum), Case B-2 (green spectrum), and Case B-3 (blue spectrum)

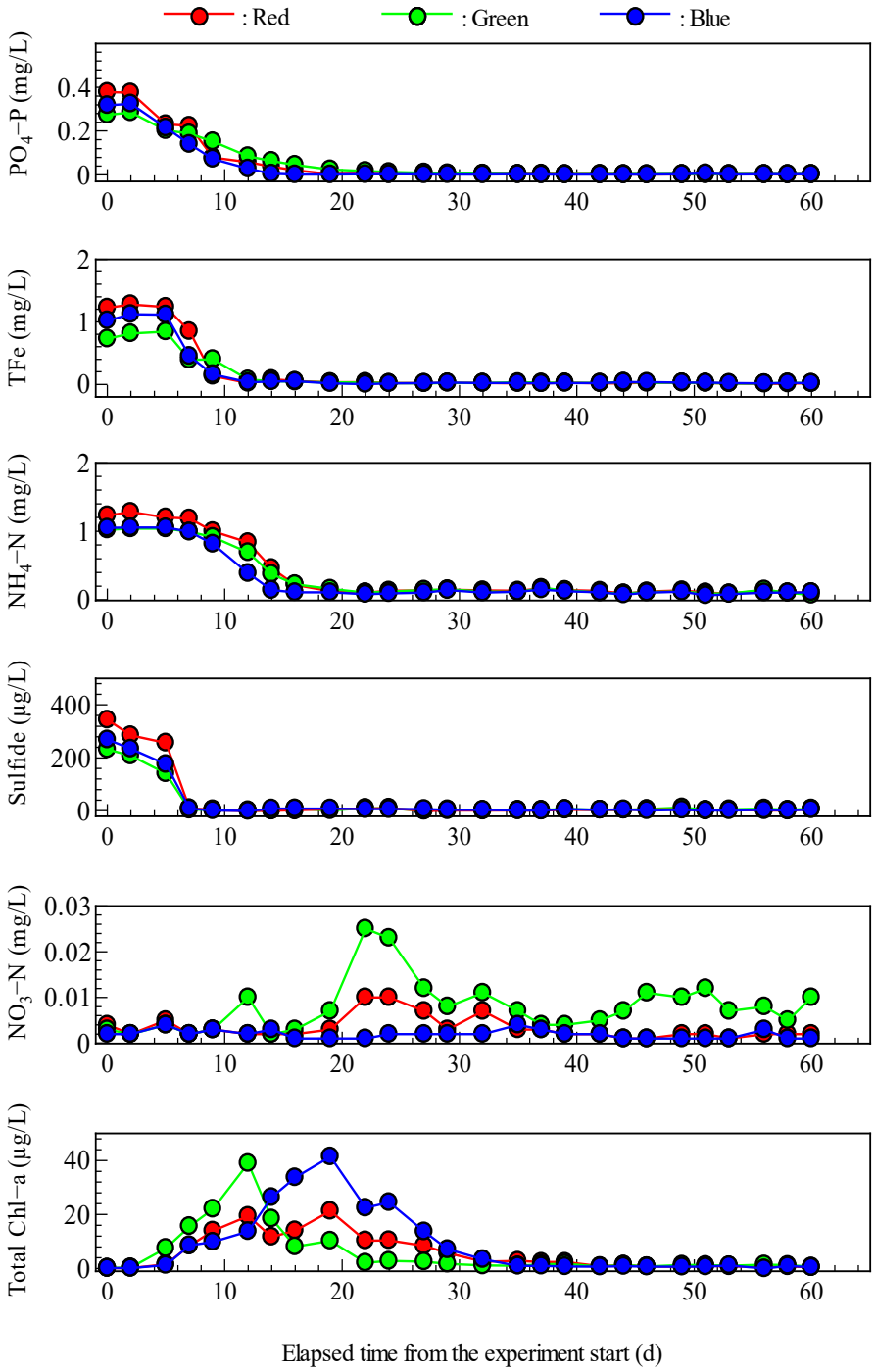

Fig.4.2 Scheduled measurements results of PO_4-P, TFe, NH_4-N, sulfide, NO_3-N and Total Chl-a in Case B-1 to Case B-3

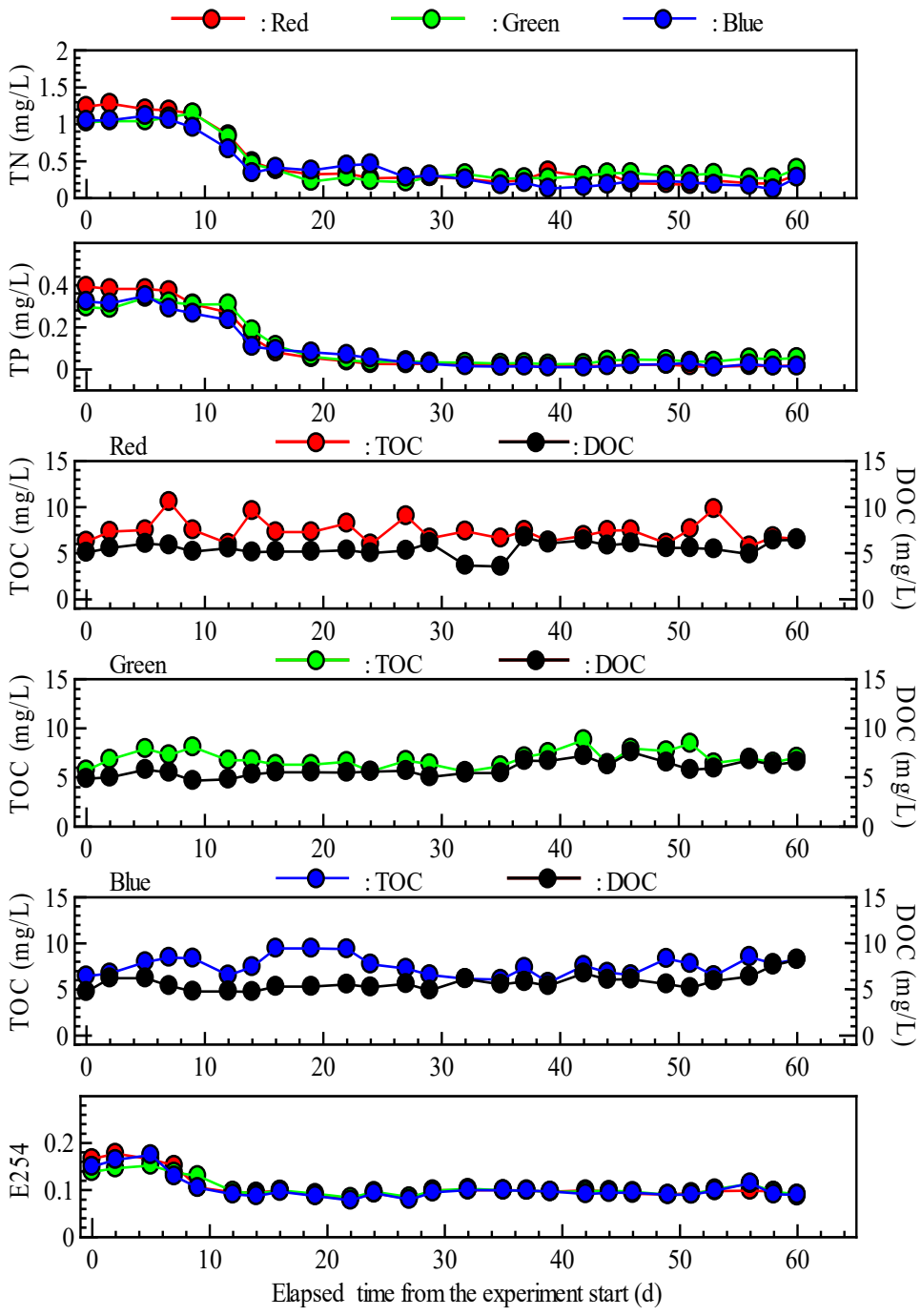

Fig.4.3 Scheduled measured results of TN, TP, TOC, DOC, and E254 in the first series

than the amount supplied; therefore, the anoxic state could not be recovered. Based on these perceptions, anoxic durations, as shown in **Fig.4.1**, are divided from the viewpoint of the presence or absence of oxygen produced by photosynthesis. Because data concerning ORP are absent, the anoxic state is considered via biochemical dynamics of oxidative substances using the scheduled measured results of sulfide and TFe contents.

In all cases, sulfide shows a decreasing trend immediately after LED irradiations began, and it rapidly decreases from a high concentration of over 150 μg/L to nearly zero in a relatively short period from t = 8 d to 10 d. Generally, sulfide decreases in the absence of oxygen due to combination with metal ions, as hydrogen sulfide becomes an insoluble metallic sulfide. Because sulfide is maintained at a high concentration of over 150 μg/L for almost one week after irradiation commenced, the gradual decrease in sulfide for t < 8 d is not because of an oxidation reaction but because of the presence of insoluble metallic sulfide (Henneberry et al. 2012; Omoregie et al. 2013). However, the abrupt disappearance of sulfide at t = 10 d denotes the oxidation of sulfide to sulfate ions; additionally, oxygen is confirmed to exist from t = 8 d to 10 d and is later consumed for oxidation. That is, a temporal boundary between the absence and presence of oxygen production is represented by t = 8 d to 10 d in all cases.

The assumption concerning oxygen production based on the sulfide concentration is supported by the TFe and PO_4-P results under the anoxic states of DO = 0. Here, an increase in TFe accompanying an increase in PO_4^{3-} under DO = 0 implies that iron ions are supplied with PO_4^{3-} into water as Fe^{2+} is released from ferric phosphate ($FePO_4$) by the reduction of trivalent iron. Conversely, a decrease in TFe accompanying a decrease in PO_4^{3-} implies that Fe^{3+} disappeared in the form of suspended small particles because it can form an insoluble iron compound with PO_4^{3-}. Particularly, when oxygen is exposed to the anoxic water containing Fe^{2+}, TFe reduced along with PO_4^{3-} because Fe^{3+} is generated instantly by the oxidation of Fe^{2+} easily formed $FePO_4$ by combining with PO_4^{3-}. According to **Fig.4.2**, TFe content shows a gradual increasing trend, followed by a sharp declining trend at t = 8 d, and is finally low to zero at t = 15 d. Additionally, PO_4-P content declines after peaking at t = 2 d. Therefore, in all cases of the first series, oxygen production by phytoplankton photosynthesis is proved to occur at t = 8 d. That is, the reduced photo-responsiveness of phytoplankton inhibits oxygen production via photosynthesis at t < 8 d, regardless of single-color irradiation, consequently, resulting in a continuous anoxic state as iron reduction progressed. Moreover, although oxygen production occur since t > 8 d, oxygen consumption via the oxidation reactions of oxidizable substances present in high concentration exceed the oxygen production, resulting in the lengthening of the anoxic

state despite LED irradiation. The time required to recover from anoxification depend on the amount of oxidizable substances and the oxygen production rate. According to **Fig.4.2**, the peak concentrations of sulfide and TFe in Case B-2 are less than those observed in other cases, while the anoxification recovery requires more time. Therefore, the oxygen production rate in Case B-2 is the lowest during single-color RGB irradiation. Furthermore, the time requires for TFe concentration to shift from the peak to zero is less in Case B-1 than in Case B-3, but the initial TFe concentration in Case B-1 is higher than that in Case B-3. Therefore, the time lag for the disappearance of oxidizable substances due to oxidation between Case B-1 and Case B-3 is because of the difference in their initial concentrations; thus, difference in the decreasing rate of TFe from the peak at t = 8 d between Case B-1 and Case B-3 is marginal. Therefore, the oxygen production rate between both cases do not majorly differ although the time requires to recover from anoxification in Case B-1 (14 d) is longer than that in Case B-3 (12 d).

The following conclusions can be drawn: 1) The time required to recover from the reduced photo responsiveness of phytoplankton do not differ among red, green, and blue spectra. 2) The time required for anoxification recovery by LED irradiation with the green spectrum is more because of low photosynthesis rate than red and blue spectra. 3) The time required for anoxification recovery between red and blue spectra is not different.

2) Dynamics of water quality after anoxification recovery

In all cases of the first series, DO concentrations change gradually during the 24-hour cycle according to the illumination of 12 hour-light on and 12 hour-light off after anoxification recovery. Additionally, the DO concentration initially reaches a peak, gradually decreases, and finally reaches a steady state. However, the three cases differ in the DO concentrations at the peak and steady state, and the time required to reach the peak value and steady state. These differences are reflected by the single-color irradiation spectrum. Subsequently, the influence of the single-color irradiation on maintaining a healthy DO level is examined from the viewpoints of the biochemical dynamics of Chl-a, DIN, and DIP. In Cases B-1 and B-3, DO concentration quickly exceed the lower limit (4 mg/L) to a healthy level after anoxification recovery, while in Case B-2, poor oxygen levels are observed (DO < 4 mg/L). These results indicates that water quality dynamics in Case B-2 evidently differs from those in the other two cases.

Here, results of Case B-1 and Case B-3 have been initially explained, after which the results of Case B-2 have been examined by comparing with the other two cases. In both Case B-1 and Case B-3, DO concentration increases from a low level approximately 2 d after the

anoxification recovery. Subsequently, the DO concentration linearly increases to a higher concentration than the saturation state (Case B-1: 150% at t = 26 d, and Case B-3: 180 % at t = 23 d). Moreover, the temporal changes in DO concentration in both cases shift to a steady state after t = 49 d, with a temporary decrease observe from t = 27 d to 47 d. However, the decreasing rate in the DO concentration from the peak to the steady state differs between Case B-1 and Case B-3. The DO concentration in Case B-1 decreases from the peak value with a decreasing amount of approximately 5 mg/L, and reaches the steady state, wherein the concentration ranged from 6 mg/L to 8 mg/L after the 24-hour illumination cycle. Moreover, DO concentration in Case B-3 reduces greatly by 11 mg/ L and shifts to the steady state, where it periodically changes from 4 mg/L to 6 mg/L during the 24-hour cycle. In both cases, DO concentration, with a saturation rate exceeding 100 %, is recovered from an anoxic state in the early period, after which a healthy DO level is finally maintained at a saturation rate of 60–80 %. These results prove that both red and blue irradiations are extremely effective to properly manage DO level to sustain aquatic life. However, the peak DO concentration in Case B-3 is higher than that in Case B-1, while DO concentration in the steady state in Case B-1 is higher than that in Case B-3. The similarities and differences between Case B-1 and B-3 as discussed previously are examined by referring to the temporal changes in the Chl-a, NO_3-N, NH_4-N, and PO_4-P contents.

Chl-a concentration in Case B-1 linearly increases at a gradient of 2.0 μg/(L d) from t = 5 d to 15 d. Further, it decreases linearly decreasing after t = 26 d and is maintained at a low level (< 1.0 μg/L) since t = 43 d. DO concentration peaked from t = 5 d to 15 d when Chl-a changes from 10 μg/L to 20 μg/L. In Case B-3, Chl-a increases linearly at the gradient of 2.4 μg/(L d) since t = 6 d, and reaches a maximum concentration (approximately 40 μg/L) at t = 22 d when DO concentration also reaches a peak value. Subsequently, Chl-a concentration sharply decreases and reaches a low level (<1.0 μg/L) since t = 36 d. Until Chl-a concentration reaches a peak value, Case B-1 and Case B-3 do not differ in the increase rate of Chl-a, and in both cases, the minimum Chl-a concentrations are less than 1.0 μg/L after reaching the peak. However, the peak Chl-a concentration in Case B-3 is almost twice as high as that in Case B-1 and unlike Case B-1, the Chl-a concentration in Case B-3 declines abruptly from the peak level to a low level without reaching a steady state. Such differences in the temporal changes in the Chl-a concentration indicate an increase in DO. First, in Case B-3, the higher Chl-a concentration at the peak is linked to the increased oxygen production, resulting in a temporary increase of DO to a maximum concentration with an oversaturation of approximately 180 %. Second, in Case B-1, DO concentration remains at a peak value for a longer duration than in Case B-3

because Chl-a concentration is relatively high (10 μg/L to 20 μg/L) for 10 d.

Light, water temperature, and nutrients are important limitation factors for phytoplankton photosynthesis (Staehr and Sand-Jensen 2006; Edwards et al. 2016; Marzetz et al. 2020). As light and water temperature are constantly controlled during the LED irradiation experiments, the temporal changes in DO and Chl-a (**Figs.4.1** and **4.2**) directly indicate the impacts of DIN and DIP on photosynthesis. In the first series, LED irradiation experiments start from the initial condition of extremely high concentrations of both NH_4-N and PO_4-P and an extremely low amount of NO_3-N. Therefore, high NH_4-N and PO_4-P concentrations serving as main nutrients for algal growth affect the temporal changes in Chl-a concentration from t = 5 d to 25 d in Case B-1 and from t = 6 d to 20 d in Case B-3. In both cases, NH_4-N began to decline at t = 10 d and reaches a low level (< 0.1 mg/L) at the almost same elapsed time (t = 22 d for Case B-1 and t = 19 d for Case B-3). Moreover, in both Case B-1 and Case B-3, PO_4-P began to decrease at t = 5 d and reaches approximately zero at t = 19–20 d. The reductions in the NH_4-N and PO_4-P concentrations when Chl-a concentration increases, indicate that these nutrients are utilized for phytoplankton photosynthesis. Here, the nutritional status for t < 22 d is determined as the strong nitrogen-control state because the N/P ratios calculated using the TN and TP results are less than 5.0. Therefore, most NH_4-N is utilized as nutrients by phytoplankton. Moreover, an extremely small volume of PO_4-P is utilized for photosynthesis, of which most decreases because of the formation of insoluble iron compound with Fe^{3+}. In addition, NO_3-N in both cases, is almost zero during the irradiation experiments although it slightly increases to 0.01 mg/L in Case B-1 during t = 24 d to 29 d, indicating that NO_3-N supplied by aerobic decomposition of organic matter after the anoxification recovery is completely used for photosynthesis. Therefore, there are no remaining nutrients after the Chl-a peak, implying that the nutrient utilization during photosynthesis and nutrient supply into the water are balanced by respiration and mineralization. In addition, the N/P ratio in both cases exceeded 10.0 after the DO peak and showed average values of 14.1 and 12.3 for Case B-1 and Case B-3, respectively, since t = 28 d. Thus, the initial state controlled strongly by nitrogen could shift to a well-balanced state including nitrogen and phosphorous for phytoplankton via LED irradiation. This indicates that the nitrogen and phosphorous cycles among planktons, organic substances, and nutrients shifts to an equilibrium state after the anoxification recovery, regardless of red and blue spectra irradiation, consequently, preserving the aerobic water environment.

The experimental results of Case B-1 and Case B-3 have been summarized here. Com-

pared with red spectrum irradiation, blue spectrum irradiation activated photosynthesis and promoted phytoplankton growth more effectively. Consequently, DO concentration under the blue irradiation reaches a highly oversaturated state early. Until DO concentration is oversaturated under both red and blue spectra irradiations, the remaining nutrients available for photosynthesis are not balanced with the proportion of living phytoplankton in water, because phytoplankton rapidly consumes large amounts of DIN and DIP. Thus, a lack in the nutrient amount (particularly DIN) inhibits oxygen production via photosynthesis, which is more evident under the blue spectrum irradiation. However, when considering the temporal changes in DO concentration of over one month, a healthy DO level could be maintained via equilibrium between the nitrogen and phosphorous cycles among planktons, organic substances, and nutrients, regardless of red and blue spectra irradiations. Therefore, both spectra irradiations have the same advantages in preserving the aerobic water environment without increasing the amount of phytoplankton.

Furthermore, DO concentration in Case B-2 start to increase at the approximately-same time as in the other two cases and peak at t = 18 d, which is earlier than that in the other two cases. Additionally, Chl-a linearly increases at a gradient of 2.8 μg/(L d) from t = 4 d and peaked at 40 μg/L at t = 12 d. Similar results are observed in Case B-3. In addition, NH_4-N and PO_4-P concentrations remarkably declined from t = 8 d to t = 15 d. Because the initial nutritional status of phytoplankton in Case B-2 is strongly controlled by nitrogen, similar to the other two cases, phytoplankton growth and increase in Chl-a depend on the initial high NH_4-N concentration (approximately 1.0 mg/L), consequently, increasing DO concentration. Although the initial NH_4-N concentration and peak Chl-a concentration in Case B-2 are as high as those in Case B-3, the peak DO concentration in Case B-2 is at a lower level (4 mg/L) than in the other two cases. Therefore, the oxygen production rate under the green spectrum irradiation is extremely lower than that under red and blue spectra irradiations. Moreover, after a peak concentration, DO in Case B-2 gradually decreases from t = 22 d, and then reaches a steady state during the 24-hour cycle, with minimum DO concentration (1 mg/L) in the dark period and maximum concentration (3 mg/L) in the light period since t = 44 d. This implies that the green spectrum irradiation could not sufficiently sustain a healthy DO level although the anoxic state improves.

In Case B-2, although NH_4-N decreases to 0.1 mg/L and PO_4-P decreases to nearly zero after DO concentration peak, the N/P ratio exhibited small values ranging from 3 to 8 until the irradiation experiment ended. This indicates that the nutritional status of phytoplankton is re-

tained in the strong nitrogen-control state (Diatta et al. 2020), unlike Cases B-1 and B-3. Moreover, NO_3-N in Case B-2 is in the range of 0.01 mg/L to 0.03 mg/L after the anoxification recovery. Only a little NO_3-N remained in water, which is not utilized by phytoplankton for photosynthesis, unlike in the other two cases. Therefore, Case B-2 do not show a uniform utilization of DIN and DIP for photosynthesis and a balance between nutrient uptake by photosynthesis and their supply into water via aerobic decomposition of organic matter. The results indicate that the impacts of the green spectrum on oxygen production efficiency and promoting effect of photosynthesis were extremely low when compared to those of red and blue spectra, and consequently, healthy DO levels are not maintained. Thus, regarding the relation between DO and nutrients after anoxification recovery, the biochemical dynamics of phytoplankton, DIN, and DIP reaches an equilibrium state using red and blue spectra LED irradiation. Consequently, a healthy DO level could be preserved even at low Chl-a concentration (< 1 μg/L), without promoting phytoplankton overgrowth. Green spectrum irradiation plays an auxiliary role for oxygen production via phytoplankton photosynthesis. Therefore, red and blue spectra are majorly essential as the light conditions to conserve aquatic environments by maintaining a healthy DO level.

3) Reduction effects in nitrogen, phosphorous and organic matter

Finally, reductions in TN, TP, TOC, DOC, and E254 are examined to estimate the effects of water environmental remediation on anoxification recovery. The final concentrations are compared with the initial concentrations in each case as shown in **Table 4.3**; additionally, the temporal changes of these parameters are shown in **Fig.4.3**. In all cases, TOC and DOC do not show a remarkably increasing trend from the initial values despite temporary increases in phytoplankton promoted by LED irradiation. Moreover, the initial E254 values in the first series significantly decrease for two months, implying that components, such as humic acid, of dissolved organic matter, which are not easily decomposable, could be decomposed under aerobic conditions.

TN and TP in all cases considerably decrease from the initial high concentration after LED irradiation for two months. As mentioned previously, the decline in TP is mainly because of the disappearance of phosphate due to the formation of insoluble $FePO_4$ under the aerobic oxidative state, and the decline in TN is because of the uptake of NH_4-N and NO_3-N

Table 4.3 Comparisons of the final and initial concentrations of TN, TP, TOC, DOC, and E254 in the first series

Water quality parameters	Case B-1		
	(a) Start	(b) End	(b) /(a)
TN (mg/L)	1.23	0.32	0.26
TP (mg/L)	0.39	0.02	0.05
TOC (mg/L)	6.39	6.56	1.02
DOC (mg/L)	5.56	6.42	1.15
E254	0.15	0.09	0.60

Water quality parameters	Case B-2		
	(a) Start	(b) End	(b) /(a)
TN (mg/L)	0.91	0.40	0.44
TP (mg/L)	0.27	0.06	0.22
TOC (mg/L)	7.23	7.04	0.97
DOC (mg/L)	7.03	6.60	0.94
E254	0.12	0.09	0.75

Water quality parameters	Case B-3		
	(a) Start	(b) End	(b) /(a)
TN (mg/L)	1.04	0.28	0.27
TP (mg/L)	0.32	0.02	0.06
TOC (mg/L)	6.49	8.29	1.28
DOC (mg/L)	5.50	8.21	1.49
E254	0.14	0.09	0.64

by phytoplankton under the strong nitrogen-control state. Such reductions in TN and TP could be attributed to water environmental remediation by the LED irradiations. Notably, the final concentrations of TN and TP in Case B-2 are evidently higher than those in Case B-1 and Case B-3. In particular, TP concentration at the end of LED irradiation experiment is relatively high (0.06 mg/L) in Case B-2, while it is low (0.02 mg/L) in the other two cases. Thus, reductions in TP are markedly different between the green spectrum irradiation, and red and blue spectra irradiations. These differences in TN and TP concentrations across different color irradiations indicate whether nitrogen and phosphorous cycles among planktons, organic substances, and nutrients reach an equilibrium state.

4.3 Influence evaluation of light intensity on water environmental remediation

4.3.1 Experimental conditions

In the second series, the optical spectrum of LED irradiation is designed such that the ratio of photon flux densities in the RGB spectra is R:B:G = 1:1:1, as shown in **Table 4.4**. This series involve in three water tanks, labeled as Case C-1, Case C-2, and Case C-BK, with different LED irradiation conditions as follows. Case C-1 and Case C-2 are irradiation experiments to monitor water quality under oxygen produced by phytoplankton while irradiating anoxic water under a 24-hour cycle (12 hour-on/12 hour-off), and these are performed under small and large photon flux density by adjusting the output electric power. Specifically, the irradiation conditions in Case C-1 are defined as the weak light intensity of 17.8 μmol/(m^2 s), which seems to seriously inhibit photosynthesis as an optical limiting factor during the experimental period. The condition in Case C-2 is set as the strong light intensity of approximately 100.0 μmol/(m^2 s) during the experimental period, and this photon flux density corresponds to sufficient light quantum for phytoplankton photosynthesis. Case C-BK, where water in the tank is maintained in the dark state without LED irradiation, is categorized as the control condition.

As mentioned above, the primary purposes in the second series is to examine the recovery from anaerobic conditions, in which a strong reductive state cause an increase in NH_4-N, PO_4-P and sulfide like the first series and beaker-scale experiments. To achieve this objective, the anaerobic water prepared in cylindrical water tanks before beginning LED irradiation experiments for two months is maintained for a long period of about two months. Therefore, the initial condition of water quality in each case of the second series is reflected by the anaerobic reductive reactions under a strongly reduced state of ORP = –400.0 mV. As shown

Table 4.4 Optical spectrum and intensity of LED irradiation in the second series

Case	LED	Intensity μmol/(m^2 s)	Visible light (360 nm~780 nm)	Blue band (435 nm~480 nm)	Red band (610 nm~710 nm)	Green band (500 nm~570 nm)	R/B ratio
C-1	RGB	Weak	17.8	5.2	5.4	5.0	1.0
C-2	RGB	Strong	99.1	30.8	29.4	30.0	1.0

Table 4.5 Initial water quality parameters at the start of LED irradiation in the second series

Case	ORP (mV)	DO (mg/L)	Chl-a (μg/L)	Sulfide (μg/L)	NH_4-N (mg/L)	PO_4-P (mg/L)	NO_3-N (mg/L)	TFe (mg/L)
C-1	-416.7	0.2	1.9	227.0	1.97	0.21	0.00	2.39
C-2	-293.8	0.2	1.5	139.3	2.04	0.19	0.00	2.63
Control	-367.1	0.2	1.5	212.6	1.32	0.20	0.00	2.15

in **Table 4.5**, the initial conditions concerning water quality are summarized as NO_3-N=0 and relatively high concentrations of NH_4-N, PO_4-P, TFe and sulfide. Therefore, the aim of the second series is to examine the influence of photon intensity on the water quality-improving effects of long-term irradiation where concentrations of nutrients and reductive substances increase due to denitrification, iron reduction, and sulfate reduction.

4.3.2 Results and Discussion

Figure 4.4 shows the continuously measured DO and ORP under three experimental conditions in the second series. Additionally, the regularly measured results for water quality parameters, including PO_4-P, TFe, NH_4-N, sulfide, NO_3-N, class-differentiated Chl-a and total Chl-a concentrations, are summarized in **Fig.4.5**. When discussing the results in the second series from the viewpoint of optical influence on water environmental remediation via the anoxification recovery, it is important to focus on the changes in DO, Chl-a, DIN, and DIP concentrations in Case C-1 (under weak light intensity conditions) corresponding to those in Case A-3. In the following, to examine the spatial range of the effect of remediating the water environment considering the decay of light intensity in the irradiating direction from LED lamp, the impacts of low photon quantum on the effect of anoxification recovery are estimated by comparing Case C-1 with Case C-BK (under dark conditions) and Case C-2 (under strong light intensity conditions).

1) Water quality dynamics until anoxification recovery

In both Cases C-1 and C-2, ORP temporally changes with remarkable variations in the negative range until the start of the increase in DO, unlike Case C-BK, and it increases or decreases according to the presence/absence of light despite anaerobic conditions. For a few days after beginning the LED irradiation experiments (t < 6 d for Case C-1 and t < 2 d for Case C-2), ORP remains at approximately –400.0 mV, which is a strong reducing state comparable to the initial condition. Meanwhile, the ORP level increases in the negative range during putting out the light between t = 6 d and 22 d for Case C-1 and t = 3 d and 9 d for Case C-2. Such an increase of ORP levels toward zero means that the strong reduction is weakened by the slight presence of oxygen. The sulfide concentration in Case C-1 decreases sharply at t = 6 d, and it reaches almost zero at t = 8 d. Also, sulfide concentration in Case C-2 decreases abruptly to zero t = 2 d. Because the disappearance of sulfide indicates the oxidation of it to SO_4^{2-}, oxygen is produced by photosynthesis after t = 6 d for Case C-1 and after t = 2 d for Case C-2. Similar to beaker-scale experiments, the time lag between the start of LED irradiation

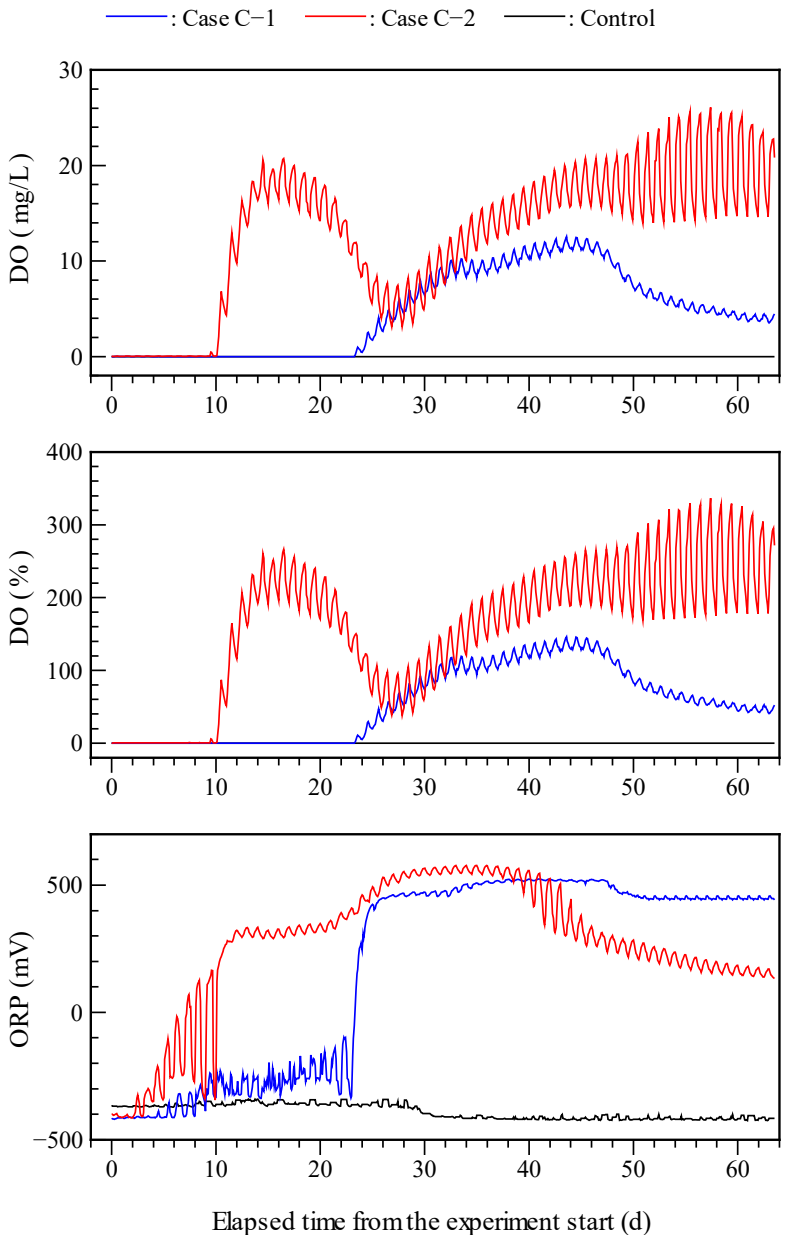

Fig.4.4 Continuously measured DO and ORP in Cases C-1 and C-2

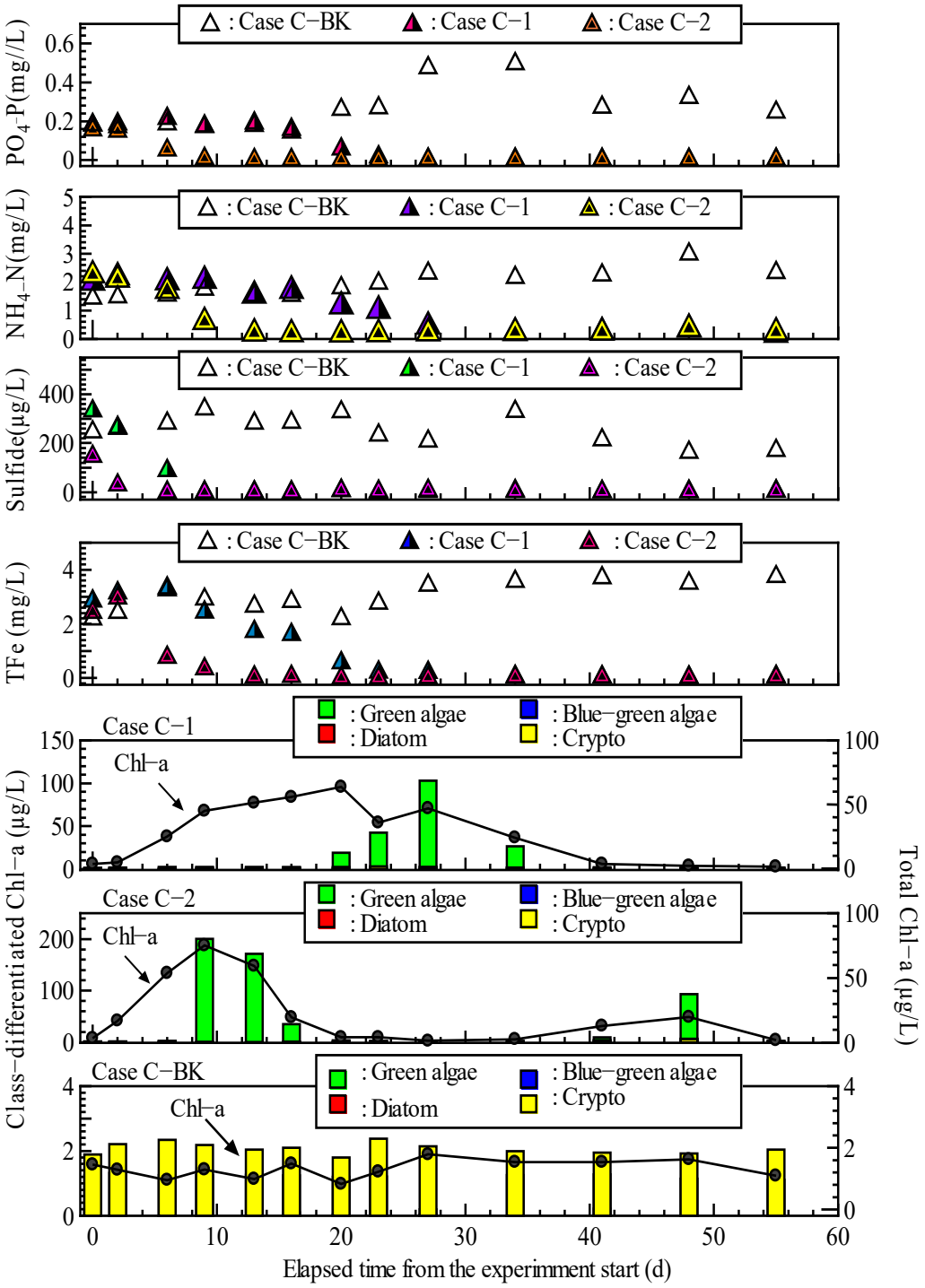

Fig.4.5 Periodically measured PO_4-P, NH_4-N, sulfide, TFe, class-differentiated Chl-a and Total Chl-a in Case C-1 and C-2

and the start of DO production is due to the reduced photo- responsiveness of phytoplankton due to long-term darkness until beginning LED irradiation experiments. Remarkably, the time lag of 6 days in Case C-1 and 2 days in Case C-2 differ under different light intensity conditions, and low light intensity remarkably slows the recovery from the reduced photo-responsiveness. The recovery times from anoxification are t = 23 d for Case C-1 and t =10 d for Case C-2. Therefore, the difference in the recovery time from anoxification between Cases C-1 and C-2 is 13 d (= 23 – 10). Meanwhile, the difference in the recovery time from the reduced photo-responsiveness between the two cases is 3 d (= 6 – 3). From the comparison of the two differences, the influence of light intensity on the initiation of oxygen production by photosynthesis is relatively small compared to the start of anoxification recovery.

In Case C-BK in the aphotic state set as a control condition, PO_4-P and TFe levels are kept at high concentrations of 0.25 mg/L and 3.75 mg/L, respectively, under the strong reducing state. Meanwhile, both concentrations in Cases C-1 and C-2 decrease to almost zero during the variation of the ORP levels regardless of DO = 0 before anoxification recovery. In Case C-2 with strong light intensity, it required 7 d (= 10 – 3) to increase DO from the anoxic state at t = 10 d, although oxygen start to be produced at t = 3 d. During the anaerobic period, TFe in Case C-2 decreased to zero at t = 9 d. This decrease results from the disappearance of Fe^{3+} ions in the subsequent process. First, Fe^{2+} ions, which make up most of TFe in the initial strong reductive state, would be oxidized to Fe^{3+} ions due to the presence of oxygen. Next, Fe^{3+} would change to the insoluble iron compound by combining with a part of the phosphate ion, levels of which would increase because of the elution from the bottom sediment under anaerobic conditions before beginning LED irradiation experiments. PO_4-P concentration in Case C-2 decreases to zero between t = 3 d and 10 d, and it is assumed that iron ions disappear and phosphate ion decreases because of the aerobic oxidizing reaction. In Case C-1, under weak light intensity, the time lag between the start of oxygen production and the recovery from DO = 0 was 17 d (= 23 − 6). In this period, TFe and PO_4-P concentrations monotonically decrease after t = 6 d, and iron ions almost disappear at t = 23 d. This result means that the oxygen produced by photosynthesis between t = 6 d and 23 d is almost consumed due to the oxidation of Fe^{2+} and sulfide, as in Case C-2.

Green algae suddenly emerge as the dominant species at t = 20 d in Case C-1 and t = 9 d in Case C-2. In particular, concentrations of Chl-a in Case C-1 reaches 23.5 μg/L at t = 20 d and 46.2 μg/L at t = 24 d before the increase of DO, and the algal growth is confirmed in the anoxic state. In addition, the anoxification in Case C-2 is solved after Chl-a increases to a high

concentration of 201.0 μg/L at t = 9 d. Therefore, in both cases, the disappearance of sulfide and iron ions, as well as the increase in ORP, resulted from the oxygen production by the green algae with high photosynthetic ability. That is the point at which the Chl-a concentration reaches a maximum over the eutrophic level almost corresponds to the point at which DO start to increase. Here, the difference in the maximum concentration of Chl-a between Cases C-1 and C-2 is attributed to the light intensity. From the above results, at t = 23 d for Case C-1 and t = 9 d for Case C-2, the oxygen consumption by the oxidation of an oxidizable substance, such as Fe^{2+} ion, as well as sulfide, exceed the oxygen production by phytoplankton photosynthesis under sufficient concentrations of Chl-a, resulting in the occurrence of a time lag between the start of oxygen production and the recovery from anoxification in both cases. In particular, the large influence of low photon condition on the recovery from anoxification is evident, such that this time lag in Case C-1 is extended to 17 days (= 23 − 6) when compared to the sufficient photon condition of Case C-2. The stronger the light intensity, the greater the photosynthetic ability, resulting in the promotion of oxygen production. Therefore, it is a natural consequence that a longer time is required for anoxification recovery in Case C-1 when compared to Case C-2 according to the light intensity. Because LED is irradiated toward the anoxic water such that the anaerobic state is maintained for 2 months in Cases C-1 and C-2, both cases strongly reflected the initial high concentration of an oxidizable substance, which increases oxygen consumption. A large number of oxidizable substances remarkably reduce the net increase in DO under the condition of low oxygen production. Therefore, the time lag between the start of oxygen production and the recovery from anoxification became longer in Case C-1 because of not only low light intensity but also high concentrations of oxidizable substances increased by biochemical reduction under long-term anaerobic conditions. That is, the speed of recovery from anoxification by LED irradiation under weak light conditions strongly depend on the duration of anoxification with a strong reductive state.

2) Water quality dynamics after anoxification recovery

When focusing on the circadian variation in DO after anoxification is recovered at t = 23 d for Case C-1 and at t = 10 d for Case C-2, the stroke in Case C-1 is smaller than that in Case C-2. This result is strongly reflected in an optical limitation on phytoplankton photosynthesis due to weak light intensity. However, the DO in Case C-1 maintains a saturation of 60 %, although it slowly decreases after t = 48 d via a supersaturation state such that the oxygen concentration temporarily reaches 10.0 mg/L. Therefore, LED irradiation could contribute to the

maintenance of a sufficient aerobic state even though the light intensity is as low as one-fifth of the optimum light intensity for photosynthesis. Chl-a concentration in Case C-1 increases to a relatively high level of 25.0 μg/L to 45.0 μg/L in the period of t = 6 d to 8 d, resulting in the solution of an anaerobic strong reducing state. Furthermore, the recovery from anoxification in Case C-2 resulted from the Chl-a concentration, which drastically increases to about 100.0 μg/L in the period of t = 6 d to 8 d. In particular, NH_4-N in both cases decrease to zero during the exponential increase in Chl-a, whereas PO_4-P levels are maintained at a low concentration after decreasing to zero due to the combination with Fe^{3+} ions, as described above. The disappearance or upkeep of low concentrations of DIN and DIP denotes the uptake of phytoplankton for photosynthesis. According to the composition ratios of the algal class, green algae proliferating as a dominant species consumes NH_4-N and PO_4-P as an applicable DIN and DIP for algal photosynthesis regardless of light intensity. Although phytoplankton biomass is at a low level after the peak Chl-a level in both cases, NH_4-N and PO_4-P remains around zero without increasing, and the aerobic state is maintained without a decrease in DO concentration to the level of poor oxygen or anoxia. These results indicate that uptake of nutrients by algae is balanced in a stable equilibrium with the supply of nutrients inside the water body via not only the respiration of zoo- and phytoplankton but also the hydrolysis of dissolved organic matter. In particular, the DO environment seems to be well preserved even though the underwater light intensity is lower than the optimum photon intensity for photosynthesis because the matter cycle among plankton, organic substances, and nutrients reach an equilibrium state even under weak light intensity The temporal changes in DO includes the decrease after recovery from the anoxic state to the saturated or supersaturated state in both cases. DO in Case C-1 gradually decreases from t = 46 d, and DO in Case C-2 lowered to 5.0 mg/L according to a sharp decline of Chl-a from 37.0 μg/L to 5.7 μg/L during t = 20 d to 28 d. Focusing on the circadian variation of DO in the decrease, the change in the oxygen production in the presence of light is smaller than the oxygen consumption in the absence of light under both strong and weak light intensity. This result indicates that the decrease after the anoxic recovery is caused by the excessive consumption of DO due to the aerobic decomposition of organic matter (i.e., respiration by phytoplankton or zooplankton) in the dark. Because DO decreases after it increases to the peak value, which reaches supersaturation, its decline started after the time when phytoplankton sufficiently proliferated. The number of herbivorous zooplankton seem to be abundantly increased by grazing phytoplankton in large quantities after the peak of DO in both Cases C-1 and C-2. As a result,

DO temporarily decreases due to oxygen consumption by plankton respiration after the peak of Chl-a concentration, regardless of light intensity. In addition, phytoplankton decreases due to grazing by zooplankton, links to the above-mentioned decline of DO, where oxygen production decreases. Chl-a concentration shows levels of 3.8 μg/L for Case C-1 and 5.6 μg/L for Case C-2 after the recovery from anoxification. However, the decline of DO never resulted in dysoxic or anoxic water, although the oxygen production by photosynthesis decreases due to the decrease in phytoplankton. Therefore, the healthy aerobic state could be maintained until the end of irradiation experiments regardless of light intensity because the relationship between algal proliferation and grazing by zooplankton is balanced from the viewpoint of oxygen circulation. However, DO under the strong light intensity condition declines earlier than that under the weak light intensity condition because a sufficient light intensity lead to a mass propagation of phytoplankton such that Chl- a concentration exceed 2.2 μg/L. The greater the photon quantity in the irradiating LED, the stronger influence of light intensity on the decrease process, which results from the aerobic oxygen consumption by zooplankton after the recovery from anoxification. That is, in the weak light intensity, the aerobic state after the recovery from anoxification temporally changes with a small amplitude of daily variation without the influence of large oxygen consumption and shows a stable fluctuation, although DO shows a saturation level of approximately 60 % and Chl-a changed to a low concentration of approximately 4.0 μg/L. Therefore, LED irradiation could contribute to the preservation of a healthy aerobic state even if the light intensity is smaller than the optimum light intensity for phytoplankton photosynthesis, as in Case C-1. When the change with time in DO after t = 26 d for Case C-2 is considered, DO gently increases for a period of 24 h and reaches a high level of supersaturation regardless of low Chl-a concentration less than 5.0 μg/L. In particular, DO after t = 46 d fluctuates in the range of 15.0 mg/L to 25.0 mg/L, and such a high concentration strongly influences the existence of algae with a high photosynthetic ability. This means that the increase in DO is not resulted from the oxygen production by phytoplankton but by an aquatic plant. This aquatic plant is a submerged plant, which is observed after t = 46 d, as shown in **Fig. 4.6**. As a result of collecting all of the submerged plants in water tank at the end of LED irradiation experiment, the sampled plant was *Ceratophyllum demersum* and has a wet weight of 15.18 g. Also, the Chl-a concentration of the submerged plant is 676.6 μg/g in wet weight. The height of the submerged plant reaches the top of LED lamp, and the water volume that the submerged plant

occupies in the experimental water tank is 13.2 L. Therefore, the spatially averages concentration of Chl-a derived from the aquatic plan could be calculated as 778.1 μg/L. This high concentration of Chl-a remarkably promotes the oxygen production algal photosynthesis and lead to a significantly high DO concentration such that the saturation exceeds 200 % under strong light intensity in the range of optimum photons for algal photosynthesis. The transition of dominant algal species from green algae to the submerged plant in Case C-2, resulted from the strong light intensity in the range of optimum photon intensity for algal photosynthesis. Therefore, the large difference between the strong and weak light intensity conditions is the main contribution to oxygen production by the submerged plant or phytoplankton.

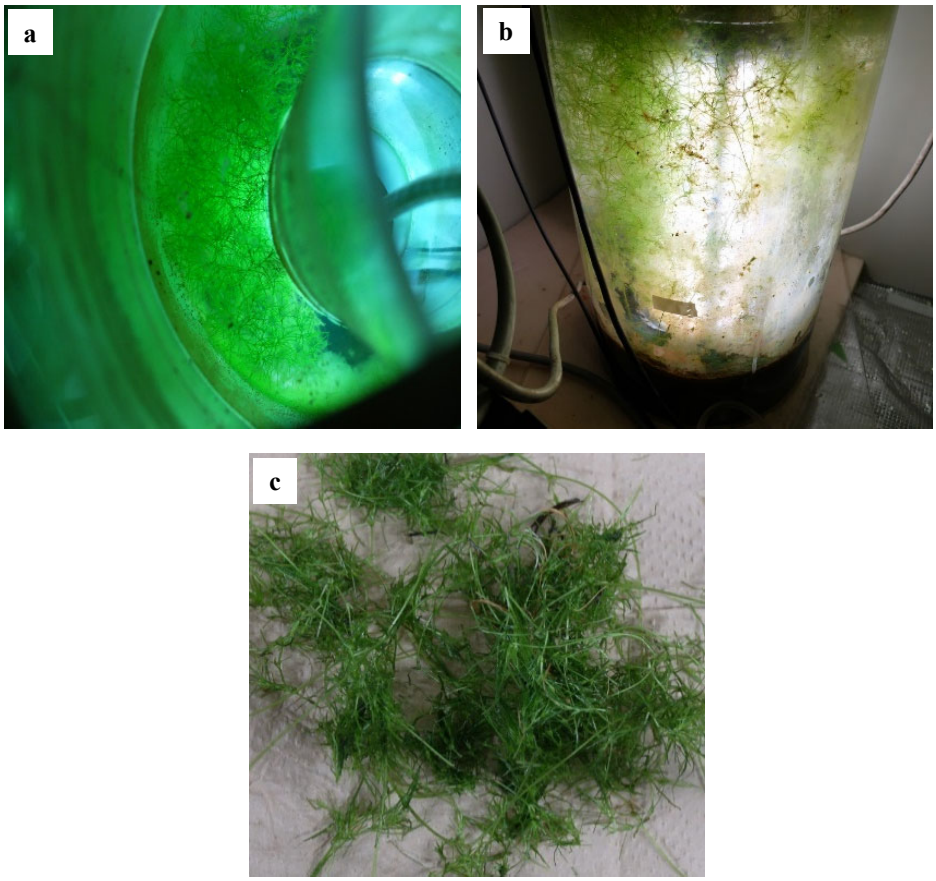

Fig.4.6 The submerged plant in the water tank in Case C-2 under the strong light intensity conditions at the end of the LED irradiation experiment. a) The aquatic plant observed after 46 days. b) The aquatic plant observed on the last day of the LED irradiation. c) A part of the submerged plant collected after finishing the experiment.

3) Reduction effects in nitrogen, phosphorous and organic matter

Figure 4.7 shows the scheduled observation results for TN, TP, TOC, DOC, and E254 levels. In addition, the comparisons of the final results with the initial concentrations in each

case, as well as the comparisons of the final results between the irradiation and control conditions are summarized in **Table 4.6**. To examine the effects of water environmental remediation upon anoxification recovery, we first focus on the reductions of TN, TP, TOC, DOC, and E254 under weak light conditions by comparing Case C-1 with Case C-BK under the control condition.

According to the results of Case C-BK, the persistent anoxic state for 2 months cause an external high TN concentration of more than 2.00 mg/L and TP concentration of approximately 0.60 mg/L because NH_4-N and PO_4-P are eluted from the bottom sediment as a result of anaerobic organic matter decomposition. Meanwhile, TN and TP in Case C-1 respectively decrease to concentrations of 0.47 mg/L and 0.03 mg/L upon LED irradiation for 2 months, and both values are lower than the standard Ministry of the Environment, Japan (2008) values for nitrogen and phosphorous levels in eutrophication (TN: 1.00 mg/L and TP: 0.10 mg/L). That is, TN and TP concentrations in Case C-1 decrease by approximately 20 % and 5 %, respectively, when compared to the control condition via LED irradiation for 2 months. NH_4-N, which occupies most of the total nitrogen in the initial condition, is used by phytoplankton for photosynthesis, resulting in a decrease in TN concentration. In addition, the decrease in TP is derived not only from the uptake of phytoplankton for its growth but also from the insoluble iron compound via combination with Fe^{3+}, as mentioned above. Actually, TFe concentration eventually decreases from 2.84 mg/L to 0.06 mg/L under aerobic conditions after the anoxic recovery, and this result indicates the reason why phosphate ion level decreases.

From the above, LED irradiation with low light intensity compared to the optimum photon for photosynthesis for 2 months could significantly inhibit the increase of nitrogen and phosphorous concentrations caused by elution from the bottom sediment under long-term anoxification. In addition, E254 levels in Case C-1 is decreased by 50 % in the control experiment, although the TOC and DOC concentrations are not significantly lower. Therefore, water environmental remediation by LED irradiation could be clearly evaluated, as refractory dissolved organic substance levels decrease. Upon comparing the results of TN, TP, TOC, DOC, and E254 at the end of LED irradiation experiment with those at the start, there is no

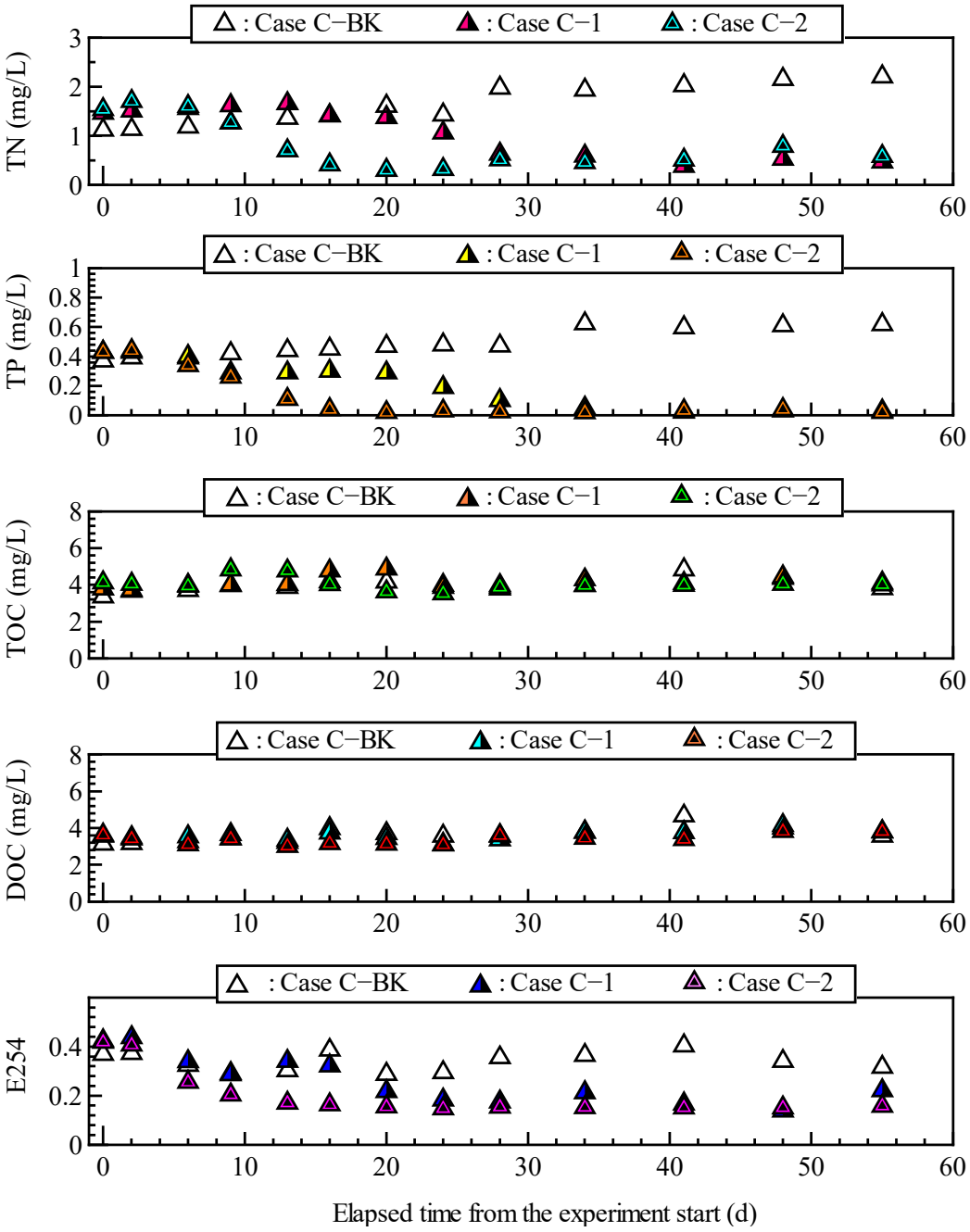

Fig.4.7 Periodically measured TN, TP, TOC, DOC, and E254 in the second series

Table 4.6 Comparisons of the initial and final TN, TP, TOC, DOC, and E254 measurements in the LED irradiation group and the final results under control conditions in the second series

Water quality parameters	Case C-1				
	(a) Start	(b) End	(c) Control	(b) /(a)	(b) /(c)
TN (mg/L)	1.46	0.47	2.21	0.33	0.21
TP (mg/L)	0.43	0.03	0.62	0.07	0.05
TOC (mg/L)	3.78	4.11	3.79	1.09	1.08
DOC (mg/L)	3.56	3.79	3.57	1.06	1.06
E254	0.43	0.22	0.32	0.51	0.69

(a) and (b) : the initial and final concentrations in the LED irradiating condition, (c): the final concentrations in the control condition.

Water quality parameters	Case C-2				
	(a) Start	(b) End	(c) Control	(b) /(a)	(b) /(c)
TN (mg/L)	1.54	0.58	2.21	0.38	0.26
TP (mg/L)	0.43	0.02	0.62	0.05	0.03
TOC (mg/L)	4.12	4.01	3.79	0.97	1.06
DOC (mg/L)	3.62	3.81	3.57	1.05	1.07
E254	0.42	0.16	0.32	0.38	0.50

(a) and (b) : the initial and final concentrations in the LED irradiating condition, (c): the final concentrations in the control condition.

significant difference between Cases C-1 and C-2. TN, TP, and E254 greatly decrease from the initial concentration upon LED irradiation for two months, while TOC and DOC concentrations shows no significant changes during LED irradiation without decreasing according to the growth of phytoplankton or aquatic plants. That is, the effect of water environmental remediation in Case C-1 is expected to be the same as Case C-2, in which light intensity is sufficiently strong for algal growth, even though the light intensity is as low as one-fifth of the optimum photon intensity for phytoplankton photosynthesis. From this comparison, the growth of submerged vegetation do not promote the reduction of nitrogen, phosphorous, and organic matter concentrations and do not significantly affect the improvement of water quality environment, except for DO. In addition, a comparison between Cases C-1 and C-2 prove that the spatial effect of water environmental remediation by LED irradiation is not limited to the vicinity of the light source, but is also effective in the wide range in which the light intensity is one- fifth of the optimum photon for phytoplankton photosynthesis.

4.4 Effects of water environmental remediation considering influence of initial anaerobic conditions under low photon intensity

4.4.1 Experimental conditions

In the third series, LED irradiation experiments are conducted with mixed RGB light to examine the improvement in anoxic water environment under two different reductive states of anoxic water (strong and a weak reductive potential). Also, optical conditions are set to low photon intensity, which would strongly affect phytoplankton photosynthesis due to optical limitation. This series aim to estimate the effects of mixed RGB irradiation, with a corresponding photon ratio of 1:1:1 (R:G:B), on water environmental remediation from the viewpoints of two experimental conditions. One is extremely low photon intensity, which strongly affects phytoplankton photosynthesis and acts as the optical limitation. The other is the initial concentrations of nutrients and oxidizable substances generated under anaerobic conditions. In the third series, water quality experiments are conducted in three water tanks labeled as Cases D-1, D-2, and D-3. The experimental conditions regarding the optical spectrum and intensity of LED irradiation in each case are summarized in **Table 4.7**. Additionally, the initial conditions of main water quality parameters are shown in **Table 4.8**.

Anoxification recovery by LED irradiation depend on the photon intensity and thus, the recovery effect would be weak at a point far from the light source due to the decay of light

Table 4.7 Optical spectrum and intensity of LED irradiation in the third series

Case	Color	Intensity μmol/(m^2 s)	Visible light (360 nm~780 nm)	Blue band (435 nm~480 nm)	Green band (500 nm~570 nm)	Red band (610 nm~710 nm)
D-1	RBG	Weak	8.12	2.52	2.86	2.74
D -2	RBG	Weak	7.97	2.50	2.69	2.78
D--3	RBG	Weak	3.98	1.24	1.44	1.30

Table 4.8 Initial conditions of main water quality parameters associated with the an-aerobic state in the third series

Case	DO (mg/L)	Chl-a (μg/L)	Sulfide (μg/L)	NH_4-N (mg/L)	PO_4-P (mg/L)	NO_3-N (mg/L)	TFe (mg/L)
D-1	0.12	0.6	83.0	1.42	0.51	0.00	2.30
D-2	1.3	0.6	9.0	1.13	0.07	0.01	0.12
D-3	0.01	0.3	5.5	0.61	0.12	0.00	0.17

intensity. To properly evaluate the spatial range, which allows for good anoxification improvement by LED irradiation, estimating the dynamics of water quality parameters, such as DO, Chl-a, DIN, and DIP, is essential under extremely low photon intensities. In both Cases D-1 and D-2, the total photon intensity of the visible light region is set to approximately 8.0 μmol/(m^2 s), which correspond to approximately one-tenth of the lower limit of the optimum light intensity required for photosynthesis. Moreover, the photon intensity in Case D-3 is set to a smaller value of 4.0 μmol/(m^2 s), which is approximately one-twentieth of the lower limit of the optimum photon intensity, to estimate water quality dynamics under strong photon limitations for photosynthesis.

The key experimental factor in the third series is the initial concentrations of water quality parameters, particularly nutrients and oxidizable substances. Because LED irradiation experiment in Case D-1 start two months after the formation of anoxic water, the initial anaerobic conditions are represented as anaerobic reductive reactions under a strongly reductive state and are reflected by high concentrations of sulfide, TFe, NH_4-N, and PO_4-P. LED irradiation experiments in Cases D-2 and D-3 start few weeks after the experimental system is set, resulting in low concentrations of oxidizable substances and nutrients regardless of DO = 0 and NO_3-N = 0. These initial anaerobic conditions in both cases denote a weak reductive state wherein the reductive reactions of iron reduction and sulfate reduction has not yet occurred as the next anaerobic reductive reactions after denitrification. Therefore, the initial conditions in Cases D-2 and D-3, unlike Case D-1, are common in the anaerobic reductive state characterized by low concentrations of NH_4-N, PO_4-P, sulfide, and TFe.

4.4.2 Results and discussion

Figure 4.8 shows the results of continuous measurement of DO in Cases D-1, D-2, and D-3. Further, the scheduled measurements in all cases in the third series are shown in **Figs.4.9** and **4.10**. Although the anoxic state could be recovered in Case D-1 and Case D-2, the variation characteristics of DO evidently differ between both cases in four aspects: the time requires to recover from the anoxic state, maximum level, average concentrations in the stationary state, and the time at which the DO concentration shifts from an increasing state to a steady state. In addition, the results of Case D-3 shows that the DO concentration is maintained at zero, and do not increase during LED irradiation experiment. Therefore, the influence of the initial anaerobic condition on anoxification recovery and water environmental remediation are examined from the following perspectives: 1) a healthy DO level, 2) phytoplankton growth,

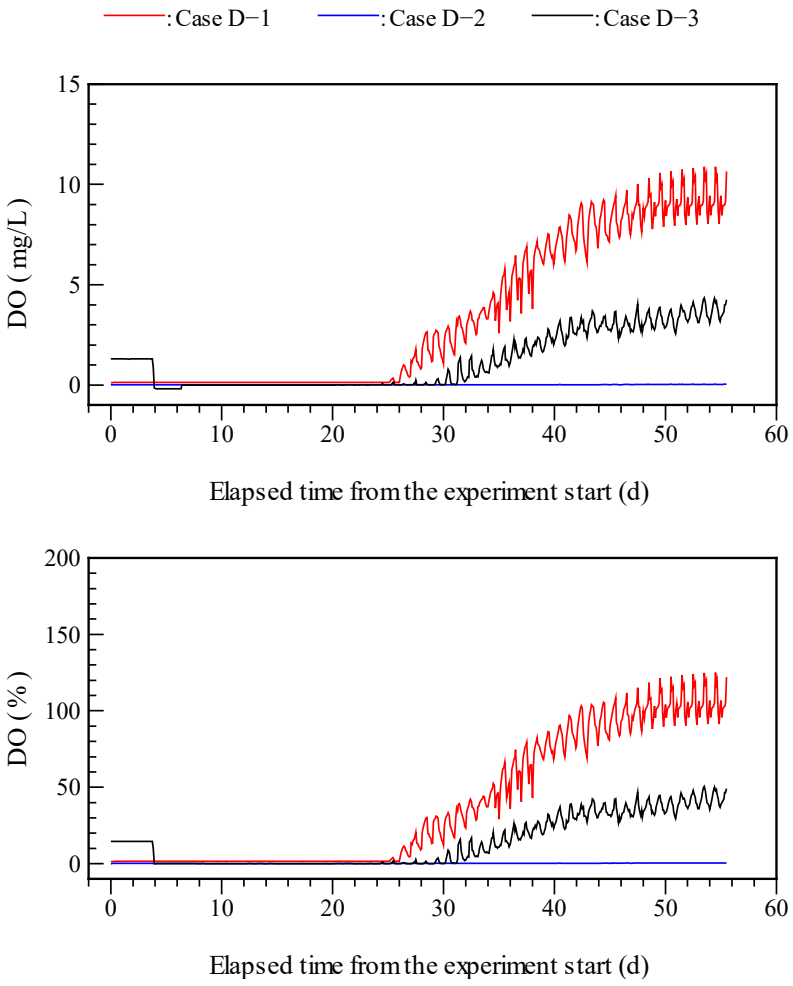

Fig.4.8 Continuously monitored DO results of in Cases D-1, D-2, and D-3

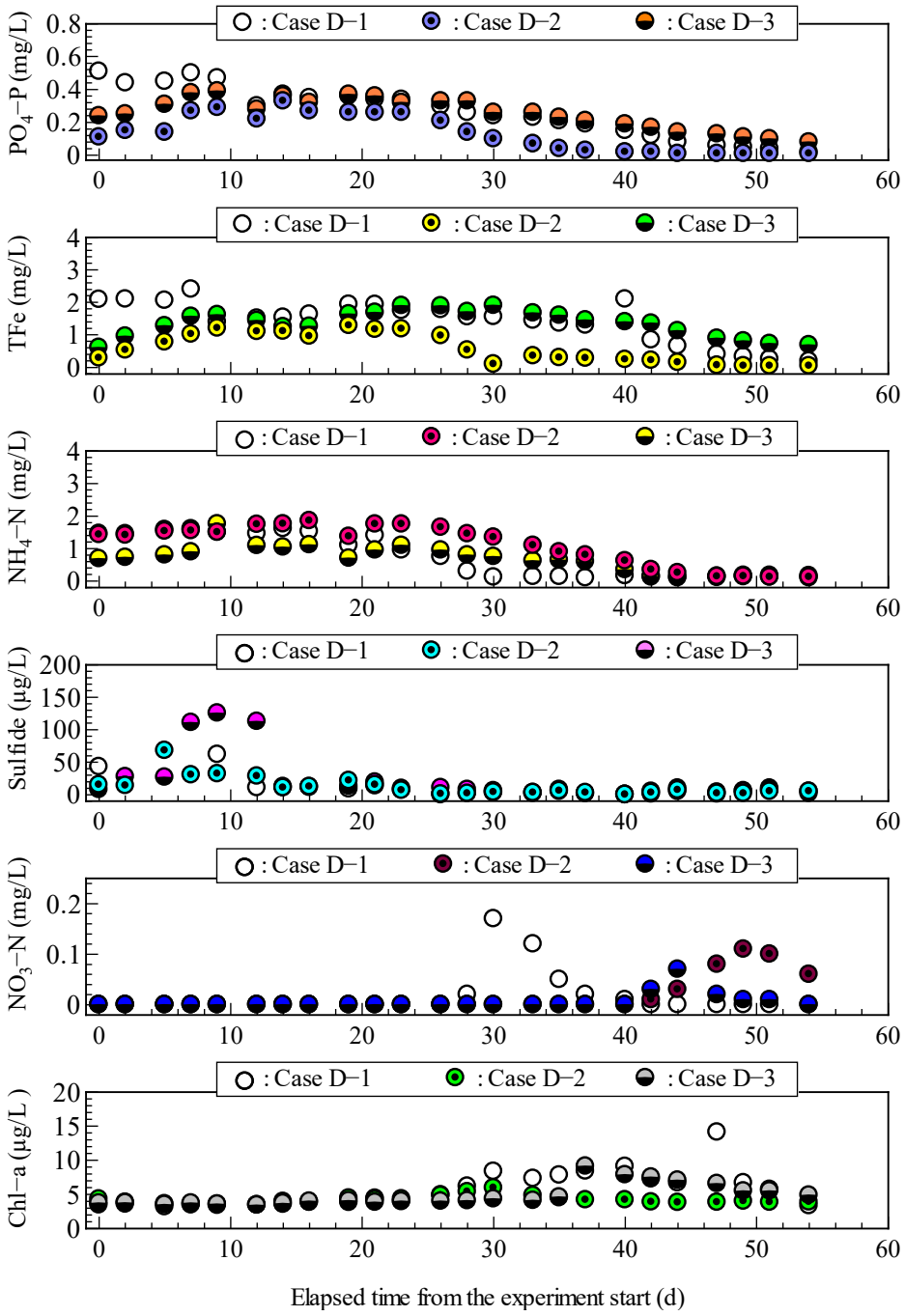

Fig.4.9 Time series variation of water quality parameters. (a) PO4-P, (b) TFe, (c) NH4-N, (d) sulfide, (e) NO3-N and (f) Chl-a in Cases D-1, D-2, and D-3

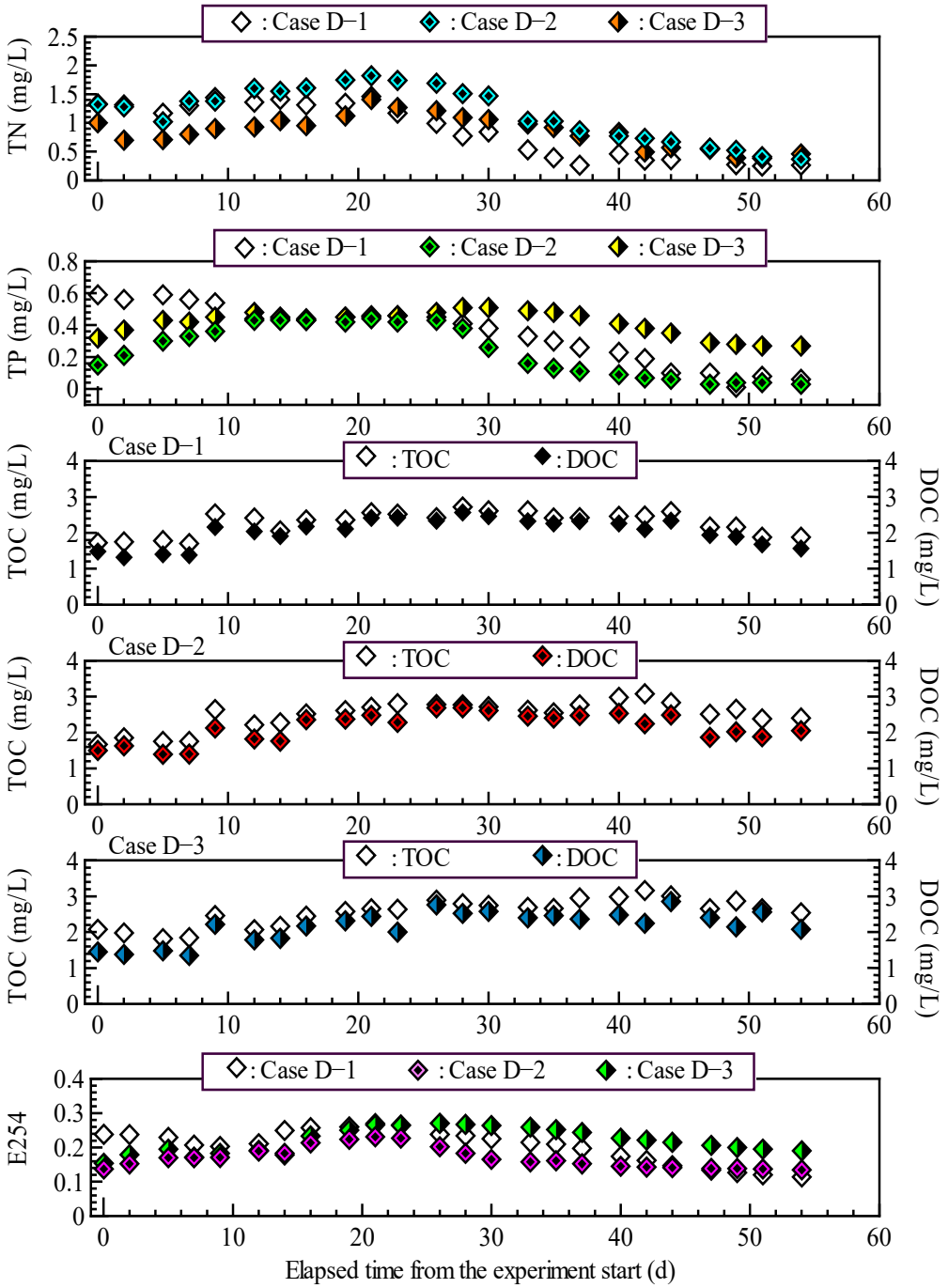

Fig.4.10 Time series variation of water quality parameters. (a) TN, (b) TP, (c) TOC, (d) DOC, and (e) E254 in the third series

3) biochemical dynamics of DIN and DIP and temporal changes in oxidizable substances (sulfide and Fe^{2+}), and 4) reductions in nitrogen, phosphorous, and organic carbon through DO variations. The key point for considering the results in the third series is the discussion under the experimental condition, which assumes that phytoplankton photosynthesis is strongly restricted by optical limitation, unlike the second series.

1) Influence of initial anaerobic conditions on anoxification recovery effects

Case D-1 and Case D-2 require more time (26 d and 31 d, respectively) to shift from the anoxic state to the aerobic state when compared to the cases of the first and second series. Similar to other series, the anoxic state in the third series may be divided into two periods from the viewpoint of the presence or absence of oxygen production by photosynthesis. First, the production and consumption of DO are considered based on the temporal changes in the sulfide content, which in both cases, increases to higher levels when compared to the initial concentrations for few weeks after initiating LED irradiation (t < 9 d for Case D-1 and t < 21 d for Case D-2). In particular, sulfide content in Case D-1 exceeds 200 μg/L from t = 2 d to 7 d, and that in Case D-2 reaches a maximum value of 68.0 μg/L at t = 5 d. Thus, both cases show an anoxic period wherein sulfate reduction progressed further under a continuous strong reductive state due to the non-production of oxygen, regardless of LED irradiation. However, high sulfide concentration in Case D-1 rapidly decrease to a low level (approximately 10 μg/L) in a short term from t = 9 d to 21 d, and sulfide disappears at t = 26 d. Additionally, in Case D-2, after a constant low sulfide concentration (10 μg/L) from t = 14 d to 21 d, sulfide concentration lower to zero at t = 26 d. Because the decrease and disappearance of sulfide resulted from the oxidation reaction under the presence of oxygen, oxygen production by photosynthesis is confirmed at t > 9 d in Case D-1 and t > 14 d in Case D-2. Therefore, until DO concentration increases, the anoxic state could be divided into the first period, which represented the non-production of oxygen due to the reduced photo-responsiveness of phytoplankton, and the second period, when the anoxic state resulted from the complete consumption of oxygen produced by phytoplankton during photosynthesis for the oxidation reaction.

Thus, the anoxic state divided based on the temporal changes in sulfide is supported by the scheduled measurement results of TFe and PO_4-P. Both TFe and PO_4-P concentrations in Case D-1 gradually decreases since t = 9 d. Additionally, the temporal changes in TFe and PO_4-P concentrations in Case D-2 shift from high values to constant values at t = 12 d, after which both concentrations abruptly start to decrease at t = 23 d. Such decreases in TFe and PO_4-P in

both cases could have been mainly caused by the formation of an insoluble iron compound, with high Fe^{3+} content due to the oxidation of Fe^{2+}, along with phosphoric acid.

These results indicate that the oxygen required for iron reduction is acquired from the DO that is slightly produced by photosynthesis after t = 9 d in Case D-1 and t = 23 d in Case D-2. These results indicate that the oxygen required for oxidizing Fe^{2+} is acquired from the DO slightly produced by photosynthesis after t = 9 d in Case D-1 and t = 23 d in Case D-2. These times correspond to the time required for oxygen consumption during sulfate reduction. Therefore, the anaerobic state of DO = 0 is maintained because the oxygen consumption during the oxidation of oxidizable substances would exceed the oxygen production during photosynthesis.

The time required for the anoxification recovery differ between Case D-1 and Case D-2 because of differences in the mass balance between oxygen production and oxygen consumption. In Case D-1, having extremely high concentrations of both sulfide and TFe, the oxygen consumption during the oxidation of oxidizable substances is higher than that in Case D-2. However, the anoxic state in Case D-1 is recovered faster than that in Case D-2. Therefore, oxygen production in Case D-1 could be judged to be more than that in Case D-2, although Chl-a concentrations in both cases remain approximately constant at a low level of approximately 3.5 μg/L until DO concentration start to increase. From the viewpoint of limiting factors (nutrients, water temperature, and light intensity) for photosynthesis, the initial high concentrations of NH_4-N and PO_4-P in Case D-1 stimulate the photosynthesis rate more than those in Case D-2 because of differences only in the nutrient limiting factor between both cases. Therefore, under similar weak light intensities, the time length for anoxification recovery in both cases depend more strongly on the initial high concentration of nutrients than that of oxidizable substances.

2) Impacts of initial anaerobic conditions on water quality dynamics after anoxification recovery

Although the light intensity is approximately one-tenth of the lower limit of the optimum light intensity required for photosynthesis, DO evidently increases after anoxification recovery with a fluctuation in the 24-hour cycle and shifted to the steady state after reaching the peak value, regardless of initial anaerobic conditions. However, Case D-1 and Case D-2 differ in the following aspects: the time required to reach the lower concentration limit (4 mg/L) required for a healthy DO level (t = 35 d for Case D-1, and t = 46 d for Case D-2), average increasing rate of DO until the maximum concentration is reached [0.5 mg/(L d) for Case D-1 and 0.2 mg/(L d) for Case D-2, DO concentration at the steady state (9.5 mg/L for Case D-1

and 3.5 mg/L for Case D-2), and daily variation in DO (3.0 mg/L for Case D-1 and 1.0 mg/L for Case D-2).

Thus, the results of Case D-1 can be summarized as follows: The photosynthesis rate is promoted after the anoxification recovery; consequently, DO promptly increases to a peak concentration with a saturation of approximately 100% and a relatively high production of oxygen, which exceeds the amount of oxygen consumed. Additionally, a healthy DO level is maintained since t = 40 d. These findings are supported by the results of the temporal changes in DIN, DIP, and Chl-a. First, NH_4-N content decreases to almost zero from t = 28 d to 37 d after recovering from the anoxic state. This decrease under increasing DO concentration might be attributable to NH_4-N uptake by the phytoplankton. Further, after NO_3-N significantly increases from the zero level to approximately 0.2 mg/L from t = 30 d to 33 d, it reaches zero again during a short time from t = 30 d to 37 d. The increase in NO_3-N resulted from the aerobic decomposition of organic matter (including the nitrification of NH_4-N) after the anoxification recovery (Hsiao et al. 2014). Compared with Case D-2, because the undecomposed organic matter in Case D-1 is high due to the prolsonged anoxic condition until the irradiation experiments began, the initial high values of TOC, DOC, and E254 are associated with the increase in NO_3-N to approximately 0.2 mg/L. Further, the decrease in NO_3-N to zero from t = 30 d to 37 d could be because of its uptake via photosynthesis because NO_3^- is a major nitrogen source for phytoplankton growth. In particular, the nutritional status of phytoplankton in Case D-1 is strongly controlled by nitrogen according to the N/P ratio (2.2) calculated by the initial TN and TP concentrations. This nitrogen-control state derived from the initial high PO_4-P concentration is due to a strong reductive potential when LED irradiation began. Therefore, Chl-a concentration increases by approximately two times more than its initial concentration based on the rapid supply of NO_3-N and the initial high NH_4-N concentration. Consequently, DO concentration reaches the saturated steady state with increased oxygen production since t = 40 d. Furthermore, PO_4-P concentration after the anoxification recovery decreases more slowly when compared to NO_3-N and NH_4-N concentrations and is almost zero at t = 51 d. Therefore, unlike DIN, determining the temporal changes in PO_4-P corresponding to the increase in DO is difficult after the anoxification recovery. PO_4-P concentration is maintained at a high level (over 0.1 mg/L) when DO reaches the saturated steady state at t = 40 d. However, the temporal changes in PO_4-P concentration are similar to those of TFe. TFe decreased from approximately 2.0 mg/L after DO reaches a peak concentration at t = 37 d, and it finally decreases to a low level of 0.2 mg/L at t

= 47 d. This decrease in TFe indicates that Fe^{3+} generated by the oxidation of Fe^{2+} due to sufficient DO concentration might combine with PO_4^{3-} and change to insoluble phosphoric acid-iron. In addition, PO_4-P available for photosynthesis (approximately 0.02 mg/L) remains in water without being consumed by phytoplankton. The strong nitrogen-control state is maintained from the initial condition because the N/P ratio changed from 1.0 to 5.3 until the end of LED irradiation. Therefore, PO_4-P mainly decreases due to the formation of insoluble phosphate compound, and the impact of its uptake by phytoplankton is relatively small.

The results of Case D-2 can be summarized as follows: The initial PO_4-P concentration (approximately 0.1 mg/L) is sufficient for phytoplankton, although it is lower than that in Case D-1. The nutritional status in Case D-2 is estimated to be in the nitrogen-control state based on the calculated initial N/P ratio of 8.0. Additionally, the initial NH_4-N concentration (1.13 mg/L) in Case D-2 is high from the viewpoint of the nitrogen source for photosynthesis, although the concentration is lower than that in Case D-1. However, NH_4-N concentration do not drastically decrease with the increase in DO during a fluctuation in the 24-hour cycle from t = 30 d to 42 d. Thus, NH_4-N is not actively consumed as a nutrient by phytoplankton, and the increase in DO from t = 30 d to 42 d is limited to a low level (<3.0 mg/L). Although NO_3-N, a main nitrogen source for phytoplankton photosynthesis, is maintained at zero for t < 42, its concentration increased from t = 47 d to 51 d due to aerobic decomposition of organic matter (including the nitrification of NH_4-N). When comparing the temporal changes of NO_3-N in Case D-2 with those in Case D-1, the time required for the concentration to increase in the former case is 17 d later than that in the latter; however, the maximum concentration in Case D-2 is approximately less than half of that in Case D-1. Such a marginal increase in the NO_3-N concentration is associated with the differences in the increasing concentrations of Chl-a and DO between Case D-1 and Case D-2. That is, Chl-a in Case D-2 changes marginally from 3 μg/L to 5 μg/L and do not increase much compared to its initial concentration. Consequently, DO production rate via photosynthesis is low in Case D-2 and is strongly limited by lower NO_3-N concentration compared to that in Case D-1; additionally, the aerobic state is preserved at a low level of DO with approximately 45% saturation. Based on this, the influences of initial anaerobic conditions on improving the anoxic environment could be determined from the viewpoint of the biochemical dynamics of NO_3-N. Both NH_4-N and PO_4-P decrease to almost zero from t = 44 d to 47 d, and the concentration of the remaining nutrients is almost negligible. Therefore, the biochemical balance between the NH_4-N and PO_4-P uptake by photosynthesis and their supply into water due to respiration and mineralization might shift to an equilibrium state after t = 44 d or 47 d.

In addition, the N/P ratio reaches a value of approximately 14.0 due to the supply of NO_3-N from t = 47 d to 51 d that represent a well-balanced state of nitrogen and phosphorous for phytoplankton, implying that the nitrogen and phosphorous cycles among planktons, organic substances, and nutrients reach an equilibrium state. Therefore, a healthy DO level could be preserved at a low level of approximately 4 mg/L although underwater light intensity is one-tenth of the lower limit of optimum light intensity required for photosynthesis.

3) Impacts of initial anaerobic conditions on reductions in nitrogen, phosphorous and organic matter

The reductions in TN, TP, TOC, DOC, and E254 are used to examine the effects of water environmental remediation on anoxification recovery in Cases D-1 and D-2. **Table 4.9** compares the final and initial concentrations. In both cases, high TN and TP concentrations are dramatically reduced in two months after their initial concentrations temporarily reached peak values due to increase in PO_4-P and NH_4-N eluted from sediment. Therefore, the actual decreasing rates of TN and TP are higher than the results shown in **Table 4.9.** Because the majority of TN and TP are incorporated in the dissolved inorganic components until the end of irradiation experiments, the decrease in PO_4-P and NH_4-N concentrations could be directly linked to the decrease in TN and TP. As stated above, the nutritional statuses in both cases are in the nitrogen-control state due to the initial high PO_4-P concentration. Consequently, the intake of PO_4-P by phytoplankton is restricted because the DIN available for photosynthesis do not remain in water. Therefore, TP mainly decreases due to the formation of insoluble phosphoric acid-iron. Additionally, phytoplankton ingests NO_3-N and NH_4-N, and an abiotic particulate organism derived from algal death settled on the bottom bed, which resulted in the disappearance of DIN and particulate organic nitrogen (PON) from water. Thus, TN (=DIN+PON) is reduced via the aerobic matter cycle among planktons, organic substances, and nutrients. Therefore, LED irradiation could be effective in reducing TN and TP concentrations although the oxygen production is strongly restricted to approximately one-tenth of the lower limit of optimum photon intensity required for photosynthesis.

In Case D-1, TOC and DOC increase after oxygen production at t = 9 d, and this increasing trend continues until DO reaches a peak value at t = 40 d. Thus, the increase in TOC corresponds to the growth period of phytoplankton. Both oxygen production and consumption

Table 4.9 Comparisons of the final results with the initial concentrations of TN, TP, TOC, DOC, and E254 in the third series

Water quality parameters	Case D-1		
	(a) Start	(b) End	(b) /(a)
TN (mg/L)	1.33	0.26	0.20
TP (mg/L)	0.59	0.06	0.10
TOC (mg/L)	1.72	1.88	1.09
DOC (mg/L)	1.48	1.56	1.05
E254	0.24	0.11	0.46

Water quality parameters	Case D-2		
	(a) Start	(b) End	(b) /(a)
TN (mg/L)	1.32	0.37	0.28
TP (mg/L)	0.15	0.03	0.20
TOC (mg/L)	1.67	2.40	1.44
DOC (mg/L)	1.50	2.05	1.37
E254	0.14	0.13	0.93

Water quality parameters	Case D-3		
	(a) Start	(b) End	(b) /(a)
TN (mg/L)	1.00	0.46	0.46
TP (mg/L)	0.32	0.27	0.84
TOC (mg/L)	2.08	2.54	1.22
DOC (mg/L)	1.45	2.08	1.43
E254	0.15	0.19	1.23

seemed to be high after DO increased at t = 26 d because the daily variations in DO were high. Thus, oxygen is sufficiently produced such that DO level reaches a saturation state, while oxygen consumption is high because of mineralization of organic matter under aerobic oxidative conditions. Consequently, TOC and DOC decrease since t = 40 d and finally reach a concentration same as the initial concentrations. Moreover, E254 level in Case D-1 reduces because of the aerobic decomposition of barely decomposable dissolved organic matter without a temporary increase. Therefore, in Case D-1, maintaining a healthy DO level could effectively reduce organic carbon.

Similar to Case D-1, TOC and DOC in Case D-2 show an increasing trend after oxygen production at t = 14 d. However, although their concentrations later decrease by aerobic oxidative decomposition after DO started increasing at t = 31 d, the decreased levels in TOC and DOC in Case D-2 is less than in Case D-1. As mentioned above, DO decreases to a low level (approximately 4 mg/L) with a small daily variation after recovering from the anoxic state, and the oxygen amount available for the aerobic oxidative reactions is insufficient. Therefore, TOC and DOC concentrations by the end of LED irradiation are higher than their initial concentrations, while E254 level is the same at the beginning and end of LED irradiation experiment. However, the effect of water environmental remediation by the anoxification recovery is evident because two months of LED irradiation inhibit the increase in the undecomposed organic matter stemming from the anaerobic state.

4) Effects of water environmental remediation under extremely low photon intensity

In Case D-3, DO level is zero until the end of LED irradiation experiment, unlike in Cases D-1 and D-2. However, despite this, the temporal changes in the water quality are determined as follows based on the oxidation-reduction reaction. Although sulfide content that increases immediately after starting LED irradiation experiment reaches a maximum concentration of 125 μg/L at t = 9 d, it abruptly decreases and reaches a low level (< 10 μg/L) since t = 9 d. Further, after TFe gradually increases from the beginning of irradiation experiment until t = 30 d, it gradually lowers to the same concentration as that observed initially. PO_4-P and NH_4-N concentrations shows a temporary similar changing pattern; that is, immediately after the LED irradiations began, both drastically increase to a maximum level (PO_4-P: 0.37 mg/L and NH_4-N: 1.76 mg/L), which is maintained for approximately one month. Subsequently, both PO_4-P and NH_4-N concentrations reduce since t = 30 d and finally decrease to nearly 0.1 mg/L.

These temporal changes indicate that anoxic state, which continues until the end of the LED irradiation experiment, could be divided into two stages by a boundary line of t = 26 d to 30 d based on the oxidation-reduction reactions. First, the strong reductive potential is maintained without oxygen production for approximately t < 28 d, consequently, promoting iron reduction and sulfate reduction. Moreover, since t = 28 d, aerobic oxidative reactions are confirmed such that sulfide almost disappear and TFe decreases to nearly zero although the anoxic state remains unchanged from the beginning to the end of LED irradiation. This indicates that oxygen is produced due to phytoplankton photosynthesis since t = 28 d. However, oxygen production is extremely low possibly because PO_4-P and NH_4-N concentrations reduce gradually and their consumption rate by phytoplankton is low. Moreover, NO_3-N is continuously maintained at zero level immediately after LED irradiations began; additionally, unlike Cases D-1 and D-2, NO_3-N concentration do not increase despite an extremely low concentration of 0.07 mg/L observed temporarily at t = 44 d. Therefore, NO_3-N, a major nitrogen source, do not assist in phytoplankton photosynthesis because it is not sufficiently supplied in water via the aerobic decomposition of organic matter due to lack of oxygen. Furthermore, Chl-a concentration in Case D-3 do not clearly increase from the initial value. Therefore, it is possible to determine the influence of extremely weak light intensity on oxygen production from the viewpoint of NO_3-N limitation for phytoplankton photosynthesis.

In addition, the oxidizable substances remarkably increase from the initial concentrations as the strong reductive state progressed for t < 28 d, consequently, increasing the oxygen consumption since t > 28 d. Therefore, both decrease in the photosynthesis rate due to light limitation and increase in the oxidizable substances due to prolonged strong reductive state prevented the anoxification recovery in Case D-3. However, determining the anoxification recovery is possible in Case D-3 based on the water quality degradation as sulfide and nutrient contents decreased to nearly zero, although a healthy DO level is not maintained to sustain aquatic life. Furthermore, TN and TP concentrations at the end of irradiation experiment are lower than those observed initially, as summarized in Table 4, and the decrease in the concentrations are similar to those observed in Case D-2. Although the final concentrations of TOC and DOC are higher than the initial concentrations, the differences do not exceed 0.5 mg/L; additionally, the increase in undecomposed organic matter is inhibited by two months LED irradiation. Therefore, the spatial range is extended by the LED irradiation because the minimum effects of water environmental remediation are observed although the light intensity is one-twentieth of the optimum photon intensity required for phytoplankton photosynthesis.

4.4 Conclusions

In this chapter, the effectiveness of anoxification recovery via oxygen production by phytoplankton photosynthesis under the condition of underwater LED irradiation in anoxic water is proved on the water tank-scale experiment from three viewpoints. Firstly, the influence of each RGB spectrum on maintaining a healthy DO level is evaluated according to the single-color irradiations, which are sufficient for phytoplankton photosynthesis despite their marginal light intensity. Secondly, the effects for remediating long-term anoxic water environment with a strong reductive state are proved considering the influence of photon intensity on the oxygen production rate. Finally, the influences of initial anaerobic conditions on the anoxification recovery are cleared up under mixed RGB irradiation having extremely low photon intensity compared to the optimal photon intensity required for photosynthesis. The significant findings of the three series of irradiation experiments have been summarized below.

Red and blue spectra largely contribute to the stable maintenance of a healthy DO level, although the oxygen production rate and maximum and stationary DO levels differ between the two spectra; further, the green spectrum plays an auxiliary role in oxygen production. Thus, red and blue spectra are essential to maintain a healthy DO level to ensure aquatic environmental conservation.

RGB irradiation (R:B:G = 1:1:1) assists healthy aerobic state preservation even though the light intensity is as low as one-fifth of the optimum photon for phytoplankton photosynthesis. Also, the water quality improvement by solving long-term anoxification under both strong and weak light intensity conditions are reflected in decreased TN and TP because of the reduction of DIN and DIP through the aerobic matter cycle, in which phytoplankton plays a leading role. In conclusion, the spatial effect of water quality improvement via LED irradiation is applicable to a wide range and is not limited to the vicinity of the light source. In addition, mixed RGB irradiations maintained a healthy DO level despite the light intensity being one-tenth of the lower limit of the optimum intensity necessary for performing photosynthesis. Moreover, under extremely weak light intensity, which is one-twentieth of the optimum intensity, large-scale reductions of sulfides and nutrients resulted from marginal oxygen production. These are regarded as minimum effects of water quality improvement, although anoxification recovery is absent. The initial anaerobic condition influences the oxygen production rate through high nutrient concentration stemming from long-term anoxification. The effects of optical conditions

and initial anaerobic conditions on maintaining a healthy DO level are determined by balanced nitrogen and phosphorous cycles via biochemical reactions.

The study findings could be applied to design the optimal spectral condition of LED irradiation. In an actual organically polluted reservoir, the area that requires water quality improvement because of long-term anoxification could be determined as a distance in the irradiating direction from the LED lamp. The required photon intensity of a light source can be estimated using the Beer–Lambert law, while considering that the light intensity for the furthermost separated point from the LED lamp should be 4–8 μmol/(m^2 s) as the minimum amount to maintain a healthy DO level. This estimation requires the light extinction coefficient value to be according to the water turbidity. The basic light energy required for a LED lamp can be set mainly using red and blue spectra, and the total photon intensity of visible light from a light source can be determined by supplying a shortage with the green spectrum, to be close to the estimated result. In this study, the effect of water quality improvement by LED irradiation is examined for the anoxic water under a strong nitrogen-control state stemming from an increase of PO_4^{3-} due to long-term anoxification.

Chapter 5 General Conclusion

In a closed water body with an excessive inflow of organic matter, a low transparency causes an anoxification in the deeper layer due to low DO levels in hot seasons. Anoxic water occurs not only because of inhibited oxygen production through phytoplankton photosynthesis under poor underwater light intensities, but also because of suppressed vertical transport of DO through thermal stratification. Anoxification leads serious environmental issues, such as the death of aquatic life because of oxygen deficiency, the pathogenic bacterial growth due to putrefaction of organic matter, the acceleration of eutrophic state by the elution of nutrients from the bottom sediment, the generation of toxic hydrosulfide, and the accumulation of sludge including metal sulfides and undecomposed organic matter on the bottom bed. Therefore, for the environmental conservation and restoration of water in organically polluted water bodies, it is important to develop effective counter measures against anoxification, and establish a technique to recover the anaerobic state.

This study focuses on a method for water environmental remediation using underwater LED treatment in an organically polluted reservoir. Anoxification can be recovered by oxygen production via phytoplankton photosynthesis via artificially improving the underwater light environment using an LED light source. In addition, this solution may be linked to the improvement of water and bottom sediment environments with recovery from anaerobic to aerobic states. The objective of this study is to examine, at the laboratory level, how much RGB full-color underwater LED lamp irradiation contributes to the quality improvement via the anoxification recovery, by considering the influences of two factors, optical spectrum of light source and initial anaerobic condition of water, on the anoxification recovery and water environmental remediation. In this study, water quality parameters, such as DO, chlorophyll-a, DIN, and DIP, are monitored via beaker and water tank experiments while using LED irradiation for 24 hour (12 hour-on/12 hour-off) for 2 months in anoxic water, where the anaerobic decomposition of organic matter progressed under reductive conditions. The knowledge and outcomes acquired by the LED irradiation experiments can be summarized as follows from four viewpoints.

In single-color irradiations, having marginally sufficient photon intensity of approximately 50 μmol/(m^2 s), the green spectrum required more time to recover from the anoxic state because of the lower photosynthesis rate compared to red and blue spectra. Additionally, the influence of oxygen production rate on the time required for the anoxification recovery is almost negligible between red and blue spectra. In these spectra, the equilibrium between nitrogen

and phosphorous cycles for phytoplankton and nutrients is linked to a healthy DO level without an overgrowth of phytoplankton; moreover, TN and TP concentrations decrease considerably because of the reductions in DIN and DIP. The red and blue spectra are essential to maintain a healthy DO level to ensure aquatic environmental conservation, although green spectrum irradiation plays an auxiliary role for oxygen production via phytoplankton photosynthesis.

The photo-responsiveness and photosynthesis rate of phytoplankton are enhanced in the presence of the green spectrum regardless of light intensity, and the anoxic state could be quickly recovered. In particular, LED irradiation with three-color mixed RGB spectra (R:G:B=1:1:1) plays an important role in promoting oxygen production compared to mixed light of red and blue color spectra under low light intensity of approximately 20 μmol/(m^2 s). Under high intensity light of approximately 100 μmol/(m^2 s), DO rapidly increases to supersaturation after anoxification recovery due to the growth of green algae regardless of the green spectrum. This is reflected by the possessing high photosynthetic capacity of green algae. Also, LED irradiation, including the green color band, has an advantage such that the healthy DO environment is preserved without a decrease to poor oxygen levels in the absence of light. The water environmental remediation by solving long-term anoxification under both strong and weak light intensity conditions are reflected in decreased TN and TP upon LED irradiation for 2 months. These results indicate the reduction of DIN and DIP through the aerobic matter cycle, in which phytoplankton play a leading role. In particular, phosphate formed a particulate inorganic chemical chelate with ferric ions generated by the oxidation of ferrous ions after recovering the anaerobic condition, resulting in the reduction of TP. In addition, Environmental water is remediated by anoxic state recovery and the inhibition of nutrient release from the sediment.

Although the light intensity of approximately 10 μmol/(m^2 s) is one-tenth of the lower limit of the optimum photon intensity required for photosynthesis, the anoxic state is finally improved to a healthy DO level. Such an effective improvement in the DO level is attributed to the equilibrated biochemical balance between the oxygen consumption during photosynthesis and oxygen supply into water due to respiration and mineralization, regardless of initial anaerobic conditions. However, the initial anaerobic condition influences the oxygen production rate. LED irradiation under high initial nutrient concentrations stemming from long-term anoxification is advantageous regarding the time required to reach a healthy DO level, average increasing DO rate, and maximum and stable concentrations. The oxygen production rate promoted by the

initial high concentrations of NH_4-N and PO_4-P are associated with the early recovery of anoxification despite the high oxygen consumption due to the presence of many oxidative substances. In addition, the rapid increase in the DO level to a saturated state due to increased oxygen production rate produced NO_3-N due to the aerobic decomposition of organic matter and the oxidation of NH_4-N. Further, the increase in NO_3-N weakened the initial strong nitrogen-limitation state required for phytoplankton photosynthesis. Consequently, a high supply of nutrients is associated with a healthy DO environment.

Under extremely weak light intensity of approximately 5 μmol/(m^2 s), which is one-twentieth of the optimum photon intensity, the photosynthesis rate decreases considerably due to the strong limitation of light linked to marginal oxygen production, which is significantly less than the oxygen consumed for oxidizing a large proportion of the oxidative substances. Consequently, the anoxic state could not be recovered despite LED irradiation. However, the minimum effects of water environmental remediation are observed wherein the marginal oxygen production could restrict water quality degradation due to the anaerobic reductive reactions.

This study indicates the spatial effect of water environmental remediation via LED irradiation is not limited to the vicinity of light source but is applicable to a wide range, in which the light intensity contributes to one-twentieth of the optimum photon intensity for phytoplankton photosynthesis. The study findings could be applied to design the optimal spectral condition of LED irradiation. In an actual organically polluted reservoir, the water area that requires to improve from long-term anoxification could be determined as setting up an irradiated distance direction from LED lamp. The required photon intensity of a light source can be estimated using the Beer–Lambert law, while considering that the light intensity for the furthermost separated point from the LED lamp should be 4–8 μmol/(m^2 s) as the minimum amount to maintain a healthy DO level. This estimation requires the light extinction coefficient value to be according to the water turbidity. The basic light energy required for a LED lamp can be set mainly using red and blue spectra, and the total photon intensity of visible light from a light source can be determined by supplying a shortage with the green spectrum, to be close to the estimated result. All of those results in this study could be used to design optimal LED irradiation techniques to mitigate anoxification to sustain a healthy aquatic environment.

Acknowledgement

This study has been implemented at the Laboratory of Water Environment Engineering, Graduate School of Bio-resource and Bio-environment Sciences, Kyushu University, Japan. The success of this study aimed to apply underwater LED irradiation as a water quality improvement technique to conserve and restore the aquatic environment of organically polluted water bodies. The Project for Human Resource Development Scholarship (JDS) is one of main contribution of my success in both master and doctoral degrees so I sincere thank you to JDS that provides me a financial support and a grateful opportunity to join an academic life at Kyushu University.

I would like to acknowledge and appreciate for all the excellent advises and encouragements to me to conduct the PhD research during 3 academic years. Indeed, I do really appreciate to Dr. Masayoshi Harada, Associate professor in the Laboratory of Water Environment Engineering who is my main supervisor for his intensive support and educated me to improve my ability in water environmental field. By doing research and experiments, I have learnt and developed my knowledge, skills and experiences in advanced level. Moreover, I would like to show gratitude to Dr. Kazuaki Hiramatsu, Professor in the Laboratory of Water Environment Engineering for his valuable comment, reminding and contribution. I would like to thank Dr.Yoshiyuki Shinogi, Professor in the Laboratory of Irrigation and Water Management, Division of Bioproduction Environmental Sciences, Department of Agro-environmental Sciences, Faculty of Agriculture, Kyushu University, for valuable comments and contribute to complete my thesis. I also feel grateful to Dr. Toshinori Tabata, Assistant professor in the Laboratory of Water Environment Engineering for his treasured feedback and enhancement. Additionally, I am thankful to Dr. Akinori Ozaki, Assistant Professor in the International Development Section, Institute of Tropical Agriculture, Kyushu University for his concentrated comment and suggestion. Without all of your supervisions, I may not handle with this research and submit the academic paper to Paddy Water and Environment Journal. I would like to express thanks to Mr. Hiroto Yamada, Ms. Yumiko Nakashima and water quality analysis groups in the Laboratory of Water Environment Engineering for our teamwork and help each other in the laboratory including main water quality parameters measurement, setup of the experiment and water sampling. Also, I would like to thank all members of the Laboratory of Water Environment Engi-

neering for their exchange experiences. Therefore, I believe that the gained ability from Doctoral course in Japan would be useful and contribute to the development of water environmental remediation in Laos.

References

Barry RC, Schnoor JL, Sulzberger B, et al (1994) Iron oxidation kinetics in an acidic alpine lake. Water Resources 28:323–333.

Beutler M, Wilshire KH, Meyer B, Moldaenke C, Lüring C, Meyerhöfer M, Hansen HP, Dau H (2002) A fluorometric method for the differentiation of algal populations *in vivo* and *in situ*. Photosynthesis Research 72(1): 39–53

Burke SP, Banwart SA (2002) A geochemical model for removal of iron(II)(aq) from mine water discharges. Applied Geochemistry 17:431–443.

Caraco NF, Cole JJ, Findlay SEG, et al (2000) Dissolved oxygen declines in the Hudson River associated with the invasion of the zebra mussel (Dreissena polymorpha). Environ Sci Technol 34:1204–1210.

Chapra SC, Canale RP (1991) Long-term phenomenological model of phosphorus and oxygen for stratified lakes. Water Resources 25: 707–715

Chen HB, Wu JY, Wang CF, Fu CC, Shieh CJ, Chen CI, Wang CY, Liu YC (2010) Modeling on chlorophyll a and phycocyanin production by Spirulina platensis under various light-emitting diodes. Biochemical Engineering Journal 53: 52–56

Diatta J, Waraczewska Z, Grzebisz W, et al (2020) Eutrophication Induction Via N/P and P/N Ratios Under Controlled Conditions—Effects of Temperature and Water Sources. Water, Air and Soil Pollution 231:149.

Do NT, Yoshimura Y, Harada M, Hiramatsu K (2015) Generation of hydrogen sulfide in the deepest part of a reservoir under anoxic water conditions. Paddy and Water Environment 13: 101–113

Edwards KF, Thomas MK, Klausmeier CA, Litchman E (2016) Phytoplankton growth and the interaction of light and temperature: A synthesis at the species and community level. Limnology and Oceanography 61:1232–1244.

Elçi Ş (2008) Effects of thermal stratification and mixing on reservoir water quality. Limnology 9: 135–142

Harada M, Hiramatsu K, Fukuda S (2014) Dynamics of water qualitites under the anaerobic and reductive state in an organically polluted closed water body. Journal of Rainwater Catchment systems 20: 49–55 (in Japanese with English abstract)

Harada M, Kawano Y, Hiramatsu K, Tabata T (2016) Experimental study on improvement effect of DO environment in an organic polluted water body using an underwater LED considering optical absorption property of chlorophyll a. Applied Hydrology 28: 1-10 (in

Japanese with English abstract)

Hasan K, Alam K, Saidul Azam Chowdhury M (2013) The Use of an Aeration System to Prevent Thermal Stratification of Water Bodies: Pond, Lake and Water Supply Reservoir. Appl Ecol Environ Sci 2: 1–7

Henneberry YK, Kraus TEC, Nico PS, Horwath WR (2012) Structural stability of coprecipitated natural organic matter and ferric iron under reducing conditions. Organic Geochemistry 48:81–89.

Honglikith D, Harada M, Hiramatsu K, Tabata T. Ozaki A. (2022) Anoxification recovery using underwater LED irradiation and influence of its optical spectrum on water quality improvement. Paddy Water Environment 20(1): 153–175

Hsiao SY, Hsu TC, Liu JW, et al (2014) Nitrification and its oxygen consumption along the turbid Chang Jiang River plume. Biogeosciences 11:2083–2098.

Hupfer M, Lewandowski J (2008) Oxygen controls the phosphorus release from lake sediments - A long-lasting paradigm in limnology. Int Rev Hydrobiol 93: 415–432

Jahan R, Khan S, Haque MM, Choi JK (2010) Study of harmful algal blooms in a eutrophic pond, Bangladesh. Environ Monit Assess 170: 7–21

Kaushik N, Tyagi B, Jayaraman G (2012) Modeling of the Dissolved Oxygen in a River with Storage Zone on the Banks. Applied Mathematics 03:699–704.

Kido K, Saito T, Uotani R, Kuwabara T, Aizaki M (2014) Estimate of the Efflux of N·P·S from Sediment in Dredging Hollow in Lake Nakaumi and Effect of Sand Capping with Granulated Coal Ash. Journal of Japan Society on Water Environment 37: 71–77 (in Japanese with English abstract)

Lijklema L (1980) Interaction of Orthophosphate with Iron(III) and Aluminum Hydroxides. Environmental Science and Technology 14:537–541.

Luther GW, Glazer B, Ma S, et al (2003) Iron and sulfur chemistry in a stratified lake: Evidence for iron-rich sulfide complexes. Aquatic Geochemistry 9:87–110.

Mackay EB, Feuchtmayr H, De Ville MM, et al (2020) Dissolved organic nutrient uptake by riverine phytoplankton varies along a gradient of nutrient enrichment. Science of the Total Environment 722:137837.

Marzetz V, Spijkerman E, Striebel M, Wacker A (2020) Phytoplankton Community Responses to Interactions Between Light Intensity, Light Variations, and Phosphorus Supply. Frontiers in Environmental Science 8:1–11.

Minato T, Yokoyama Y, Oishi T, Sato Y (2012) Improvement of Anoxic Condition on Bottom Water Layer and Sediment by Supplying Light with Light Emitting Diode. Journal of

Japan Society of Civil Engineers, Ser. B2 (Coastal Engineering) 68(1): 54–59 (in Japanese with English abstract)

Minato T, Sato Y, Yokoyama Y, Oishi T (2014) Oxygen Evolution on Bottom Water Layer by Supplying Light with Light Emitting Diode. Journal of coastal zone studies 27(1): 15–25 (in Japanese with English abstract)

Morse JW (1990) Aquatic chemical kinetics: Reaction rates of processes in natural waters. Limnology and Oceanography 35:1865–1865.

Nielsen AH, Vollertsen J (2021) Model parameters for aerobic biological sulfide oxidation in sewer wastewater. Water (Switzerland) 13: 981.

Ogawa D, Murakami K, Katakura N (2009) Field Experiments on the Lasting of Sand Capping Technique on Nutrient Release Reduction and the Influence of Suspended Sediments on the Effects. Journal of Japan Society of Civil Engineers, Ser. B2 (Coastal Enggineering) 65: 1181–1185 (in Japanese with English abstract)

Omoregie EO, Couture RM, Van Cappellen P, et al (2013) Arsenic bioremediation by biogenic iron oxides and sulfides. Applied and Environmental Microbiology 79:4325–4335.

Oniki A, Harada M, Hiramatsu K, Tabata T (2017) Experimental Study on Dynamics of Water Qualities near Bed Material in Anoxic Water Area Focused on Nitrate Nitrogen. Journal of Rainwater Catchment Systems 22(2): 31–39 (in Japanese with English abstract)

Radwan M, Willems P, El-Sadek A, Berlamont J (2003) Modelling of dissolved oxygen and biochemical oxygen demand in river water using a detailed and a simplified model. International Journal of River Basin Management 1:97–103.

Robert Hamersley M, Woebken D, Boehrer B, et al (2009) Water column anammox and denitrification in a temperate permanently stratified lake (Lake Rassnitzer, Germany). Syst Applied Microbiology 32:571–582.

Roden EE, Edmonds JW (1997) Phosphate mobilization in iron-rich anaerobic sediments: Microbial Fe(III) oxide reduction versus iron-sulfide formation. Archiv fur Hydrobiologie 139:347–378.

Sahoo GB, Luketina D (2006) Response of a Tropical Reservoir to Bubbler Destratification. Journal of Environmental Engineering 132: 736–746

Staehr PA, Sand-Jensen KAJ (2006) Seasonal changes in temperature and nutrient control of photosynthesis, respiration and growth of natural phytoplankton communities. Freshwater Biology 51:249–262.

Takada J, Murase N, Abe M, Noda M, Suda Y (2011) Growth and Photosynthesis of *Ulva pro-*

lifera under Different Light Quality form Light Emitting Diodes (LEDs). Aquaculture Science 59(1): 101-107 (in Japanese with English abstract)

Thach TT, Harada M, Hiramatsu K, Tabata T (2018a) Estimation of water quality dynamics under long - term anoxic state in organically polluted reservoir by field observations and improved ecosystem model. Paddy and Water Environment 16: 665–686

Thach TT, Harada M, Hiramatsu K, Tabata T (2018b) The Influence of Bottom Sediment Redox State on Water Quality Dynamics under Long-term Anoxic Conditions in an Organically Polluted Reservoir. Journal of Rainwater Catchment Systems 24(1): 23-31

Thach TT, Harada M, Oniki A, Hiramatsu K, Tabata T (2017) Experimental study on the influence of dissolved organic matter in water and redox state of bottom sediment on water quality dynamics under anaerobic conditions in an organically polluted water body. Paddy and Water Environment 15(4): 889–906

Vadeboncoeur Y, Jeppesen E, Vander Zanden MJ, et al (2003) From Greenland to green lakes: Cultural eutrophication and the loss of benthic pathways in lakes. Limnology and Oceanography 48: 1408–1418

Wang X, Han X, Shi X, et al (2006) Kinetics of nutrient uptake and release by phytoplankton in East China Sea: Model and mesocosm experiments. Hydrobiologia 563:297–311.

Wang CY, Fu CC, Liu YC (2007) Effects of using light-emitting diodes on the cultivation of Spirulina platensis. Biochemical Engineering Journal 37: 21–25

Wendt-Potthoff K, Kloß C, Schultze M, Koschorreck M (2014) Anaerobic metabolism of two hydro-morphological similar pre-dams under contrasting nutrient loading (Rappbode Reservoir System, Germany). International Review of Hydrobiology 99:350–362

Whitmire SL, Hamilton SK (2005) Rapid Removal of Nitrate and Sulfate in Freshwater Wetland Sediments. Journal of Environmental Quality 34:2062–2071.

Yamanaka R, Kozuki Y, Okegawa H, Sawada K, Maeda M, Kutsukake Y, Hirai S, Isshiki K (2012) Development of water quality improve technique for the water improvement cannel using LED light at night in Amagasaki Canal. Journal of Japan Society of Civil Engineers, Ser. B2 (Coastal Engineering) 68(2): I_1166– I_1170 (in Japanese with English abstract)

Zerkle AL, Kamyshny A, Kump LR, et al (2010) Sulfur cycling in a stratified euxinic lake with moderately high sulfate: Constraints from quadruple S isotopes. Geochimica et Cosmochimica Acta 74:4953–4970.

Zhang C, He J, Yao X, et al (2020) Dynamics of phytoplankton and nutrient uptake following dust additions in the northwest Pacific. Science of the Total Environment 739:139999.